

TNO-VOEDING ZEIST  
BIBLIOTHEEK

P: 102 (1)

Matrix-assisted laser desorption/ionization  
mass spectrometry in biological sciences

Sonja Jespersen



**Matrix-Assisted Laser Desorption/Ionization Mass Spectrometry  
in Biological Sciences**

Proefschrift  
ter verkrijging van de graad van Doctor  
aan de Universiteit Leiden,  
op gezag van de Rector Magnificus Dr. W.A. Wagenaar,  
hoogleraar in de faculteit der Sociale Wetenschappen,  
volgens besluit van het College voor Promoties  
te verdedigen op donderdag 18 februari 1999  
te klokke 15.15 uur

door

**Sonja Jespersen**

geboren te Hanning sogn, Denmark in 1963

## Promotiecommissie

Promotor: Prof. dr. J. van der Greef

Co-promotor: Dr. W.M.A. Niessen  
Dr. U.R. Tjaden

Referent: Prof. P. Roepstorff

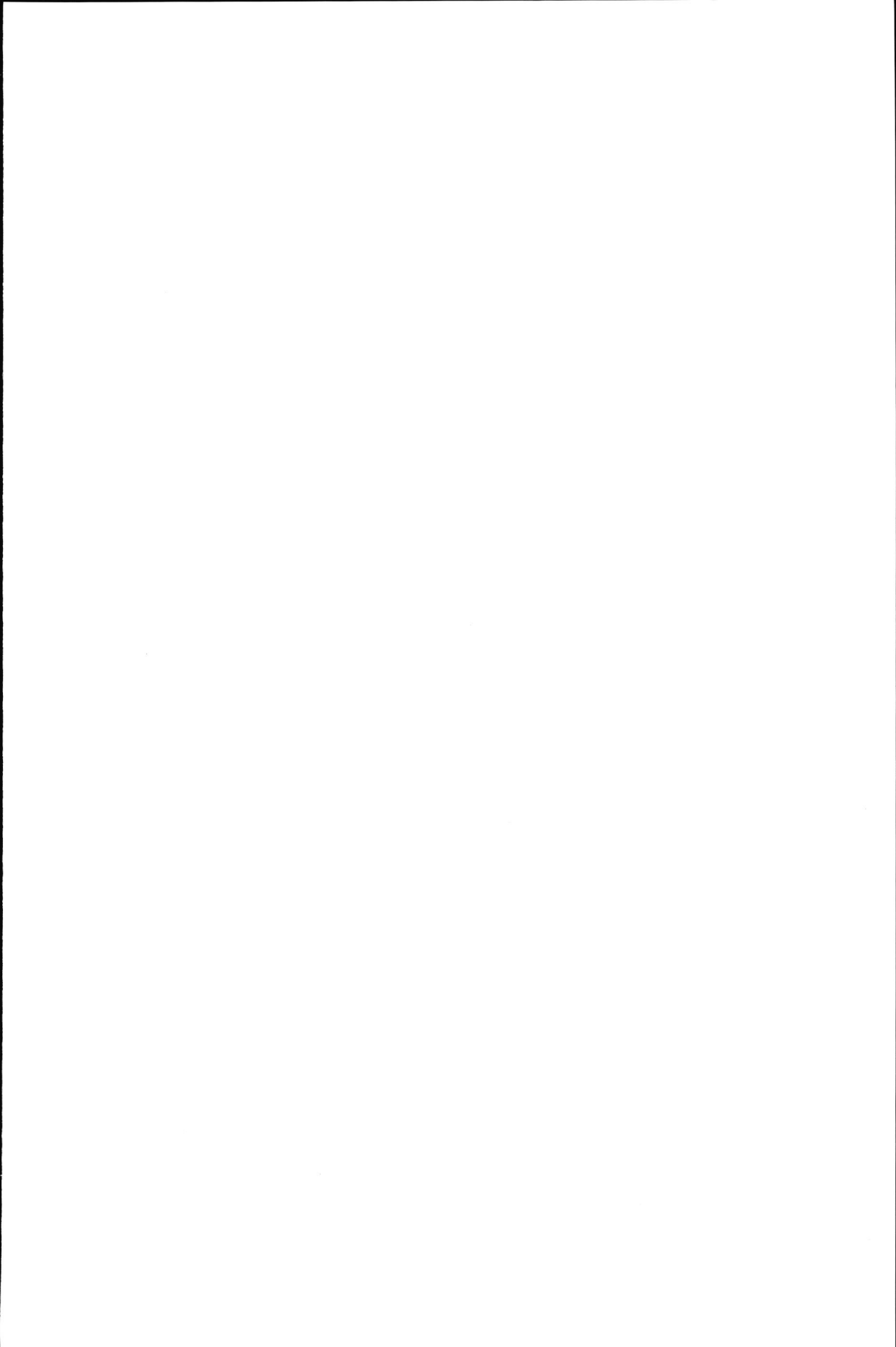
Overige leden: Prof. dr. D.D. Breimer  
Prof. dr. E.R. de Kloet  
Prof. dr. R. Verpoorte

Printed by Grafisch bedrijf Ponsen & Looijen B.V., Wageningen, The Netherlands

Publication of this thesis was financially supported by:

Thermo BioAnalysis, BioMolecular Instruments,  
Santa Fe, New Mexico, USA

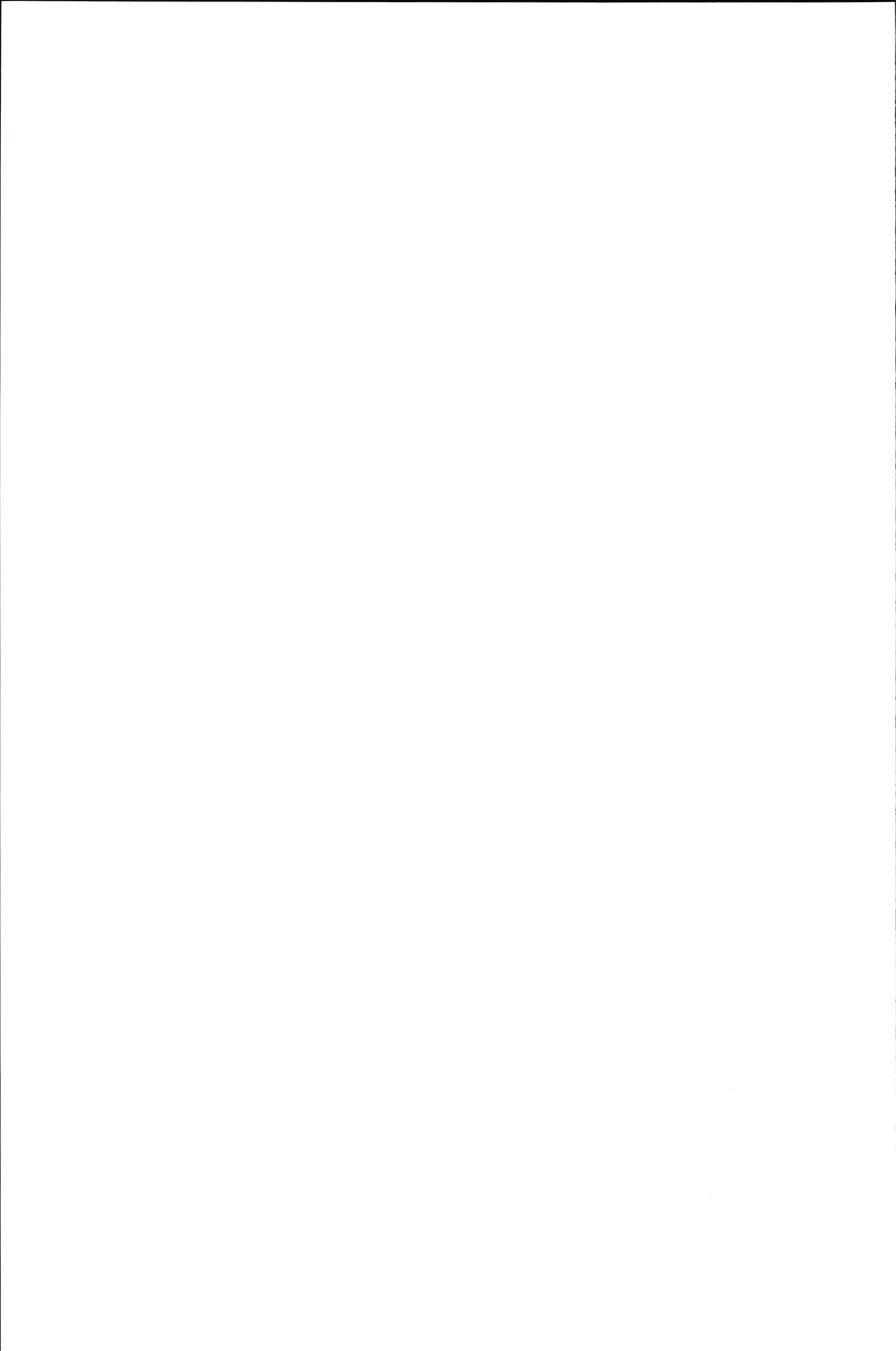
TNO Nutrition and Food Research Institute,  
Zeist, The Netherlands



# Contents

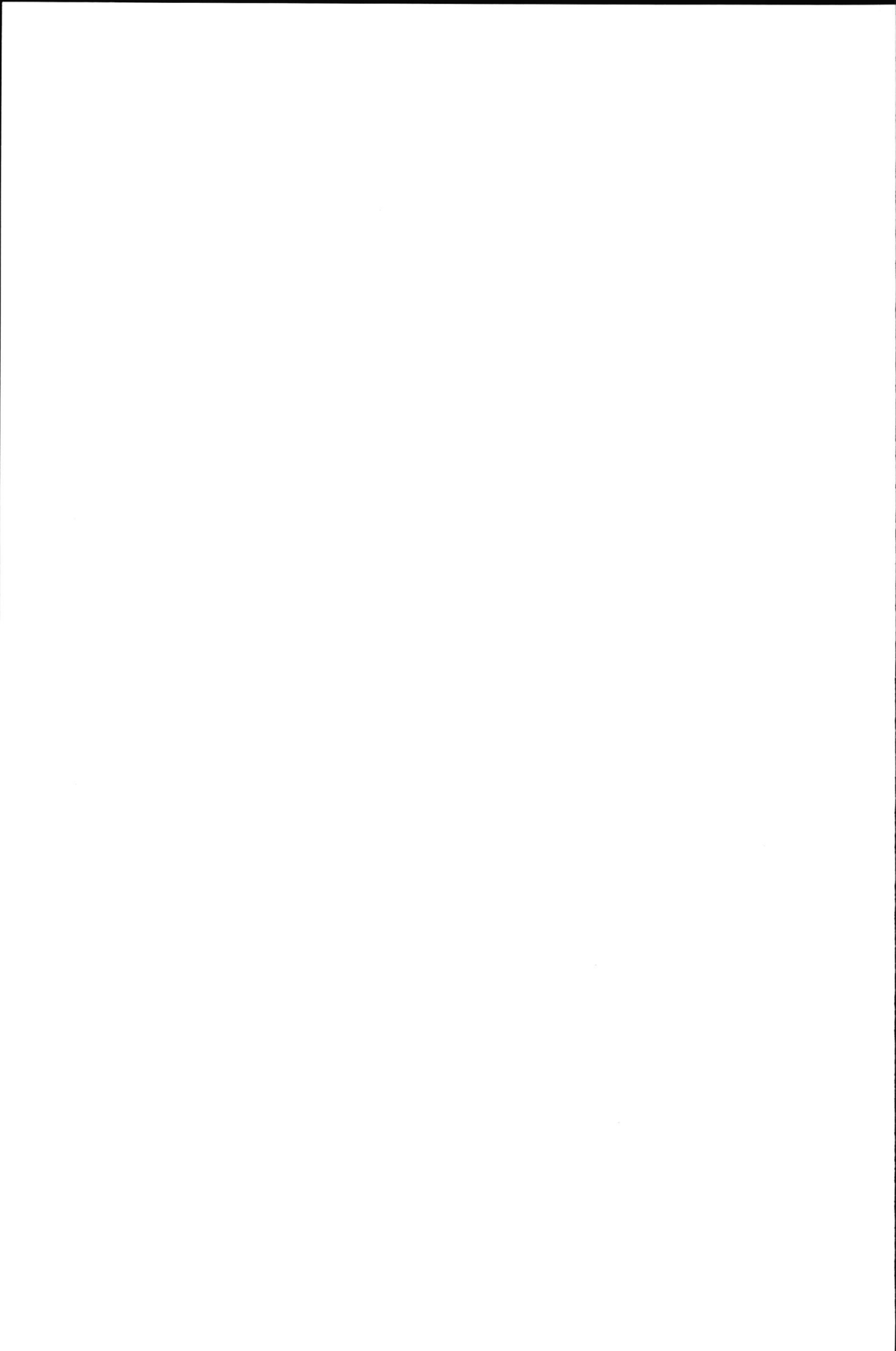
<b>Chapter 1.</b>	Introduction	
1.1	General introduction	9
1.2	Discovery of MALDI	9
1.3	Matrices	11
1.4	Sample preparation	12
1.5	Mechanism of MALDI	13
	Photochemical ionization model (UV)	14
	Non-ionized matrix model (UV)	14
	Phase transition model (IR)	15
1.6	Instrumentation	16
	Ion source	16
	Time-of-flight (TOF) mass spectrometry	17
	Ion detection and data collection	19
	Calibration	19
1.7	Performance specifications	19
	Sensitivity	20
	Mass range	20
	Mass accuracy	20
1.8	Post-source decay	20
1.9	Delayed extraction	23
1.10	Applications	24
	Proteins	24
	Peptide profiling	25
	In combination with gel electrophoresis	25
	In combination with databases	26
	Oligonucleotides	26
	Synthetic polymers	26
	Quantitative aspects	27
	Non-covalent complexes	27
1.11	Scope of this thesis	28

<b>Chapter 2.</b>	Attomol detection of proteins by MALDI-MS with the use of picolitre vials	37
<b>Chapter 3.</b>	Quantitative bioanalysis using MALDI-MS	53
<b>Chapter 4.</b>	Basic matrices in the analysis of non-covalent complexes by MALDI-MS	63
<b>Chapter 5.</b>	Identification of multiple target sites for a glutathione conjugate on glutathione-S-transferase by MALDI-MS	77
<b>Chapter 6.</b>	Characterization of O-glycosylated precursors of insulin-like growth factor II by MALDI-MS	91
<b>Chapter 7.</b>	Identification of POMC processing products in single melanotrope cells by MALDI-MS	109
<b>Chapter 8.</b>	Direct sequencing of neuropeptides in biological tissue by MALDI-MS	123
<b>Chapter 9.</b>	Conclusion and perspectives	141
	Summary	143
	Sammenvatting	145
<b>Curriculum Vitae</b>		147
<b>Acknowledgement</b>		149
<b>List of publications</b>		151



---

**Chapter 1**  
Introduction



---

# Introduction

## 1.1 General introduction

During the past two decades, important achievements in biological mass spectrometry (MS) have been made by the development of new ionization techniques for the analysis of biopolymers such as proteins, carbohydrates and nucleotides. Conventional mass spectrometric methods, which proved so useful in organic chemistry for analyzing compounds with low molecular masses, exclude the possibility of measuring compounds with high molecular masses. The general problem was to convert non-volatile biopolymer macromolecules into intact, isolated ionized molecules in the gas phase. Once formed, the ions can be directed into a mass analyzer that differentiates the ions according to their mass-to-charge ratio ( $m/z$ ).

Two desorption techniques, fast atom bombardment (FAB) [1] and plasma desorption (PD) [2], initiated the development of strategies for protein characterization by mass spectrometry. Though very successful, their general use was restricted by a limitation in the mass range; routinely below 5000 Da for FAB and 15 000 Da for PDMS. The breakthrough for the mass spectrometry of biomolecules at higher molecular masses came in 1988 with the introduction of electrospray ionization (ESI) [3] and matrix-assisted laser desorption/ionization (MALDI) [4], ESI and MALDI mass spectrometry extended the accessible mass range to above several hundred thousand Daltons. They provide a rapid, simple and accurate means of obtaining molecular mass information for a wide range of non-volatile biopolymers at excellent sensitivity.

## 1.2 Discovery of MALDI

With the invention and development of lasers in the early 1960's it was demonstrated that irradiation of solid surfaces with a high intensity laser pulse could produce ions in the gas-phase for mass spectrometric analysis [5]. In the years to follow, lasers throughout the wavelength range from far-infrared (IR) to far-ultraviolet (UV) were combined with virtually every available type of mass spectrometer. During the 1970's the laser desorption (LD) technique extended from mainly elemental analysis to the analysis of non-volatile polar biological and organic molecules [6-9]. Especially the desorption of intact quasimolecular ions of thermally labile compounds, such as oligosaccharides, glycosides and peptides [7] was an important step in the development of LD.

Two general mechanisms of LD were discovered: First, an efficient and controllable energy transfer to the sample requires resonant absorption of photons by the molecule at the laser wavelength used. Second, to avoid thermal decomposition of thermally labile molecules the energy from the laser beam must be transferred within a very short time. However the success of LD for the analysis of intact larger biomolecules was quite limited i.e. in the mass range up to 10 kDa for IR-LD [10,11] and up to 3 kDa for UV-LD [12-14]. This limitation was believed to be due to the fact that the energy needed for resonant absorption and successful energy transfer was greater than the energy required for the dissociation of the larger biomolecules [15].

A major breakthrough in LD was achieved in 1988, when it was discovered that, similarly as in FAB, the use of a matrix compound in LD greatly extends the applicability range of the ionization technique. Simultaneously but independently, two matrix techniques were introduced [16,17]. Tanaka *et al.* [16] used a slurry of metal particles in glycerol as the absorbing matrix and a nitrogen ( $N_2$ ) laser, emitting radiation at 337 nm for desorption. Since laser light at 337 nm passed through glycerol without any interaction, it was necessary to introduce a finely dispersed metal powder. Because of their ability to produce thermal excitation in response to laser irradiation, the metal particles were the coupling between the light and the liquid matrix. The matrix technique chosen by Karas and Hillenkamp was conceptually different. In earlier studies, they observed that small, non-absorbing molecules (amino acids) could be desorbed intact if dispersed in a suitable matrix, consisting of small highly absorbing species [14,18]. Under these conditions the role of the metal substrate, used as sample support, in energy deposition could be excluded. The breakthrough towards higher masses came with the discovery that nicotinic acid had special properties as matrix for larger polypeptide analytes [17]. Nicotinic acid is solid at room temperature and shows a high molar absorptivity at 266 nm, a frequency of the neodymium-doped yttrium aluminium garnet (Nd-YAG) laser used. Irradiation of a dried mixture of nicotinic acid and the analyte mediated both the desorption and ionization of intact molecular ion of proteins exceeding 10 000 Da [17].

The major difference between the two methods of sample preparation was sensitivity. The sample preparation of Tanaka's required nanomoles of protein, whereas only picomoles were required for the Karas and Hillenkamp sample preparation. The signals obtained for the latter method were also more intense and had a higher signal-to-noise ratio. These factors indicated that for an analytical method, the nicotinic acid matrix was perceived to be more promising. The name given to this new method of ion production was "matrix assisted laser desorption/ionization" (MALDI).

Principles and various practical aspects of MALDI-MS are discussed in the next sections, i.e. the choice of matrix, sample preparation and ionization mechanisms in MALDI. This is followed by the instrumental set-up, including the principles of the time-of-flight analyzers. After listing some general performance specifications, advanced techniques like post-source decay and delayed extraction are explained. Finally, the general application area of MALDI-MS is briefly overviewed.

**Table 1** The most commonly used matrices for MALDI-MS

Matrix	Wavelength	Application
Nicotinic acid [17]	266 nm	proteins
Sinapinic acid [23]	337, 355 nm	proteins and glycoproteins
2,5-Dihydroxybenzoic acid (DHB) [24]	337, 355 nm 2.94 $\mu\text{m}$	proteins and glycoproteins carbohydrates, synthetic polymers peptide-mapping biological samples
$\alpha$ -Cyano-4-hydroxycinnamic acid [31]	337, 355 nm	peptides and glycoproteins peptide-mapping PSD analysis
3-Hydroxy picolinic acid [33]	337, 355 nm	oligonucleotides and carbohydrates
DHB + 10% 2-hydroxy-5-methoxy benzoic acid (sDHB) [34]	337, 355 nm	high mass range; $M_r > 20\,000$

### 1.3 Matrices

Since the introduction of nicotinic acid, several different organic compounds, selected for their UV absorbing properties have been investigated [see e.g. 19-22]. Most of these compounds are substituted aromatic compounds containing a carboxylic acid group. Different matrix compounds or mixtures of matrix compounds are used for MALDI analysis, depending on the laser wavelength used, the solubility of the analyte and the class of compounds. A list of the most commonly used substances is given in Table 1. Cinnamic acid derivatives, including ferulic acid and sinapinic acid evaluated by Beavis and Chait [23] enabled MALDI analysis at laser wavelengths extending from 266 to 355 nm. Compared to nicotinic acid, these matrices improved the sensitivity and reduced the abundance of adduct ions. The matrix 2,5-dihydroxybenzoic acid (DHB), introduced by Strupat *et al.* [24], performs as well as or better than the cinnamic acid derivatives

and in conjugation with both UV and IR lasers [25,26]. This matrix is extremely useful for the analysis of a large variety of macromolecules such as proteins [27], carbohydrates [28], synthetic polymers [29] and enzymatic digest [30]. Besides, it has shown a high tolerance to contaminants such as inorganic salts, buffer and ionic detergents like sodium dodecyl sulphate (SDS) [24]. Another matrix,  $\alpha$ -cyano-4-hydroxycinnamic acid (HCCA) produces intense signals of peptides and glycopeptides [31]. In addition, a high degree of metastable fragmentation is induced with HCCA as matrix [32], making it a suitable matrix for post-source decay analysis. Among the few matrix compounds that have been found to desorb/ionize intact DNA, 3-hydroxypicolinic acid (3-HPA) is probably the most widely used [33]. More recently, the use of the matrix DHB, along with 2-hydroxy-5-methoxy benzoic acid, (super DHB, sDHB) have enhanced the MALDI performance and extended the accessible mass range of DHB [34].

#### 1.4 Sample preparation

Proper sample preparation is crucial for successful analyses by MALDI-MS. The earliest and most widely used procedure for analyte-matrix preparation is the "dried droplet" method [35]. The matrix compounds are typically dissolved in an aqueous solution containing 30-70% acetonitrile and/or 0.1% trifluoroacetic acid (TFA). The analyte is prepared in a solvent compatibility with the matrix. Micro volumes of the matrix and the analyte solution are deposited on a sample probe either sequentially to mix them thoroughly on the probe tip or together in the form of an admixture of the two solutions and allowed to dry. Optimal molar ratios are in the 1:1000 to 1:10000 (analyte to matrix) range. Depending on the matrix used, finely dispersed crystallites or extended crystalline areas at the rim of the droplet can be observed by microscopic inspection. Incorporation of analyte into matrix crystals, taking place upon evaporation of the solvent [24,36,37] provides an in-situ purification of the sample and is the reason for the relatively high tolerance against contaminants.

However, high concentrations of impurities commonly found in biological samples can significantly reduce or totally eliminate the analyte ion yield. For such complex systems, it is necessary to optimize the matrix-sample preparation and/or add a sample pretreatment step to desalt the sample [38]. Significant improvements in the tolerance of MALDI to high levels of involatile additives has been demonstrated using a slow matrix crystallization technique [39]. Several immobilization/washing strategies have also been fairly successful in decreasing salt levels where either thin layer of micro/poly-crystalline film [35,40], a membrane [41-44], or a C-18 derivatized target [45] is used to adsorb analytes, allowing extensive washing of the sample.

## 1.5 Mechanism of MALDI

The role of the matrix is generally thought to be threefold [27-46]:

*(1) Matrix isolation.*

The biomolecules are incorporated in a large excess of matrix molecules, separating analyte molecules from each other, strong intermolecular forces are thereby reduced, preventing aggregation of the biomolecules.

*(2) Absorption of energy from the laser light.*

The matrix molecules absorb the energy from the laser pulse and transfer it into excitation energy of the solid system, initiating the process of desorption.

*(3) Ionization of the biomolecules.*

Suitable matrices are thought to induce the ion formation of the analyte molecules by photoexcitation or photoionization of matrix molecules, followed by proton transfer to the analyte molecules.

The precise mechanisms involved in the concept of matrix assistance to laser desorption/ionization are still uncertain. Efforts have been made in order to understand the fundamental aspects of desorption and ionization. Such investigations include the examination of compounds for their efficacy as matrices [21,31,47-49], determination of the initial velocity distribution of laser desorbed analyte ions [50-52], the influence of laser wavelength and pulse width [49,53], studies of exchangeable protons in the matrix molecule [51,54] determination of common matrices proton affinities [48,55] and studies of matrix-ion suppression [37,56,57].

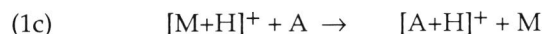
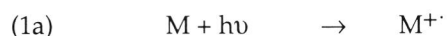
The mechanism for transferring the biomolecules, embedded in the matrix, into gas-phase ions involves a rapid phase change from solid to gas. It is generally accepted that the matrix molecules, upon absorption of the laser beam energy, rapidly sublime, forming a dense plume that undergoes supersonic expansion into vacuum, carrying the embedded molecules into the gas phase [51,52,58].

As far as ion formation processes are concerned several observations support the model that the ionization of analyte molecules takes place as a separate process in the expanding plume of desorbed particles as a result of matrix analyte reactions [47,50,59,60], whereas the chemical step leading to ionization is still a matter of considerable debate and research. For UV-MALDI mainly two different models have been proposed: a photochemical ionization model, where highly reactive matrix radical ions are formed

by photoionization, followed by subsequent ion-molecule reactions with the neutral analyte molecules, i.e. chemical ionization and the non-ionized matrix model which involves excited-state proton transfer between electronically excited matrix molecules and neutral analyte molecules.

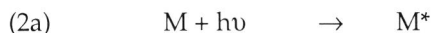
*Photochemical ionization model (UV)*

This model is based on the observation of both radical molecular ions ( $M^{\cdot+}$ ) and protonated ions ( $[M+H]^+$ ) for several matrix compounds [47], whereas the peptides/proteins (analytes) are observed essentially as protonated molecules ( $[A + H]^+$ ). The key idea is that ionization of highly absorbing compounds by UV lasers is initiated by a photoionization step yielding intermediate radical molecular ions (reaction 1a). The radical molecular ions which usually are very reactive species, then undergo chemical reactions with neutral molecules, thereby directly protonating the analyte (reactions 1b) and/or another matrix molecule (reactions 1b') [47,51,59,61]. Protonation of the analyte may also include an additional step, where the proton originates from the protonated matrix ions (reaction 1c) [32,54,62,63].



*Non-ionized matrix model (UV)*

The low relative intensity of matrix related ions compared to analyte ions and the existence of specific conditions in which matrix ions are fully suppressed [31,37,56,57,64,65] suggest non-ionized matrix as precursor for protonated analyte ions. In this model the electronically excited matrix molecule ( $M^*$ ) formed in reaction 2a acts as an acid, transferring a proton to the analyte molecule (reactions 2b). There should be a similar pathway for matrix ions when analyte is not in the vicinity (reactions 2b'). The intermolecular proton transfer depends on the relative proton affinities of the matrix and analyte molecules.



*Phase transition model (IR)*

For both the above models at least, two UV photons or two UV excited matrix molecules are needed to provide the necessary ionization energy [47,66]. Since MALDI of large ions has been demonstrated for IR laser wavelengths as well, requiring 20-80 photons [25,26,47,64,66,67], the formation of radical ions and/or neutral photoexcited matrix appears not to be an essential prerequisite for ion formation.

Recently Niu, Zhang and Chait [68] made the first direct comparison of UV- and IR-MALDI mass spectra of proteins obtained from the same analyte-matrix mixture (sample spot). Strikingly similar IR- and UV-MALDI mass spectra were obtained for a given protein from the same matrix. This lead to the suggestion that the ionization occurs as a natural consequence of the solid-to-gas phase transition induced by the IR irradiation and that ionization takes place through proton exchange reactions in the intermediate phase between solid and gas, with the protons derived from dissociation of the acidic matrix in this intermediate phase, and that the driving force for ionization is the relative high proton affinity of the protein molecules. They further propose that ionization in UV-MALDI may also be a natural consequence of the phase transition and that electronic excitation may not play a primary role in the ionization process.

Although a number of models for the processes underlying the phase transition and ionization have been proposed, insufficient experimental data has been obtained to assess definitively their relative merits. And it must be kept in mind, that ion formation can be sensitive to both the matrix material and the analyte.

## 1.6 Instrumentation

*Ion source*

A schematic drawing of an MALDI instrument is shown in Figure 1. The ion source consists of a sample stage/probe that is used to load the matrix-analyte mixture into the vacuum system of the mass spectrometer. Lasers emitting in the UV wavelength range of 260-360 nm are almost exclusively used in MALDI instruments. The most common are the  $N_2$  laser emitting at 337 and the Nd-YAG laser, whose emission wavelength of 1064 nm can be transformed to 355 nm or 266 nm by frequency tripling or quadrupling using non-linear optical crystals. The few IR-MALDI related studies have mainly been carried out with the erbium-yttrium aluminium garnet (Er-YAG) laser emitting at 2.94  $\mu\text{m}$ .

For the required irradiance in the range of  $10^6 - 10^7 \text{ W/cm}^2$  the laser beams are focused onto the sample spot, to diameters in the 50-500  $\mu\text{m}$  range by suitable optical lenses. Tuning of the applied irradiance is achieved by finely attenuating the laser beam.

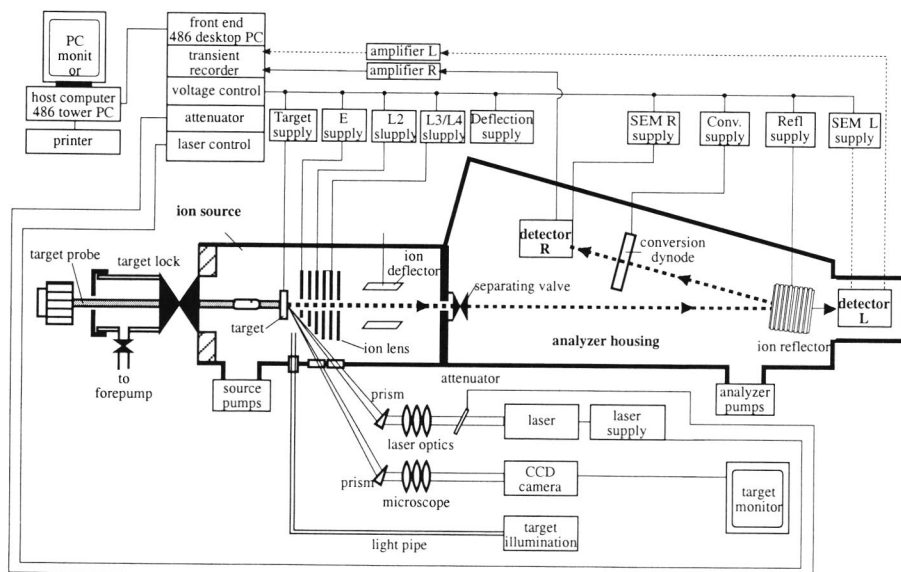


**Figure 1.** Schematic diagram of the Finnigan MAT, VISION 2000, a MALDI-TOF instrument (courtesy Finnigan MAT).

*Time-of-flight (TOF) mass spectrometry*

MALDI of large molecules is usually coupled to a time-of-flight (TOF) mass analysis, although several applications have been performed on fourier-transform ion cyclotron resonance (FT-ICR) [69,70], magnetic sector [71,72] and ion trap mass analyzers [73-77]. In TOF analyzers (Figure 2a), the mass-to-charge ( $m/z$ ) of an ion is determined by measuring its flight time. The analyte ions together with the matrix ions, form a dense plume just above the sample probe, which is held at high potential. These gas-phase ions are accelerated through a grid held at ground potential, into a field-free drift region. Because all ions are accelerated by a fixed potential difference, they will have the same kinetic energy:  $1/2 (m/z)v^2 = E$ , where  $E$  is the energy imparted on the charged ions as a results of the voltage that is applied by the instrument and  $v$  is the velocity of the ions in the field-free region. The velocity of the ion will then be proportional to  $(m/z)^{-1/2}$  where  $m/z_i$  is the mass-to-charge ratio of a particular ion species. As the ions travel through the length ( $D$ ) of a field-free region, they separate into a series of spatially discrete individual ion packets, each travelling with a velocity characteristic of its  $m/z$  ratio. A detector positioned at the end of the field-free flight-tube produces a signal as each ion species that strikes it. The difference between the start time, set by the occurrence of the laser pulse and common to all ions, and the arrival time of an individual ion at the detector is proportional to  $(m/z)^{1/2}$

$$(1) \quad t = \left(\frac{m}{2zE}\right)^{1/2} D$$

and can be used to calculate the ions  $m/z$  ratio

$$(2) \quad \frac{m}{z} = 2E \left(\frac{t}{D}\right)^2$$

One problem in TOF mass analysis results from the initial kinetic energy distribution of the ions prior to acceleration, due to the desorption/ionization process. This initial energy spread results in slight differences in times of flight which leads to peak broadening at the detector and thus a limited mass resolution ( $m/\delta m$ ). The peak broadening can be reduced by using a reflectron (ion mirror) TOF analyzer (Figure 2b). The reflectron compensates for the difference in flight times of ions with the same  $m/z$  but slightly different kinetic energies by means of retarding them in an electrical deceleration field and reversing their flight direction. Ions with excess kinetic energy (and slightly faster velocities) penetrate the retarding field more deeply than those with less kinetic energy. Hence, the more energetic ions will be slightly delayed relative to

the less energetic ions and if the retarding field of the reflectron is adjusted properly the arrival time spread will be largely corrected for at the detector, increasing the mass resolution. For reflectron TOF mass analyzers in the combination of MALDI ion sources, mass resolution of up to 6000 at full width half maximum (FWHM) have been obtained for peptides up to about 3000 Da [78], whereas the mass resolution with linear TOF analyzer is limited to about 700 [27].

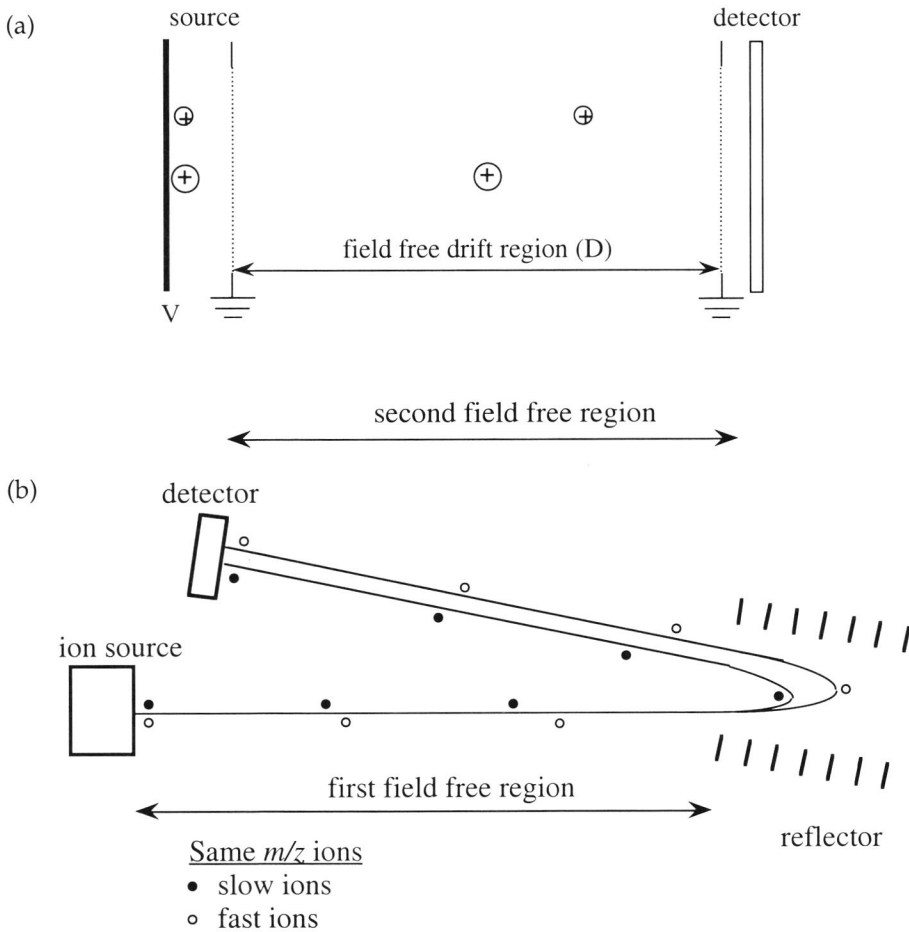


**Figure 2.** Schematic drawing of the basic components and principles of time-of-flight mass spectrometer. In linear mode (a) the ions are separated according to their mass dependent velocities. The reflectron (b) compensates for the differences in flight times of ions with the same  $m/z$  but different initial velocity distributions.

### *Ion detection and data collection*

To detect ions from MALDI, secondary electron multipliers (SEM) are used. The high mass ions produce either electrons or low-mass ions at the conversion dynode of the multiplier. These particles are then used to start the multiplication cascade in an electron multiplier. The surfaces used for the conversion are either copper-beryllium or the lead glass inner surface of a microchannelplate. The yield of secondary electrons and ions from the conversion dynode is a function of the velocity of the ions to be detected. MALDI instruments using low ion acceleration energy need post acceleration of high mass ions in order to compensate for the lower detection efficiency at lower ion velocities. This is achieved by a separated dynode, held at a potential of typically 20 kV, placed in front of the multiplier.

The detector signal is either amplified with a fast linear amplifier or directly digitized by a digital oscilloscope (transient recorder). The data are then transferred to a PC for spectrum averaging, mass calibration and storage. Typically 10-50 spectra, each from a single laser shot are summed to improve the signal-to-noise ratio and allow mass determination.

### *Calibration*

The time-of-flight data are converted into appropriate  $m/z$  values for ions using the elementary equation:

$$(3) \quad t = a(m/z)^{1/2} + b$$

where the constant  $a$  can be calculated from the geometry of the ion source and mass analyzer, and  $b$  is the total time offset introduced by the registration system. However, in practice, more accurate results are achieved by selecting two peaks of known  $m/z$  and calculating the constants  $a$  and  $b$  from their measured time-of-flight in the spectrum. This is usually carried out with well defined reference compounds either internally by adding them to the analyte-matrix mixture or externally by measuring their masses from a separate sample spot.

## **1.7 Performance specifications**

The technique of MALDI mass spectrometry has now emerged as a highly sensitive and accurate method for determining the molecular mass of large nonvolatile biomolecules, particularly with respect to its applications in protein chemistry.

### *Sensitivity*

The outstanding sensitivity achieved under standard sample preparation conditions is a strength of the MALDI technique. The amount of sample used is typically in the low picomole to high femtomole range. Since the amount of material consumed for the analysis is much less than the total amount loaded onto the sample support, significant improvement in the absolute detection limits has been demonstrated by decreasing the analyte-matrix volume [Chapter 2]. Enhanced sensitivity has also been achieved utilizing microcrystalline matrix surfaces prepared by fast evaporation of a matrix solution prior to application of the analyte solution [40]. Though 5-10 attomoles of peptide/protein have shown to be sufficient, using the above sample handling/preparation methods, it is not straightforward to use these extremes of sensitivity for routine analysis.

### *Mass range*

The accessible mass range for MALDI using time-of-flight instrument has extended to more than 1 MDa. The largest functional protein entity published so far is the monomer ion signal of human immunoglobulin M at 982,000 Da [79].

### *Mass accuracy*

The mass accuracy depends on instrumentation characteristics, as well as the sample preparation [80]. A mass accuracy of 0.01 % (100 ppm) for proteins up to 30,000 Da has been demonstrated using internal calibration [81]. In practice, for peptides < 3000 Da the mass accuracy is limited to typically 300-700 ppm for linear TOF and 100-300 ppm for reflectron TOF, with internal calibration. Considerable improvement has been achieved with the incorporation of delayed extraction to MALDI-TOF [see section 1.9]. Using internal calibration, mass accuracy better than 50 ppm is obtained routinely for peptides < 4000 Da [82-84].

## **1.8 Post-source decay**

MALDI has historically been considered a "soft" ionization technique that produces almost exclusively intact analyte ion species. Prompt fragmentation is generally not observed or restricted to loss of small molecules such as water and CO<sub>2</sub>, hence standard MALDI-MS lacks the ability for structure analysis. This deficiency was overcome when Spengler and Kaufmann [85-87], demonstrated that desorbed analyte ions undergo extensive fragmentation during their flight and that the resulting fragment ions can be analyzed and detected in a reflectron instrument by lowering the potential applied to the reflectron. This technique is referred to as post-source decay (PSD) (review, see [88]) and its principle is illustrated in Figure 3.

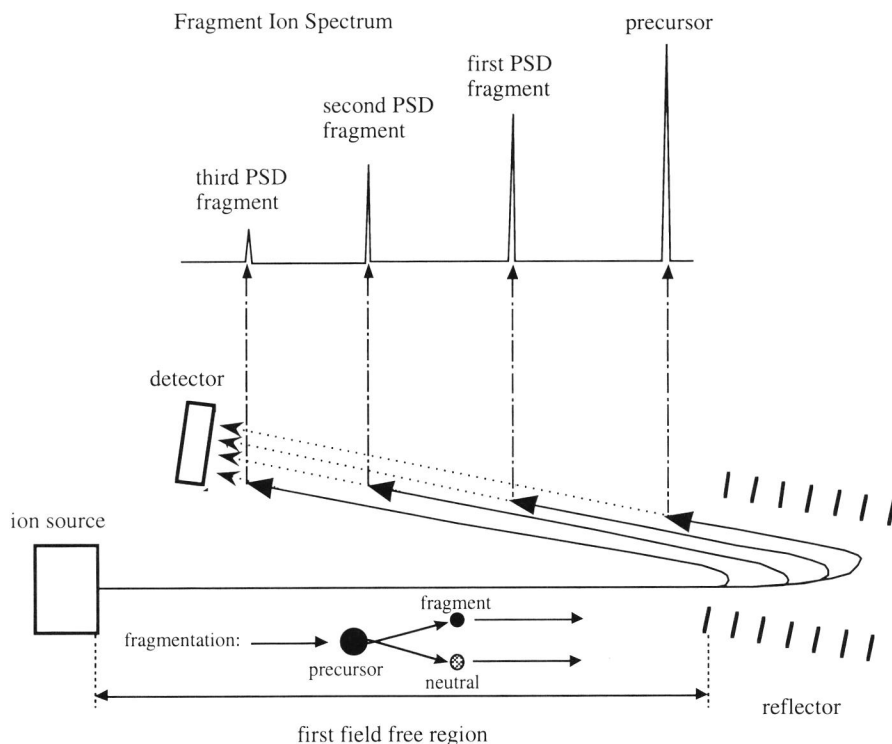


**Figure 3.** Principle of post-source decay analysis. Consecutive lowering of the reflectron potential allows for PSD ions to be imaged as well resolved ion signals in front of the signal of the stable precursor ion signal.

In the PSD process, the laser desorbed ions undergo unimolecular decomposition [87,89] in the first-field-free region before the reflectron. The resulting fragment ions retain basically the same velocity as their precursor ion and hence will enter the reflectron at the same time. However, because these fragment ions have lower kinetic energies (related to their  $m/z$  value), they do not penetrate the retarding field of the reflectron as deeply as their precursor ions, thus they will leave the reflectron and arrive at the detector earlier than their respective precursors. The reflectrons, however can only transmit a limited range of kinetic energies, i.e. those fragment ions which have sufficient kinetic energy to penetrate the retarding field. Therefore, in order to acquire a complete mass spectrum of fragment ions, it is necessary to stepwise reduce the reflectron voltage so as to bring lower energy ions into the retarding field.

The major application of the MALDI-PSD technique has so far been peptide sequencing. The ions observed in PSD analysis of peptide favours backbone cleavages producing predominately a, b and y type of fragment ions (Figure 4). Identification of these ions provide valuable sequence information of unknowns [88,90,91], confirmation of putative identities [92,93] and localization and mass characterization of conjugated modifications [92,94-99]. The routine performance of sequence analysis by PSD is limited to peptides smaller than 3000 Da. Beside peptide sequencing, PSD analysis of other biomolecules such as oligosaccharides [100-105] and oligonucleotides [106,107] is possible. In addition, distinct ions in a mixture (e.g. in a enzymatic digest of a protein) can be selected without separation by means of a precursor ion selector [96-98,108, Chapter 8]. The interpretation of the fragment pattern for unknown peptides can be relatively complex. However, by gaining a partial sequence of only a few amino acids (a sequence tag) the identifications of peptide/proteins can be received by database search [109,110, Chapter 8].

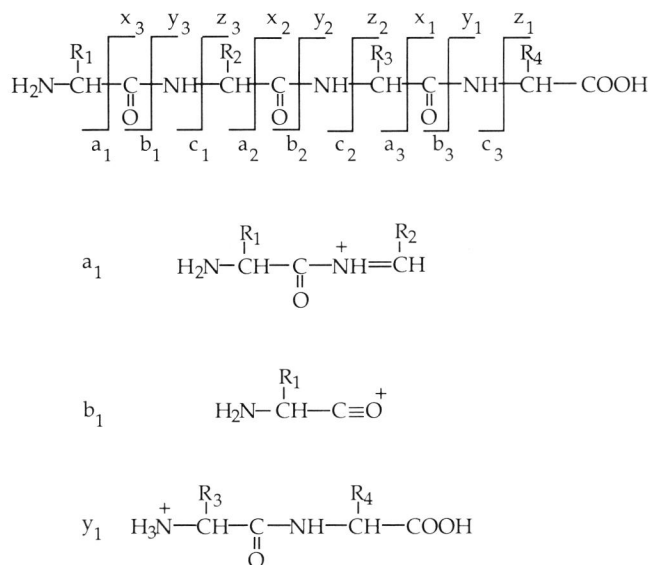


**Figure 4.** Illustration of fragment ions formed through bond cleavages along the backbone of protonated linear peptides (a) and proposed structures of a-, b- and y-type of ions common in a typical PSD spectrum (b).

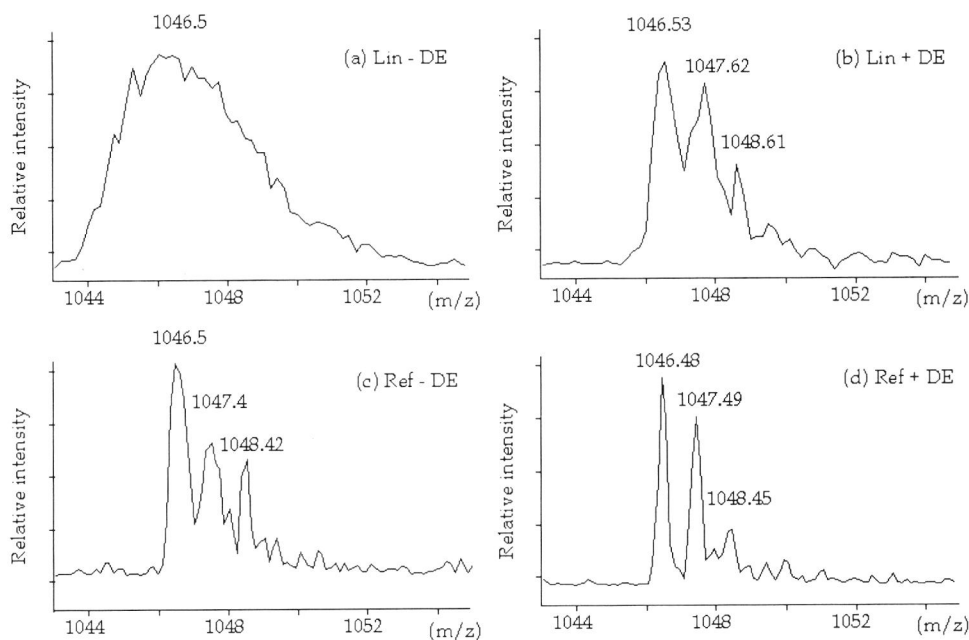


**Figure 5.** MALDI mass spectra of Angiotensin II, comparing mass resolution in linear mode (a and b) and reflectron mode (c and d) utilizing continuous ion extraction (a and c) and delayed ion extraction (b and d). Matrix: DHB. (courtesy M. Karas).

### 1.9 Delayed extraction

MALDI MS performance has improved considerably over the last few years. One of the most exciting developments arises from the implementation of the recently introduced method of delayed extraction [82,111-113]. The technique is not new; Wiley and McLaren [114] already described time-lag energy focusing to correct for initial velocity distribution in 1955. The most striking feature of delayed extraction (DE) MALDI-TOF is the dramatic increase in mass resolution in both linear [82,111-113] and reflectron [113] mode analysis compared to instruments without DE (Figure 5).

With delayed extraction, ions are generated with the extraction field switched off, i.e. no electric field, and first extracted after a short (100 to 500 ns) time delay. Within the delay time, the initial velocity difference of MALDI generated ions allow any ion (same  $m/z$ ) with higher initial velocities to travel further toward the second grid of the two stage acceleration ion source than those with lower initial velocities. When the extraction field is pulsed on, an electrostatic field gradient is established between the two source plates. The slower moving ions will experience a larger electrostatic extraction field than the faster moving ions. This results in the slower moving ions achieving a slightly higher final velocity upon exiting the ion source than those ions which were initially moving faster. By appropriate choice of delay time and pulse voltage amplitude, slower ions can be made to catch up to faster ions at the plane of the detector.

To date the potential of DE has been demonstrated mainly for peptides and proteins, with mass resolution in excess of 10 000 (FWHM) for analytes in the 1000-6000 Da mass range [82,84,113] and above 1000 for larger proteins up to the 30 kDa range. [82,112,115,116]. Other classes such as glycoproteins [98], oligonucleotide [117,118] and polymers [119-121] which are more difficult to analyze by conventional MALDI-TOF has also benefited from DE.

## 1.10 Applications

Different classes of compounds have enjoyed varying degrees of success with the MALDI technique. Clearly one of the most successful applications has been the analysis of proteins which have been reviewed over the years (recently reviewed in [122,123]).

### *Proteins*

MALDI-MS can be used for characterization and identification of proteins, by mass determination of the protein, peptide mapping and sequencing by PSD. Molecular mass of high accuracy can be utilized as verification of structural identity and to establish possible modifications and molecular heterogeneity of the protein. Direct MALDI mass analysis of peptide mixtures generated by chemical or enzymatic digestion of proteins (peptide mapping) has become a well-established and rapid method for protein identification [124,125]. The relative tolerance to many buffer systems and high sensitivity of MALDI-MS means that only small quantities of material are required and time consuming purification steps can be avoided. MALDI-MS peptide mapping is used to confirm the sequence of recombinant proteins [126,127] and to locate chemical and posttranslational modification sites to specific proteolytic fragments within proteins

of known sequences. Comparison of the measured mass with the expected mass yields information on the nature of modification e.g., phosphorylation, acetylation and glycosylation [see Chapter 5 and 6]. Finally, MALDI-PSD mass spectrometry has shown to be valuable not only for peptide sequencing but also for the parallel localization and mass characterizations of modifications [92,94,96,98,128].

#### *Peptide profiling*

A great strength of the MALDI technique over other ionization methods is its ability to analyze mixtures directly. This includes analysis of peptide/protein mixtures from biological sources, such as whole tissue and body fluid. Among the most elegant achievements is the successful analysis of neuropeptides directly out of single neurons from the fresh water snail *Lymnaea stagnalis* [129,130]. The method includes dissecting out individual, peptide containing neurons from the brain of *Lymnaea stagnalis*, placing and rupturing a single neuron in a DHB matrix solution and obtaining high quality mass spectra of the peptides present in individual cells. Although the peptides were in physiological environment, neither sample pretreatment nor separation steps were necessary. This example demonstrates how extraordinarily sensitive MALDI can be for peptides even in complex mixtures.

The *Lymnaea stagnalis* study revealed the presence of known processing products, as well as peptides which could not be directly identified from their mass alone. In a present study, pars intermedia of the pituitary of *Xenopus laevis* were used to show the feasibility of obtaining sequence information of neuropeptides directly from tissue samples using MALDI MS combined with PSD fragment ion mass analysis. MALDI-PSD combined with database searching is shown to be a promising method for rapid structural characterization of specific neuropeptides directly from tissue samples [Chapter 8]. Model cases like this provide for the fascinating possibility that expression and processing of gene products can be monitored by MALDI-MS on a cellular level.

#### *In combination with gel electrophoresis*

For more than twenty years, two-dimensional polyacrylamide gel electrophoresis (PAGE) [131] has been used to simultaneously separate and visualize by suitable staining thousands of proteins present in complex mixtures, e.g. cell lysates. This powerful methodology allows the creation of a protein map for individual cell lines based on molecular mass and pI characteristics. The identification of the proteins corresponding to each stained spot has been greatly improved with the introduction of MALDI-MS. Accurate mass determination of gel separated proteins has been performed either directly from gels [132-134] electroblotted membranes [135-137], or gel extracted samples

[138,139]. Further information can be obtained by either in gel [140-143] or on membrane [136,144] digestion, followed by solvent extraction and subsequent MALDI analysis of the derived peptides. This approach has the advantage of combining the separation power of gel electrophoresis with the mass measurement accuracy of MALDI mass spectrometry [reviewed in [145,146].

#### *In combination with databases*

The availability of several large databases of known protein sequences represent a substantial resource to the protein biochemist. Proteins can be identified by comparing experimental peptide mass maps with the profiles predicted for each entry in a protein database [140,147,148]. This method has found significant applications in the rapid identifications of peptide mixtures obtained from gel separated proteins [149]. Recently Mann and co-workers [109,110] described the "sequence tag" search approach that uses the mass of the peptide in combination with partial sequence information contained in e.g. a MALDI-PSD mass spectrum to search protein and nucleotide databases. This approach can be used in addition to the peptide mass, and as such provides a significant amount of additional information. The "sequence tag" approach combined with MALDI-PSD is shown to be a very powerful method for structural characterization of specific neuropeptides directly from tissue samples [Chapter 8].

#### *Oligonucleotides*

The analysis of oligonucleotides by MALDI has enjoyed a reasonable degree of success (review see [150,151]) especially with the development of new matrices. Several groups have further demonstrated that MALDI may be useful in DNA sequencing [152]. The largest DNA species detected with UV laser is a 500 base double stranded DNA molecule amplified with polymerase chain reaction (PCR) from the bacteriophage lambda genome [153]. Whereas, IR MALDI mass spectra of oligonucleotides up to more than 2000 bases have recently been reported [154].

#### *Synthetic polymers*

Initial attempt to extend the experimental approach to the characterization of synthetic polymers gave promising results on narrow molecular mass dispersion homopolymer standards (see e.g. [29,155,156]). However, currently the MALDI technique cannot be applied to all classes of polymers due to very practical consideration such as lack of suitable matrix, cationizing reagent and/or solvent system for sample preparation [157-159].

*Quantitative aspects*

Another useful development has been the application of MALDI-MS for quantitative analysis of biological compounds [160-163] and drugs [164-166], where the use of internal standards has been observed to realise a good linear response between the peak height ratios of the analyte/internal standard ion signals and the applied amounts of analyte [Chapter 3].

*Non covalent complexes*

Non-covalent bound complexes almost always dissociate into individual components during the MALDI analysis. Accordingly, there are only a few examples where specific oligomeric complexes have been observed by this technique (most recently [167-169, Chapter 4]). The ability to detect non-covalent complex ions in MALDI-MS appears to be independent of the pH stability range of the sample but highly dependent on the choice of matrix [168, Chapter 4]. In addition, the hydrophobic forces holding the subunit together are sufficiently strong to prevent dissociation of certain protein complexes but not of others under the same conditions [Chapter 4]. At the current state no guidelines for sample preparation and choice of matrix have been proposed, further understanding of the desorption and the mechanism of ion formation is required.

## 1.11 Scope of this thesis

The basic principles, fundamental and instrumental aspects of MALDI time-of-flight mass spectrometry are outlined in this introductory chapter. Quantitative aspects of MALDI-MS are discussed in the following two chapters. In Chapter 2, the absolute detection limit of MALDI-MS is studied via minimalization of the size of the sample spot. In Chapter 3, the ability of MALDI-MS in quantitative analysis of both low and high molecular mass analytes is investigated, with the use of internal standards. Chapter 4 evaluates the potential of MALDI-MS for the mass measurement of specific non-covalent complexes of biomolecules. While it was initially thought that the pH of the matrix solution would be of utmost importance in such studies, the results indicate that the situation is more complicated.

The remaining four chapters are devoted to various aspects and methods for structure elucidation and characterization of peptides and proteins. MALDI-MS enables detection of individual components directly from complex mixtures. In this way labour-intensive and time-consuming sample purification and separation steps can be avoided. MALDI-MS is therefore, ideally suited for the characterization of peptide mixtures, e.g. peptide mapping. In Chapter 5 and 6 peptide mapping by MALDI-MS is applied to confirm the sequence of proteins and to localize and identify chemical and posttranslational modifications of proteins.

Direct peptide profiling such as characterization of neuropeptides directly from intact biological cells and tissue samples dissected from animal brains can be achieved by MALDI-MS. This is demonstrated in Chapter 7 where, peptide profiling of melanotrope cells from the South African toad, *Xenopus laevis*, allows the identification of POMC derived peptides. More advanced technology in MALDI time-of-flight MS, e.g. post-source decay and delayed extraction, have enhanced the ability of MALDI-MS in structural characterization of peptides. Post source decay sequencing of peptides directly from tissue samples combined with database searching is shown to be a promising method for rapid confirmation and structural characterization of specific neuropeptides [Chapter 8]. Improvements in both mass resolution and mass accuracy via delayed extraction further facilitates the quality and interpretation of the data, as demonstrated in Chapter 8.

References

- [1] M. Barber, R. S. Bordoli, G. Elliot, R. D. Sedgwick and A. N. Tyler, *Anal. Chem.*, **1982**, 54, 645A-657A.
- [2] R. D. Macfarlane and D. F. Torgerson, *Science*, **1976**, 191, 920-925.
- [3] J. B. Fenn, M. Mann, C. K. Meng, S. F. Wong and C. M. Whitehouse, *Mass Spectrom. Rev.*, **1990**, 9, 37-70.
- [4] F. Hillenkamp and H. Ehring, in M. L. Gross (Eds), *Mass Spectrometry in the Biological Sciences*, Dordrecht, The Netherlands, Kluwer Academic, **1992**, 165-179.
- [5] R. E. Honig and J. R. Woolston, *Appl. Phys. Lett.*, **1963**, 2, 138-139.
- [6] F. J. Vastola, R. O. Mumma and A. J. Pirone, *Org. Mass Spectrom.*, **1970**, 3, 101-104.
- [7] M. A. Posthumus, P. G. Kistemaker, H. L. C. Meuzelaar and M. C. T. N. de Brauw, *Anal. Chem.*, **1978**, 50, 985-991.
- [8] R. Stoll and F. W. Röllgen, *Org. Mass Spectrom.*, **1979**, 14, 642-645.
- [9] E. D. Hardin and M. L. Vestal, *Anal. Chem.*, **1981**, 53, 1492-1497.
- [10] C. F. Ijames and C. L. Wilkins, *J. Am. Chem. Soc.*, **1988**, 110, 2687.
- [11] S. F. Wong, C. K. Meng and J. B. Fenn, *J. Phys. Chem.*, **1988**, 92, 546.
- [12] D. E. Mattern and D. M. Hercules, *Anal. Chem.*, **1985**, 57, 2041-2046.
- [13] R. J. Cotter, J. P. Honovich and J. K. Olthoff, *Macromolecules*, **1986**, 19, 2996-3001.
- [14] M. Karas, D. Bachmann, U. Bahr and F. Hillenkamp, *Int. J. Mass Spectrom. Ion Processes*, **1987**, 78, 53-68.
- [15] F. Hillenkamp, M. Karas, R. C. Beavis and B. T. Chait, *Anal. Chem.*, **1991**, 63, 1193-1203.
- [16] K. Tanaka, H. Waki, Y. Ido, S. Akita, Y. Yoshida and T. Yoshida, *Rapid Commun. Mass Spectrom.*, **1988**, 2, 151-153.
- [17] M. Karas and F. Hillenkamp, *Anal. Chem.*, **1988**, 60, 2299-2301.
- [18] M. Karas, D. Bachmann and F. Hillenkamp, *Anal. Chem.*, **1985**, 57, 2935-2939.
- [19] R. C. Beavis and B. T. Chait, *Rapid Commun. Mass Spectrom.*, **1989**, 3, 233-237.
- [20] M. C. Fitzgerald, G. R. Parr and L. M. Smith, *Anal. Chem.*, **1993**, 65, 3204-3211.
- [21] J. Krause, M. Stoeckli and U. P. Schlunegger, *Rapid Commun. Mass Spectrom.*, **1996**, 10, 1927-1933.
- [22] H. Nonami, S. Fukui and R. Erra-Balsells, *J. Mass Spectrom.*, **1997**, 32, 287-296.
- [23] R. C. Beavis and B. T. Chait, *Rapid Commun. Mass Spectrom.*, **1989**, 12, 432-435.
- [24] K. Strupat, M. Karas and F. Hillenkamp, *Int. J. Mass Spectrom. Ion Processes*, **1991**, 111, 89-102.
- [25] J. Kampmeier, K. Dreisewerd, M. Schurenberg and K. Strupat, *Int. J. Mass Spectrom. Ion Processes*, **1997**, 169, 31-41.
- [26] K. Strupat, J. Kampmeier and V. Horneffer, *Int. J. Mass Spectrom. Ion Processes*, **1997**, 169, 43-50.
- [27] M. Karas, U. Bahr and U. Giessman, *Mass Spectrom. Rev.*, **1991**, 10, 335-357.
- [28] B. Stahl, M. Steup, M. Karas and F. Hillenkamp, *Anal. Chem.*, **1991**, 63, 1463-1466.
- [29] U. Bahr, A. Deppe, M. Karas, F. Hillenkamp and U. Giessmann, *Anal. Chem.*, **1992**, 64, 2866-2869.

- [30] P. Juhasz, I. A. Papayannopoulos, C. Zeng and K. Biemann, (Eds), *Proceedings of the 40th Annual Conference on Mass Spectrometry and Allied Topics*, Santa Fe, **1992**, 1913-1914 .
- [31] R. C. Beavis, T. Chaudhary and B. T. Chait, *Org. Mass Spectrom.*, **1992**, *27*, 156-158.
- [32] M. Karas, U. Bahr, K. Strupat, F. Hillenkamp, A. Tsarbopoulos and B. N. Pramanik, *Anal. Chem.*, **1995**, *67*, 675-679.
- [33] K. J. Wu, A. Steding and C. H. Becker, *Rapid Commun. Mass Spectrom.*, **1992**, *7*, 142-146.
- [34] M. Karas, H. Ehring, E. Nordhoff, B. Stahl, K. Strupat, F. Hillenkamp, M. Grehl and B. Krebs, *Org. Mass Spectrom.*, **1993**, *28*, 1476-1481.
- [35] F. Xiang and R. C. Beavis, *Rapid Commun. Mass Spectrom.*, **1994**, *8*, 199-204.
- [36] S. J. Doktycz, P. J. Savickas and D. A. Krueger, *Rapid Commun. Mass Spectrom.*, **1991**, *5*, 145-148.
- [37] T.-W. D. Chan, A. W. Colburn, P. J. Derrick, D. J. Gardiner and M. Bowden, *Org. Mass Spectrom.*, **1992**, *27*, 188-194.
- [38] M. Kussmann, E. Nordhoff, H. Rahbek-Nielsen, S. Haebel, M. Rossel-Larsen, L. Jakobsen, J. Gobom, E. Mirgorodskaya, A. Kroll-Kristensen, L. Palm and P. Roepstorff, *J. Mass Spectrom.*, **1997**, *32*, 593-601.
- [39] F. Xiang and R. C. Beavis, *Rapid Commun. Mass Spectrom.*, **1993**, *28*, 1424-1429.
- [40] O. Vorm, P. Roepstorff and M. Mann, *Anal. Chem.*, **1994**, *66*, 3281-3287.
- [41] K. K. Mock, C. W. Sutton and J. S. Cottrell, *Rapid Commun. Mass Spectrom.*, **1992**, *6*, 233-238.
- [42] E. J. Zaluzec, D. A. Gage, J. Allison and J. T. Watson, *J. Am. Soc. Mass Spectrom.*, **1994**, *5*, 230-237.
- [43] J. A. Blackledge and A. J. Alexander, *Anal. Chem.*, **1995**, *67*, 843-848.
- [44] M. E. McComb, R. D. Oleschuk, D. M. Manley, L. Donald, A. Chow, J. D. J. O'Neil, W. Ens, K. G. Standing and H. Perreault, *Rapid Commun. Mass Spectrom.*, **1997**, *11*, 1716-1722.
- [45] A. H. Brockman, B. S. Dodd and N. Orlando, *Anal. Chem.*, **1997**, *69*, 4716-4720.
- [46] F. Hillenkamp, M. Karas, A. Ingendoh and B. Stahl, in A. L. Burlingame and J. A. McCloskey (Eds), *Biological Mass Spectrometry*, Amsterdam, Elsevier Science Publishers B. V., **1990**, 49-60.
- [47] H. Ehring, M. Karas and F. Hillenkamp, *Org. Mass Spectrom.*, **1992**, *27*, 472-480.
- [48] R. D. Burton, C. H. Watson, J. R. Eyler, G. L. Lang, D. H. Powell and M. Y. Avery, *Rapid Commun. Mass Spectrom.*, **1997**, *11*, 443-446.
- [49] D. A. Allwood, R. W. Dreyfus, I. K. Perera and P. E. Dyer, *Applied Surface Sciences*, **1997**, *110*, 154-157.
- [50] J. Zhou, W. Ens, K. G. Standing and A. Verentchikov, *Rapid Commun. Mass Spectrom.*, **1992**, *6*, 671-678.
- [51] V. Bökelmann, B. Spengler and R. Kaufmann, *Eur. J. Mass Spectrom.*, **1995**, *1*, 81-93.
- [52] W. Z. Zhang and B.T.Chait, *Int. J. Mass Spectrom. Ion Processes*, **1997**, *160*, 259-267.
- [53] K. Dreisewerd, M. Schürenberg, M. Karas and F. Hillenkamp, *Int. J. Mass Spectrom. Ion Processes*, **1996**, *154*, 171-178.

- [54] M. E. Gimon, L. M. Preston, T. Solouki, M. A. White and D. H. Russell, *Org. Mass Spectrom.*, **1992**, 27, 827-830.
- [55] R. J. J. M. Steenvoorden, K. Breuker and R. Zenobi, *Eur. J. Mass Spectrom.*, **1997**, 3, 339-346.
- [56] T. W. D. Chan, A. W. Colburn and P. J. Derrick, *Org. Mass Spectrom.*, **1991**, 26, 342-344.
- [57] R. Knochenmuss, F. Dubois, M. J. Dale and R. Zenobi, *Rapid Commun. Mass Spectrom.*, **1996**, 10, 871-877.
- [58] A. Vertes, R. Gijbels and R. D. Levine, *Rapid Commun. Mass Spectrom.*, **1990**, 4, 228-233.
- [59] B. H. Wang, K. Dreisewerd, U. Bahr, M. Karas and F. Hillenkamp, *J. Am. Soc. Mass Spectrom.*, **1993**, 4, 393-398.
- [60] P.-C. Liao and J. Allison, *J. Mass Spectrom.*, **1995**, 30, 408-423.
- [61] H. Ehring, C. Costa, P. A. Demirev and B. U. R. Sundqvist, *Rapid Commun. Mass Spectrom.*, **1996**, 10, 821-824.
- [62] G. Grigorean, R. I. Carey and I. J. Amster, *Eur. J. Mass Spectrom.*, **1996**, 2, 139-143.
- [63] M. Gimon-Kinsel, L. M. Preston-Schaffter, G. R. Kinsel and D. H. Russell, *J. Am. Chem. Soc.*, **1997**, 119, 2534-2540.
- [64] P. Juhasz, B. H. Wang and K. Biemann, (Eds), *Proceedings of the 40th Annual Conference on Mass Spectrometry and Allied Topics*, Santa Fe, **1992**, 372-373.
- [65] J. Bai, Y.-H. Liu, T. C. Cain and D. M. Lubman, *Anal. Chem.*, **1994**, 66, 3423-3430.
- [66] B. Spengler, M. Karas, U. Bahr and F. Hillenkamp, *J. Phys. Chem.*, **1987**, 91, 6502-6506.
- [67] S. Berkenkamp, C. Menzel, M. Karas and F. Hillenkamp, *Rapid Commun. Mass Spectrom.*, **1997**, 11, 1399-1406.
- [68] S. Niu, W. Zhang and B. T. Chait, *J. Am. Soc. Mass Spectrom.*, **1998**, 9, 1-7.
- [69] J. A. Castoro and C. L. Wilkins, *Anal. Chem.*, **1993**, 65, 2621-2627.
- [70] M. V. Buchanan and R. L. Hettich, *Anal. Chem.*, **1993**, 65, 245A-259A.
- [71] J. A. Hill, R. S. Annan and K. Biemann, *Rapid Commun. Mass Spectrom.*, **1991**, 5, 395-399.
- [72] V. S. K. Kolli and R. Orlando, *Anal. Chem.*, **1997**, 69, 327-332.
- [73] V. M. Doroshenko, T. J. Cornish and R. J. Cotter, *Rapid Commun. Mass Spectrom.*, **1992**, 6, 753-757.
- [74] D. M. Chambers, D. E. Goeringer, S. A. McLuckey and G. L. Glish, *Anal. Chem.*, **1993**, 65, 14-20.
- [75] K. Jonscher, G. Currie, A. L. McCormack and J. R. Yates III, *Rapid Commun. Mass Spectrom.*, **1993**, 7, 20-26.
- [76] J. C. Schwartz and M. E. Bier, *Rapid Commun. Mass Spectrom.*, **1993**, 7, 27-32.
- [77] J. Qin and B. T. Chait, *Anal. Chem.*, **1997**, 69, 4002-4009.
- [78] A. Ingendoh, M. Karas, F. Hillenkamp and U. Giessmann, *Int. J. Mass Spectrom. Ion Processes*, **1994**, 131, 345-354.
- [79] R. W. Nelson, D. Dogruel and P. Williams, *Rapid Commun. Mass Spectrom.*, **1995**, 9, 625.
- [80] O. Vorm and M. Mann, *J. Am. Soc. Mass Spectrom.*, **1994**, 5, 955-958.

- [81] R. C. Beavis and B. T. Chait, *Anal. Chem.*, **1990**, 62, 1836-1840.
- [82] R. M. Whittal and L. Li, *Anal. Chem.*, **1995**, 67, 1950-1954.
- [83] O. N. Jensen, A. Podtelejnikov and M. Mann, *Rapid Commun. Mass Spectrom.*, **1996**, 10, 1371-1378.
- [84] R. D. Edmondson and D. H. Russell, *J. Am. Soc. Mass Spectrom.*, **1996**, 7, 995-1001.
- [85] B. Spengler, D. Kirsch and R. Kaufmann, *Rapid Commun. Mass Spectrom.*, **1991**, 5, 198-202.
- [86] B. Spengler, D. Kirsch, R. Kaufmann and E. Jaeger, *Rapid Commun. Mass Spectrom.*, **1992**, 6, 105-108.
- [87] B. Spengler, D. Kirsch and R. Kaufmann, *J. Phys. Chem.*, **1992**, 96, 9678-9684.
- [88] B. Spengler, *J. Mass Spectrom.*, **1997**, 32, 1019-1036.
- [89] R. Kaufmann, B. Spengler and F. Lützenkirchen, *Rapid Commun. Mass Spectrom.*, **1993**, 7, 902-910.
- [90] H. Schluter, D. Mentrup, I. Gross, H. E. Meyer, B. Spengler, R. Kaufmann and W. Zidek, *Anal. Biochem.*, **1997**, 246, 15-19.
- [91] M. Moormann, U. Zähringer, H. Moll, R. Kaufmann, R. Schmid and K. Altendorf, *J. Biol. Chem.*, **1997**, 272, 10729-10738.
- [92] R. Kaufmann, D. Kirsch, J. L. Tourmann, J. Machold, F. Hucho, Y. Utkin and V. Tsetlin, *Eur. J. Mass Spectrom.*, **1995**, 1, 313-325.
- [93] K. Ambihapathy, T. Yalcin, H.-W. Leung and A. G. Harrison, *J. Mass Spectrom.*, **1997**, 32, 209-215.
- [94] G. Talbo and M. Mann, J. W. Crabb (Eds), *Techniques in Protein Chemistry V*, San Diego, CA, Academic Press, Inc. **1994**, 105-113
- [95] J. Machold, Y. Utkin, D. Kirsch, R. Kaufmann, V. Tsetlin and F. Hucho, *Proc. Natl. Acad. Sci. USA*, **1995**, 92, 7282-7286.
- [96] S. Goletz, M. Leuck, P. Franke and U. Karsten, *Rapid Commun. Mass Spectrom.*, **1997**, 11, 1387-1398.
- [97] N. X. Xu, Z. H. Huang, B. L. M. d. Jonge and D. A. Gage, *Anal. Biochem.*, **1997**, 248, 7-14.
- [98] A. Tsarbopoulos, U. Bahr, B. N. Pramanik and M. Karas, *Int. J. Mass Spectrom. Ion Processes*, **1997**, 169, 251-261.
- [99] J. Vinh, D. Loyaux, V. Redeker and J. Rossier, *Anal. Chem.*, **1997**, 69, 3979-3985.
- [100] B. Spengler, D. Kirsch, R. Kaufmann and J. Lemoine, *J. Mass Spectrom.*, **1995**, 30, 782-787.
- [101] D. J. Harvey, T. J. P. Naven, B. Küster, R. H. Bateman, M. R. Green and G. Critchley, *Rapid Commun. Mass Spectrom.*, **1995**, 9, 1556-1561.
- [102] R. L. Hettich and E. A. Stemmler, *Rapid Commun. Mass Spectrom.*, **1996**, 10, 321-327.
- [103] J. Lemoine, F. Chirat and B. Domon, *J. Mass Spectrom.*, **1996**, 31, 908-912.
- [104] D. Garozzo, V. Nasello, E. Spina and L. Sturiale, *Rapid Commun. Mass Spectrom.*, **1997**, 11, 1561-1566.
- [105] T. Yamagaki, Y. Mitsuishi and H. Nakanishi, *Rapid Commun. Mass Spectrom.*, **1998**, 12, 307-311.
- [106] G. Talbo and M. Mann, *Rapid Commun. Mass Spectrom.*, **1996**, 10, 100-103.
- [107] J. K. Gooden, J. Byun, L. Chen, E. G. Rogan, E. L. Cavalieri and M. L. Gross, *Int. J. Mass Spectrom. Ion Processes*, **1997**, 169, 241-249.

- [108] C. L. Nilsson, C. M. Murphy and R. Ekman, *Rapid Commun. Mass Spectrom.*, **1997**, *11*, 610-612.
- [109] M. Mann and M. Wilm, *Anal. Chem.*, **1994**, *66*, 4390-4399.
- [110] M. Wilm, T. Houthaeye, G. Talbo, R. Kellner, P. Mortensen and M. Mann, A. L. Burlingame & S. A. Carr (Eds), *Mass Spectrometry in the Biological Sciences*, Clifton, NJ, Humana Press. **1996**, 245-265
- [111] S. M. Colby, T. B. King and J. P. Reilly, *Rapid Commun. Mass Spectrom.*, **1994**, *8*, 865-868.
- [112] R. S. Brown and J. J. Lennon, *Anal. Chem.*, **1995**, *67*, 1998-2003.
- [113] M. L. Vestal, P. Juhasz and A. S. Martin, *Rapid Commun. Mass Spectrom.*, **1995**, *9*, 1044-1050.
- [114] W. C. Wiley and I. H. McLaren, *Rev. Sci. Instrum.*, **1955**, *26*, 1150-1157.
- [115] U. Bahr, J. Stahl-Zeng, E. Gleitsmann and M. Karas, *J. Mass Spectrom.*, **1997**, *32*, 1111-1116.
- [116] D. H. Russell and R. D. Edmondson, *J. Mass Spectrom.*, **1997**, *32*, 263-276.
- [117] P. Juhasz, M. T. Roskey, I. P. Smirnov, L. A. Haff, M. L. Vestal and S. A. Martin, *Anal. Chem.*, **1996**, *68*, 941-946.
- [118] M. T. Roskey, P. Juhasz, I. P. Smirnov, E. J. Takach, S. A. Martin and L. A. Haff, *Proc. Natl. Acad. Sci. USA*, **1996**, *93*, 4724-4729.
- [119] R. M. Whittall, D. C. Schriemer and L. Li, *Anal. Chem.*, **1997**, *69*, 2734-2741.
- [120] A. T. Jackson, H. T. Yates, C. I. Lindsay, Y. Didier, J. A. Segal, J. H. Scrivens, G. Critchley and J. Brown, *Rapid Commun. Mass Spectrom.*, **1997**, *11*, 520-526.
- [121] I. A. Mowat, R. J. Donovan and R. R. Maier, *Rapid Commun. Mass Spectrom.*, **1997**, *11*, 89-98.
- [122] M. Mann and G. Talbo, *Curr. Opin. Biotechnol.*, **1996**, *7*, 11-19.
- [123] J. R. Yates III, *J. Mass Spectrom.*, **1998**, *33*, 1-19.
- [124] R. C. Beavis and B. T. Chait, *Proc. Natl. Acad. Sci. USA*, **1990**, *87*, 6873-6877.
- [125] T. M. Billeci and J. T. Stults, *Anal. Chem.*, **1993**, *65*, 1709-1716.
- [126] J. S. Andersen, *Biochemical Society transactions*, **1995**, *23*, 917-923.
- [127] J. S. Andersen, B. Svensson and P. Roepstorff, *Nature Biotechnology*, **1996**, *14*, 449-457.
- [128] P. A. Schindler, C. A. Settineri, X. Collet, C. J. Fielding and A. L. Burlingame, *Protein Sci.*, **1995**, *4*, 791-803.
- [129] P. A. v. Veelen, C. R. Jiménez, K. W. Li, W. C. Wildering, P. M. Geraerts, U. R. Tjaden and J. v. d. Greef, *Org. Mass Spectrom.*, **1993**, *28*, 1542-1546.
- [130] C. R. Jiménez, P. A. v. Veelen, K. W. Li, W. C. Wildering, P. M. Geraerts, U. R. Tjaden and J. v. d. Greef, *J. Neurochem.*, **1994**, *62*, 404-407.
- [131] P. H. O'Farrell, *J. Biol. Chem.*, **1975**, *250*, 4007-4021.
- [132] R. R. O. Loo, T. I. Stevenson, C. Mitchell, J. A. Loo and P. C. Andrews, *Anal. Chem.*, **1996**, *68*, 1910-1817.
- [133] R. R. O. Loo, C. Mitchell, T. I. Stevenson, S. A. Martin, W. M. Hines, P. Juhasz, D. H. Patterson, J. M. Peltier, J. A. Loo and P. C. Andrews, *Electrophoresis*, **1997**, *18*, 382-390.
- [134] J. R. Strahler, Y. Smelyanskiy, G. Lavine and J. Allison, *Int. J. Mass Spectrom. Ion Processes*, **1997**, *169*, 111-126.

- [135] K. Strupat, M. Karas, F. Hillenkamp, C. Eckerskorn and F. Lottspeich, *Anal. Chem.*, **1994**, 66, 464-470.
- [136] M. M. Vestling and C. Fenselau, *Anal. Chem.*, **1994**, 66, 471-477.
- [137] C. Eckerskorn, K. Strupat, D. Schleuder, D. Hochstrasser, J. C. Sanchez, F. Lottspeich and F. Hillenkamp, *Anal. Chem.*, **1997**, 69, 2888-2892.
- [138] S. L. Cohen and B. T. Chait, *Anal. Biochem.*, **1997**, 247, 257-267.
- [139] H. Ehring, S. Strömberg, A. Tjernberg and B. Norén, *Rapid Commun. Mass Spectrom.*, **1997**, 11, 1867-1873.
- [140] W. J. Henzel, T. M. Billeci, J. T. Stults, S. C. Wong and C. Grimley, *Proc. Natl. Acad. Sci. USA*, **1993**, 90, 5011-5015.
- [141] A. Shevchenko, M. Wilm, O. Vorm and M. Mann, *Anal. Chem.*, **1996**, 68, 850-858.
- [142] G. Li, M. Waltham, N. L. Anderson, E. Unsworth, A. Treston and J. N. Weinstein, *Electrophoresis*, **1997**, 18, 391-402.
- [143] K. L. O'Connell and J. T. Stults, *Electrophoresis*, **1997**, 18, 349-359.
- [144] S. D. Patterson, *Electrophoresis*, **1995**, 16, 1104-1114.
- [145] S. D. Patterson and R. Aebersold, *Electrophoresis*, **1995**, 16, 1791-1814.
- [146] P. Jungblut and B. Thiede, *Mass Spectrom. Rev.*, **1997**, 16, 145-162.
- [147] D. J. C. Pappin, P. Højrup and A. J. Bleasby, *Curr. Biol.*, **1993**, 3, 327-332.
- [148] M. Mann, P. Højrup and P. Roepstorff, *Biol. Mass Spectrom.*, **1993**, 22, 338-345.
- [149] O. N. Jensen, A. Podtelejnikov and M. Mann, *Rapid Commun. Mass Spectrom.*, **1996**, 10, 1371-1378.
- [150] E. Nordhoff, F. Kirpekar and P. Roepstorff, *Mass Spectrom. Rev.*, **1996**, 15, 67-138.
- [151] P. A. Limbach, *Mass Spectrom. Rev.*, **1996**, 15, 297-336.
- [152] K. K. Murray, *J. Mass Spectrom.*, **1996**, 31, 1203-1215.
- [153] K. Tang, N. I. Taranenko, S. L. Allman, L. Y. Cháng and C. H. Chen, *Rapid Commun. Mass Spectrom.*, **1994**, 8, 727-730.
- [154] S. Berkenkanp, F. Kirpekar and F. Hillenkamp, *Sci.*, **1998** 281, 260-262.
- [155] P. O. Danis, D. E. Karr, F. Mayer, A. Holle and C. H. Watson, *Org. Mass Spectrom*, **1992**, 27, 843-846.
- [156] P. M. Lloyd, K. G. Suddaby, J. E. Varney, E. Scrivener, P. J. Derrick and D. M. Haddleton, *Eur. J. Mass Spectrom.*, **1995**, 1, 293-300.
- [157] A. M. Belu, J. M. DeSimone, R. W. Linton, G. W. Lange and R. M. Friedman, *J. Am. Soc. Mass Spectrom.*, **1995**, 7, 11-24.
- [158] D. C. Schriemer and L. Li, *Anal. Chem.*, **1997**, 69, 4176-4183.
- [159] D. C. Schriemer and L. Li, *Anal. Chem.*, **1997**, 69, 4169-4175.
- [160] K. Tang, S. L. Allman, R. B. Jones and C. H. Chen, *Anal. Chem.*, **1993**, 65, 2164-2166.
- [161] R. W. Nelson, M. A. McLean and T. W. Hutchens, *Anal. Chem.*, **1994**, 66, 1408-1415.
- [162] B. A. Bruenner, T.-T. Yip and T. W. Hutchens, *Rapid Commun. Mass Spectrom.*, **1996**, 10, 1797-1801.

- [164] W. R. Wilkinson, A. I. Gusev, A. Proctor, M. Houalla and D. M. Hercules, *Fresenius J. Anal. Chem.*, **1997**, 357, 241-248.
- [165] A. J. Nicola, A. I. Gusev and D. M. Hercules, *Applied Spectroscopy*, **1996**, 50, 1479-1482.
- [166] R. R. Hensel, R. C. King and K. G. Owens, *Rapid Commun. Mass Spectrom.*, **1997**, 11, 1785-1793.
- [166] Y. C. Ling, L. N. Lin and Y. T. Chen, *Rapid Commun. Mass Spectrom.*, **1998**, 12, 317-327.
- [167] M. O. Glocker, S. H. J. Bauer, J. Kast, J. Volz and M. Przybylski, *J. Mass Spectrom.*, **1996**, 31, 1221-1227.
- [168] L. R. H. Cohen, K. Strupat and F. Hillenkamp, *J. Am. Soc. Mass Spectrom.*, **1997**, 8, 1046-1052.
- [169] M. Moniatte, C. Lesieur, B. Vécsey-Semjén, J. T. Buckley, F. Pattus, F. G. v. d. Goot and A. V. Dorsselaer, *Int. J. Mass Spectrom. Ion Processes*, **1997**, 169, 179-199.



## **Chapter 2**

---

# Quantitative bioanalysis using matrix-assisted laser desorption/ionization mass spectrometry



---

## Quantitative bioanalysis using matrix-assisted laser desorption/ionization mass spectrometry

*The application of matrix-assisted laser desorption mass spectrometry (MALDI-MS) for quantitative analysis was investigated with the use of internal standards. Three peptides/proteins in the mass range 1000-12000 Da were tested and the effect of various internal standards was evaluated. Horse cytochrome c was used as an internal standard for bovine cytochrome c, melittin for renin and an undecapeptide B analogue was employed as an internal standard for the decapeptide A. Linear response was found between the measured peak height ratio and the applied amount of analyte when an appropriate internal standard was used. The quantitative abilities of MALDI-MS were finally applied to the bioanalysis of the drug amperozide in plasma. The biological samples were prepared for analysis using liquid-liquid extraction prior to MALDI mass spectrometry. A linear calibration curve was obtained using the  $^{13}\text{C}_4$  stable isotopically labelled amperozide as internal standard.*

---

### Introduction

Matrix-assisted laser desorption/ionization mass spectrometry (MALDI-MS) was first described in 1988 by Karas and Hillenkamp [1]. It has become a powerful analytical method for biological mass spectrometry. It is capable of producing ions of proteins up to a molecular mass of a few hundred thousand Da [2,3]. Mass accuracy of 0.1-0.2% can easily be obtained. This can be improved to the level of 0.01% with the use of internal calibrants [4]. In addition to proteins, other classes of macromolecules such as oligosaccharides [5], oligonucleotides [6] and polymers [7] have been shown to be amenable to this technique. The matrix tolerance to buffer and salts make MALDI-MS well suited for direct analysis of complex mixtures such as enzymatic digests [8] without further purification.

While MALDI-MS has proven to be an invaluable qualitative technique for accurate determinations of relative molecular mass, the potential for quantitative analysis still has to be investigated with this technique. Several attractive features make MALDI-MS an interesting technique for quantitative analysis. It is suitable for the analysis of complex mixtures and higher molecular masses. The detection limits, although widely varying for different compounds, permit measurement in the femtomol range.

A number of quantitative methods for different compounds and using different matrices have recently been published [9-13]. For both proteins [9,11], oligosaccharides [10], oligonucleotides [11] and low molecular mass compounds [12] a good linear response

was obtained with the use of internal standards. Preston *et al.* [13] report a linear response without internal standards by the use of nitrocellulose in the sample preparation.

In the present paper, special attention was paid to the choice of the internal standard. The application of MALDI-MS for quantitative analysis was explored for various peptides and proteins in a mass range from 1000 to 12000 Da using an internal standard. Proteins and peptides selected as model analytes/internal standards were bovine cytochrome c/horse cytochrome c, renin/melittin and peptide A, LQTTIHDIIL/peptide B, ELQTTIHDIIL. Furthermore, the possibilities of MALDI-MS for quantitative bioanalysis of the drug amperozide (4-[4',4'-bis(p-fluorophenyl)butyl]-N-ethyl-1-piperazine-carboxamide) in plasma were investigated. In the quantification of amperozide an isotope-labelled amperozide was used as internal standard.

## Experimental

### *Materials*

The 2,5-dihydroxybenzoic acid (DHB) used as matrix was purchased from Aldrich Chemie (Steinheim, Germany). The test proteins, bovine heart cytochrome c (molecular mass 12230.9), horse heart cytochrome c (molecular mass 12360.1), porcine renin substrate (molecular mass 1759.0) and bee venom melittin (molecular mass 2846.5), were all purchased from Sigma Chemical Co. (St. Louis, MO, USA). Peptide A (sequence LQTTIHDIIL, molecular mass 1166.4) and peptide B (sequence ELQTTIHDIIL, molecular mass 1295.5) were kindly provided by Dr. J. W. Drijfhout (Academic Hospital Leiden, The Netherlands), human plasma, amperozide (molecular mass 401.5) and [<sup>13</sup>C<sub>4</sub>]-amperozide (molecular mass 405.5) were kindly provided by Dr. A. Björk and Dr. A.-M. Olsson (Pharmacia Therapeutics, Lund, Sweden).

### *Mass spectrometry*

The experiments were carried out on a VISION 2000 (Finnigan MAT, Bremen, Germany) MALDI mass spectrometer. This is a reflectron time-of-flight (TOF) instrument operating with a nitrogen laser at 337 nm. The laser beam was focused by a quartz lens system to a spot size of 100 µm in diameter. The samples were mounted on a *x, y* movable target, allowing an irradiation of selected sample areas. Up to eight samples can be prepared on the target. The sample spots can be inspected on a monitor via a high resolution camera during operation. The ions were accelerated to a potential of 6.5 kV in the ion source and post-accelerated by a conversion dynode to a potential of either 10 or 20 kV depending on the sample analyzed. The effective drift length of the instrument was 1.7

meters. Ions were detected by a secondary electron multiplier and the signal was amplified and digitized by a high speed transient recorder (Finnigan Board) linked to a 486 personal computer.

#### *Sample preparation*

Aqueous stock solutions of the analytes and the internal standards were prepared. The different sample ratios were obtained by mixing a fixed volume of the internal standard with different volumes of analyte and diluting the mixture with water to a total volume. The DHB matrix was dissolved at a concentration of 10 g/l in water. A 0.5  $\mu\text{l}$  of the matrix solution together with a 0.5  $\mu\text{l}$  of the aqueous analyte-internal standard solution were mixed directly on the target. For each series of experiments the matrix concentration was kept constant, giving a diverse molar ratio between matrix and analyte. The sample was dried in a cold air stream before loading into the mass spectrometer.

#### *Running procedure*

The stability of ion signal ratios was studied for bovine cytochrome c. Five sample spots were prepared on a target. From each spot successive mass spectra were accumulated for 10, 25, 50 and 100 laser shots fired at the same spot on the sample surface.

The quantitative measurements were performed in the following way: for each sample/internal standard ratio a target with four sample spots was prepared and loaded into the mass spectrometer. A spot on the sample surface was selected for further investigation, when the signal from both analyte and internal standard could be visually identified with a relative good resolution. The laser power was tuned by means of a variable attenuator to keep the  $[\text{M}+\text{H}]^+$  signals between 0-150 mV in amplitude. Then ten or twenty spectra, depending on the sample, were accumulated from the same laser spot on the sample surface. This was repeated five to eight times, every time from a new position on the four sample spots. Generally, all four sample spots were used to generate the data. All spectra were acquired in the positive-ion mode.

The intensities of the analyte and the internal standard peaks were measured by means of peak height and peak height ratios. Means, standard deviations and relative standard deviations of the 5-8 measurements were calculated for each concentration.

#### *Extraction procedure*

Plasma samples containing amperozide were made from an aqueous standard solution of amperozide/ $^{13}\text{C}_4$ -amperozide. The aqueous standard solution was mixed 1:1 with human plasma (100  $\mu\text{l}$  of each). The samples were then prepared for quantitative analysis

by a single liquid-liquid extraction procedure. The samples were mixed with 400  $\mu\text{l}$  of acetonitrile and the test-tubes were centrifuged for 3 min at 14 000 g. The organic phase was then transferred to a clean test tube and dried under a stream of nitrogen gas. The dried samples were reconstituted with 50  $\mu\text{l}$  of 50% acetonitrile. The reconstituted samples were then analysed as described above.

## Results and discussion

Absolute quantitation of MALDI ion yield from sample to sample depends strongly on shot-to-shot reproducibility, which requires a uniform sample surface and a laser pulse kept at constant energy. Mass spectra obtained from individual laser shots greatly vary in signal intensity and mass resolution, both over the sample surface and with successive shots at a given sample spot. However, the addition of a related compound as an internal standard enables quantitative information to be obtained, since experimental variation equally affects the signals from the analyte and the internal standard.

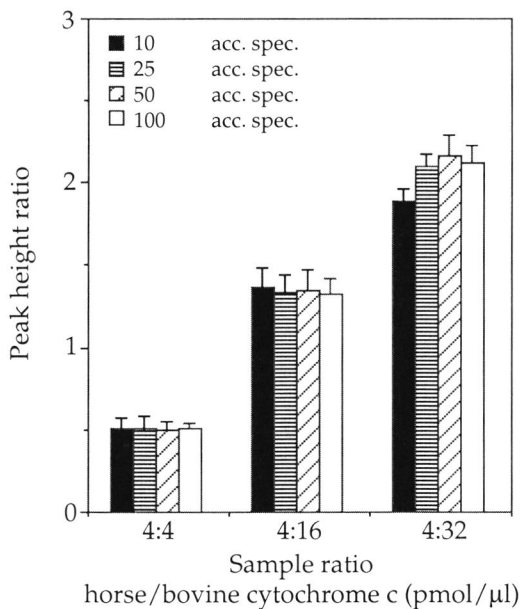


**Figure 1.** Variation of the ion signal ratio with the number of accumulated spectra obtained from the same sample spot on the sample surface at three different sample ratios of horse cytochrome c versus bovine cytochrome c. Error bars are  $\pm$  standard deviation of five measurements from five different target spots

*Stability of the ion signal ratio*

With the use of an internal standard, the stability of the ion signal ratio was compared with increasing number of spectra accumulated. A given spot on the test sample was irradiated by laser pulses and the integrated peak intensities were successively recorded for 10, 25, 50 and 100 accumulated spectra. This was repeated five times by moving the target to a new spot on the sample surface. In each case the ratio of peak heights for the analyte and the internal standard was measured and means and standard deviations of five measurements were calculated. Bovine cytochrome c was used as the analyte and horse cytochrome c as the internal standard. The experiment was carried out at three different sample ratios 4:4, 4:16 and 4:32 pmol/ $\mu$ l. The results are presented in Figure 1. In all three cases, the ratio in peak height between bovine and horse cytochrome c is independent of the number of spectra that were accumulated. The stability in the ion signal ratio indicate that the variation in signal strength can be compensated for by the use of an internal standard and that 10 summed spectra are sufficient for the quantitative analysis of cytochrome c.

**Table 1** Calculated average, measured peak-height ratios with standard deviation (SD) and relative standard deviation (RSD) in percentage of the measured peak height ratios for bovine cytochrome c, renin and peptide A. Each value listed represents peak height ratio obtained from 5-8 (n) replicate sample analyses.

	Sample ratio	applied (pmol)	Average Peak-height ratio	SD	RSD (%)	n
bovine/horse cytochrome c	0.5	1	0.28	0.03	9.5	5
	1	2	0.51	0.07	14.1	5
	2	4	0.78	0.11	14.2	5
	4	8	1.34	0.10	7.8	5
	6	12	1.61	0.12	7.2	5
	8	16	2.10	0.07	3.5	5
renin/melittin	0.25	1.25	0.16	0.04	26.5	8
	0.5	2.50	0.29	0.05	18.0	8
	1	5.00	0.82	0.17	21.2	8
	2	10.00	2.25	0.31	13.6	8
	3	15.00	4.13	1.17	28.3	8
peptide A/B	0.125	1	0.10	0.02	16.2	8
	0.25	2	0.20	0.04	21.3	8
	0.5	4	0.42	0.09	21.4	8
	1	8	0.82	0.12	14.6	8
	2	16	1.35	0.15	10.9	8
	3	24	2.48	0.56	22.6	8
	4	32	4.19	0.90	21.4	8
	5	40	5.29	1.30	24.6	8

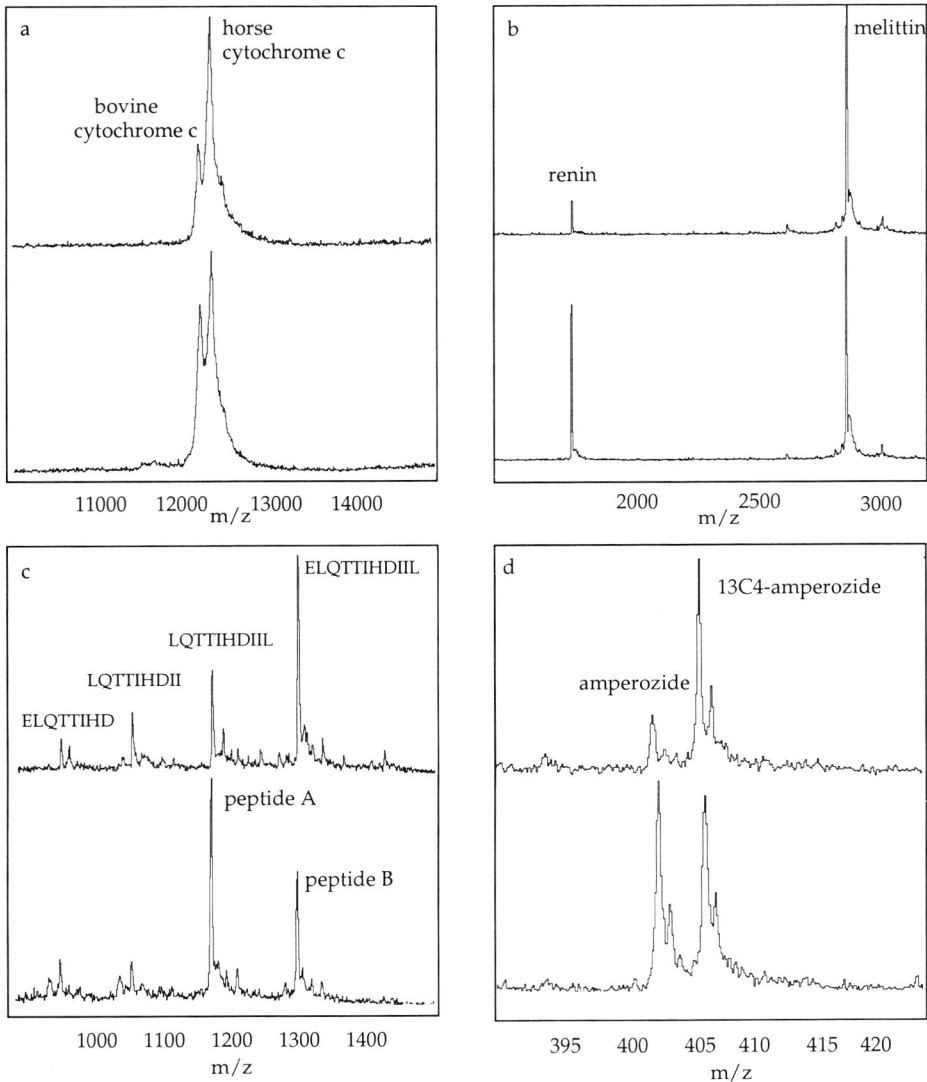


**Figure 2.** MALDI mass spectra of the four test samples with DHB as matrix. Each set of spectra represent the internal standard at constant concentration and the analyte at two different concentrations. (a) Bovine cytochrome c/horse cytochrome c; applied amount 2:2 pmol top and 4:2 pmol bottom, number of accumulated spectra = 10. (b) Renin/melittin; applied amount 1.25:5 pmol top and 5:5 pmol bottom, number of accumulated spectra = 20. (c) Peptide A (LQTTIHDIIIL)/peptide B (ELQTTIHDIIIL); applied amount 8:8 pmol top and 24:8 pmol bottom, number of accumulated spectra = 20. (d) Amperozide/ $^{13}\text{C}_4$ -amperozide in water; concentration 2.5:10 pmol/ $\mu\text{l}$  top and 10:10 pmol/ $\mu\text{l}$  bottom; number of accumulated spectra = 10.

### *Quantitative analysis*

Quantitative analysis was applied to various peptides and proteins in a mass range from 1000 to 12000 Da using appropriate internal standards. The applied procedure is described under experimental. Table 1 gives the calculated average, standard deviation (SD), relative standard deviation (RSD) in percentage of the measured peak height ratios and the number of measurements performed for each sample loading.

#### *Bovine/horse cytochrome c*

An internal standard should mimic the behaviour of the analyte during sample preparation and analysis. Horse cytochrome c was selected as internal standard in the quantitative analysis of bovine cytochrome c, because the cytochromes are functionally identical proteins. However, as they differ by three amino acids in their amino acid sequence, i.e., Thr at position 47 in horse cytochrome c is replaced by Ser in bovine cytochrome c, Lys at position 60 by Gly, and Thr at position 89 by Gly, they most likely also differ in proton affinity. Perhaps, the selection of a protein with similar proton affinity as horse cytochrome c would have been more appropriate.

Figure 2a shows the mass spectra obtained for the analysis of bovine cytochrome c with the use of horse cytochrome c as the internal standard. The internal standard was applied at a constant concentration and the analyte concentration was varied.

When the amount of bovine cytochrome c loaded per sample spot is plotted against the peak heights ratio for bovine cytochrome c and horse cytochrome c a linear response is obtained (product-moment correlation coefficient  $R = 0.992$ ) over the range 1-16 pmol bovine cytochrome c with horse cytochrome c kept at 2 pmol (Figure 3a).

#### *Renin/melittin*

In the second example renin and melittin, two functional and structural different proteins, were tested. Mass spectra obtained with renin as analyte and melittin as internal standard are shown in Figure 2b. In the renin/melittin case obviously much better mass spectral resolution is achieved owing to the lower molecular mass of the peptides. It is expected that this would result in more precise results, especially for the more extreme concentration ratios where in the cytochrome c case, peak overlap might distort proper peak height measurements.

Figure 3b shows the correlation between the amount of renin loaded and peak height ratio for renin/melittin. A linear response was found for renin with melittin as internal standard over the range 1.25 to 15 pmol ( $R=0.992$ ). The applied amount of melittin is 5 pmol. The results are not significantly better in terms of precision, which probably can be explained from the structural differences between renin and melittin, resulting in different behaviour in MALDI.

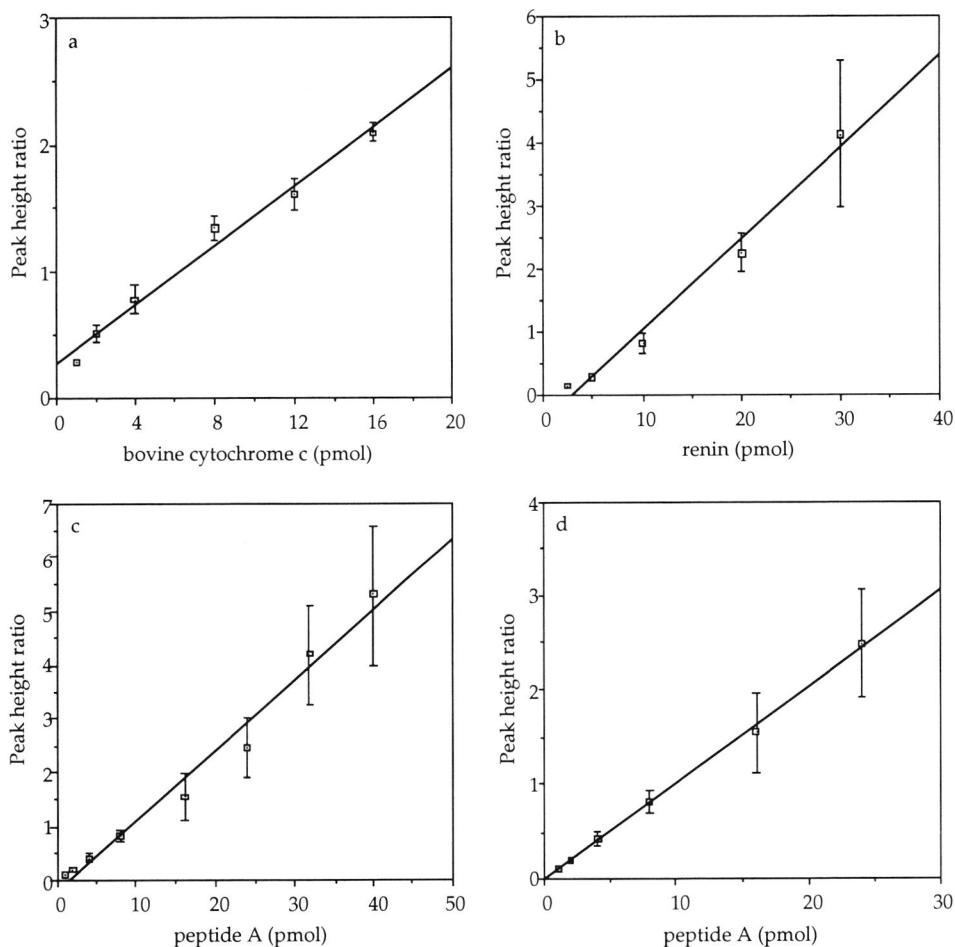


**Figure 3.** Peak height ratio plotted against the applied amount of analyte for the three proteins/peptides. (a) bovine cytochrome c ranging from 1-16 pmol with horse cytochrome c used as internal standard. (b) renin ranging from 1.25-15 pmol with melittin used as internal standard. (c) peptide A ranging from 1-40 pmol with peptide B used as internal standard and (d) peptide A ranging from 1-24 pmol with peptide B used as internal standard. Error bars are  $\pm$  standard deviation of 5 measurements for bovine cytochrome c and 8 for both renin and peptide A.

#### Peptide A/peptide B

In order to discriminate between mass spectral resolution-related effects and structural effects, two structural analogous peptides, differing only one amino acid in length at the N-terminus were explored. For this instance, peptide B, ELQTTIHDIIL was

synthesized as an internal standard for the quantification of peptide A, LQTTIHDIIL. Two spectra obtained with the internal standard peptide B applied at a constant concentration and peptide A at two different concentrations are shown in Figure 2c. A plot of the peak height ratio versus the amount of peptide A loaded is shown in Figure 3c. A linear relationship is observed with the applied amount of peptide A ranging from 1 to 40 pmol ( $R=0.991$ ). The applied amount of peptide B is 8 pmol.

#### Comparison

In all three cases a good linearity between peak height ratios and the sample quantity was obtained. The linear response indicates that the sample ratio in the solution is related to the ion signal ratio obtained by irradiation of the crystallized sample/matrix surface. The linear response was generally obtained over one order of magnitude. This is considered sufficient, since in most cases the analyte can be concentrated or diluted in solution to fit the range of the calibration curve. It must be emphasised, that although linearity is observed over only one order of magnitude the dynamic range of the instrument allows a shift of the linear range over a larger range of amounts. This requires another amount of internal standard to be applied to the sample in order to keep the peak height ratios between ca 4:1 and 1:4 ratio. For all three samples, dilution of the calibration series permitted measurements in the fmol range, as demonstrated by a spectrum obtained for the two analogous peptides A and B in the fmol range, given in Figure 4. It was selected from a 16-fold diluted calibration series (125-2500 fmol peptide A with 500 fmol peptide B as internal standard).

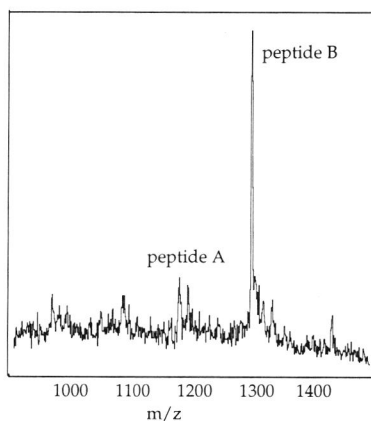


**Figure 4.** MALDI Mass Spectrum of 125 fmol peptide A and 500 fmol peptide B. Number of accumulated spectra = 20.

The dynamic range in peak height ratio obtained for bovine cytochrome c is relatively low (0.3-2.1). This can be explained by the insufficient resolution of the two peaks, corresponding to bovine and horse cytochrome c (Figure 2a). Furthermore, the incomplete resolution of the peaks of bovine and horse cytochrome c results in considerable uncertainty in determining the base line of the peaks, which may be reflected in the errors related to the calibration plot, e.g. the calibration line does not pass through the origin.

Peptide A and renin both show a relatively higher variation in peak height ratio (RSD 11-25% and 14-28%) than bovine cytochrome c (RSD 3-14%). For renin this might be explained by the choice of internal standard. Renin and melittin are two functional and structural different proteins. Events during sample preparation and mass spectrometric analysis for renin and melittin might not be comparable. Peptide A and B are nevertheless analogues and therefore the variation in peak height ratio was expected to be similar to that of cytochrome c. The relative large variation might be explained by impurities of smaller peptides in the stock solution of both peptides. The presence of impurities can be detected from the mass spectra (Figure 2c). These C-terminal truncated impurities appear to be primarily present in peptide B, explaining the fact that they are detected more readily in the spectra from the sample in which the amount of the internal standard peptide B exceeds the amount of peptide A (at the low A/B ratio, cf. upper and lower trace in Figure 2c).

The correlation between the sample loading and the peak height ratio for peptide A is roughly linear over the range 1-40 pmol. However, an improved linearity ( $R=0.9991$ ) is obtained in the 1-24 pmol range (Figure 3d). The non-linear behaviour observed at higher amounts of peptide A possibly represents a saturation of the matrix. In these experiments, like in all proper quantitative experiments, a fixed amount of matrix was used with increasing amount of sample. At a too-high sample concentration the matrix isolation, which is crucial for a successful desorption, is no longer guaranteed, resulting in a decrease in signal quality.

The above results show a broader dynamic range in both peak height ratio and sample ratio compared to the quantitative results obtained by Nelson *et al.* [9] for bovine insulin and Tang *et al.* [11] for lysozyme and myoglobin.

#### *Quantitation bioanalysis of amperozide*

Quantitative analysis has also been performed on a clinically significant compound, amperozide, in plasma. First, the experiments were performed with the analyte in water. A stable isotope-labelled compound, [ $^{13}\text{C}_4$ ]-amperozide, was used as internal standard. Figure 5a shows a linear relationship between peak height ratio and the amount of

amperozide loaded ( $R=0.9994$ ). In this case, the slope for the calibration curve approximately equals one, reflecting an equal intensity of the ion signal for amperozide and  $[^{13}\text{C}_4]$ -amperozide (Figure 2a). This was not obtained for any of the other samples tested, indicating that amperozide and the labelled internal standard show identical behaviour throughout sample preparation and MALDI-MS analysis.

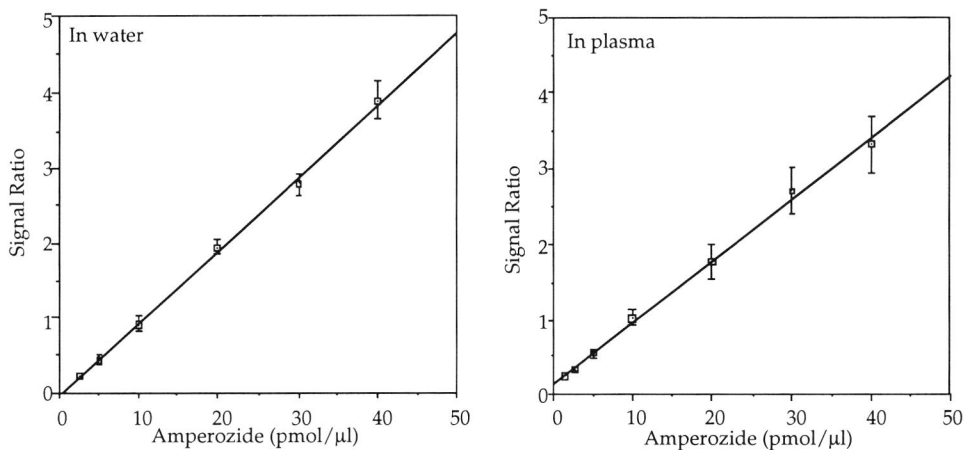


**Figure 5.** Peak height ratio plotted against the concentration of amperozide obtained (a) in water and (b) in plasma with  $[^{13}\text{C}_4]$ -amperozide used as internal standard. Error bars are  $\pm$  standard deviation of 5-6 measurements.

An aqueous sample with an unknown amount of amperozide was also analyzed after a known amount of the  $[^{13}\text{C}_4]$ -amperozide was added. From the calibration curve the unknown concentration was determined to 14.4 pmol/μl, while the actual concentration was 12.5 pmol/μl, giving an error of 13%. This is acceptable, accounting the relative standard deviation for the calibration curve, ranging from 5.4 to 13.4% (Table 2).

Finally, the experiments were performed with amperozide added to plasma. Preliminary experiments were performed with spiked plasma samples with different sample pretreatments, ranging from direct analysis of spiked plasma to the liquid-liquid extraction procedure described. The latter turned out to be necessary because the high concentration of proteins in plasma prevents matrix crystallization. Following liquid-liquid extraction (see Extraction procedure), quantitative MALDI-MS was applied to the finally reconstituted samples. The calibration curve for amperozide extracted from plasma (Figure 5b) shows good linearity ( $R=0.998$ ). Compared with the calibration curve obtained for amperozide in water the relative standard deviation (Table 2) is slightly

larger for each point of the calibration curve in plasma and the slope is smaller than one. Most likely these differences are due to interference of the biological components which are co-extracted together with amperozide. However, from the data shown it can be concluded that quantitative bioanalysis of amperozide in plasma from the concentration range from 1-40 pmol/ $\mu$ l is possible. By changing the amount of internal standard added the linear range may be shifted over larger concentration range, as previously indicated.

**Table 2** Calculated average, standard deviation (SD) and relative standard deviation (RSD) in percentage of the measured peak height ratios for amperozide obtained in water and from plasma. Each value listed represent peak height ratio obtained from 5-6 (n) replicate sample analyses.

	Sample ratio	Concentration pmol/ $\mu$ l	Average Peak height ratio	SD	RSD %	n
Amperozide in water	0.25	2.50	0.23	0.02	8.8	6
	0.5	5.00	0.44	0.06	13.4	6
	1	10.00	0.91	0.10	10.6	6
	2	20.00	1.95	0.10	5.3	6
	3	30.00	2.78	0.15	5.4	6
	4	40.00	3.88	0.25	6.3	6
Amperozide in plasma	0.125	1.25	0.23	0.03	13.2	5
	0.25	2.50	0.32	0.04	13.3	5
	0.5	5.00	0.54	0.06	10.5	5
	1	10.00	1.01	0.11	10.8	5
	2	20.00	1.77	0.23	12.9	5
	3	30.00	2.70	0.31	11.6	5
	4	40.00	3.30	0.39	11.8	5

## Conclusion

A linear correlation was found between measured peak height ratio and sample loading, when an analogous compound was used as internal standard. Together with the use of DHB as matrix this method shows great promise for quantitative applications. The most critical parameter seems to be the choice of internal standards. The best results were obtained for amperozide with the use of [ $^{13}\text{C}_4$ ]-amperozide as internal standard. Because of the mass resolution of the instrument the use of isotope-labelled forms as internal standards is only possible in the low mass range. However, a structural analogue can be used as an internal standard in the high mass range. In this respect the results obtained for bovine cytochrome c with horse cytochrome c as internal standard and peptide A with peptide B as internal standard were better than those for the renin/melittin combination.

The potential of MALDI-MS as a quantitative tool for biological applications was proven by a simple one step liquid-liquid extraction procedure. This method provides the required sensitivity and selectivity for the quantitation of unlabelled and labelled amperozide. This leads to the possibility of using MALDI-MS as a detection device for quantitative analysis in bioanalytical problems.

### Acknowledgements

Dr. A. Björk and Dr. A. M. Olsson (Therapeutic Pharmacia, Sweden) are thanked for providing the amperozide and the human plasma spiked with amperozide. Dr. J. W. Drijfhout (Blodbank, Academic Hospital Leiden, Leiden, The Netherlands) is thanked for providing the peptides A and B.

### References

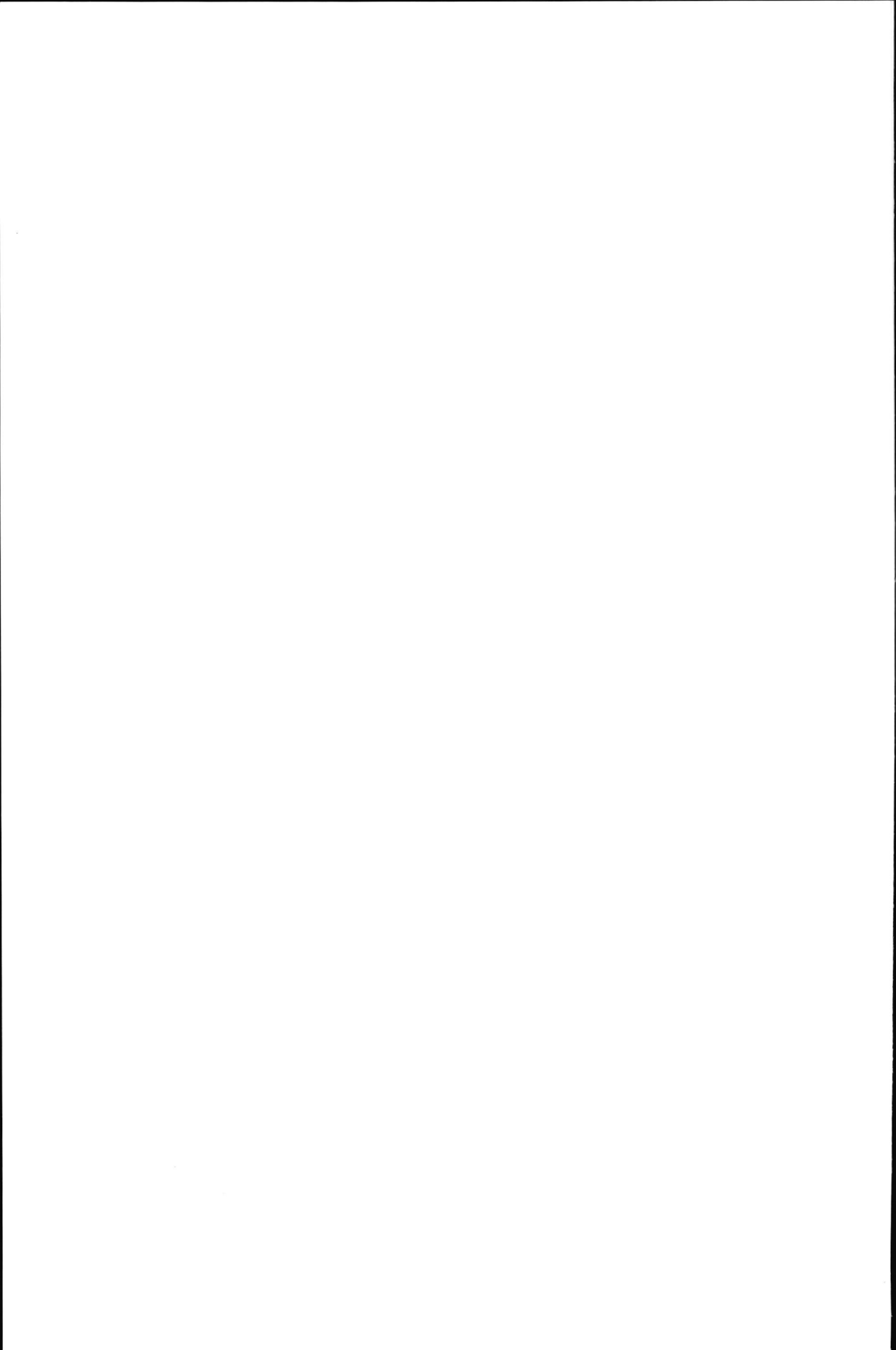
- [1] M. Karas and F. Hillenkamp, *Anal. Chem.*, **1988**, 60, 2299-2301.
- [2] M. Karas, U. Bahr, A. Ingendoh and F. Hillenkamp, *Angew. Chem. Int. Ed. Engl.*, **1989**, 28, 760-761.
- [3] M. Karas, U. Bahr, A. Ingendoh, E. Nordhoff, B. Stahl, K. Strupat and F. Hillenkamp, *Anal. Chim. Acta*, **1990**, 241, 175-185.
- [4] R. C. Beavis and B. T. Chait, *Anal. Chem.*, **1990**, 62, 1836-1840.
- [5] B. Stahl, M. Steup, M. Karas and F. Hillenkamp, *Anal. Chem.*, **1991**, 63, 1463-1466.
- [6] A. Overberg, A. Hassenbürger and F. Hillenkamp, in M. L. Gross (Eds), *Mass Spectrometry in the Biological Sciences*, Mass Spectrometry in the Biological Sciences, Dordrecht, The Netherlands, Kluwer Academic, **1992**, 181-197.
- [7] U. Bahr, A. Deppe, M. Karas, F. Hillenkamp and U. Giessmann, *Anal. Chem.*, **1992**, 64, 2866-2869.
- [8] R. C. Beavis and B. T. Chait, *Proc. Natl. Acad. Sci. USA*, **1990**, 87, 6873-6877.
- [9] R. W. Nelson, M. A. McLean and M. L. Vestal, *Proceedings of the 40th ASMS Conference on Mass Spectrometry and Allied Topics.*, Washington, DC, **1992**, 1919-20.
- [10] D. J. Harvey, *Rapid Commun. Mass Spectrom.*, **1993**, 7, 614-619.
- [11] K. Tang, S. L. Allman, R. B. Jones and C. H. Chen, *Anal. Chem.*, **1993**, 65, 2164-2166.
- [12] M. W. Ducan, G. Matanovic and A. Cerpa-poljak, *Rapid Commun. Mass Spectrom.*, **1993**, 7, 1090-1094.
- [13] L. M. Preston, K. K. Murray and D. H. Russell, *Biol. Mass Spectrom.*, **1993**, 22, 544-550.



## **Chapter 3**

---

Attomole detection of proteins by MALDI-MS with the  
use of picoliter vials



---

# Attomole detection of proteins by MALDI-MS with the use of picoliter vials

*Significant improvements in the absolute detection limits for proteins in matrix-assisted laser desorption/ionization mass spectrometry (MALDI-MS) are demonstrated by the application of so-called picoliter vials. By the reduction of the sample volume from a few  $\mu\text{l}$  down to 250 pl and simultaneous reduction of the sample spot area from a few  $\text{mm}^2$  down to  $0.01 \text{ mm}^2$  low attomole detection limits are obtained for bradykinin and cytochrome c. The detection limit in a single-shot mass spectrum of bradykinin is estimated to be as low as 250 zeptomole. These are currently the lowest amounts of protein and the smallest volumes analyzed by MALDI-MS.*

---

## Introduction

Matrix-assisted laser desorption/ionization mass spectrometry (MALDI-MS) pioneered by Hillenkamp and Karas [1,2] has become a standard analytical technique for mass analysis of biomolecules with molecular masses of up to several hundred thousand dalton [3]. The method is applicable to the analysis of different classes of biomolecules such as proteins, glycoproteins, oligosaccharides [4,5] and oligonucleotides [6,7], as well as synthetic polymers [8].

One of the analytical strengths of MALDI-MS is that it can be applied to any protein and provides a practical absolute detection limit of typically  $\sim 0.1\text{-}1 \text{ pmol}$ , depending on the molecular mass. However, the amount of protein actually consumed during the analysis is much less. It has been estimated that the analyte consumption per single spectrum is as low as  $10 \text{ amol}$  ( $10^{-18} \text{ mol}$ ) [9]. A possible approach in lowering the absolute detection limit for MALDI-MS lies in a reduction of the sample volume used in the sample preparation, if the surface area and thus the spread of the dried sample spot can be decreased proportionally. The standard sample preparation for MALDI-MS comprises on-target mixing of  $0.5 \mu\text{l}$  of the analyte solution and  $0.5 \mu\text{l}$  of a matrix solution, e.g. 2,5-dihydroxybenzoic acid (DHB). The dried droplet typically spreads over a few cubic millimetres. Absolute detection limits as low as  $1 \text{ fmol}$  for cytochrome c have been reported by reducing the sample/matrix volume down to  $100 \text{ nl}$  [10].

In this paper, a new approach to the reduction of the sample/matrix volume is described. So-called picoliter vials, basically consisting of small cavities in a thin gold-covered silicon chip, allow for a significant reduction of both the sample volume applied and the surface covered. Three orders of magnitude improvement in detection limits for bradykinin and cytochrome c using this approach are demonstrated.

---

## Experimental

### *Mass spectrometry*

The mass spectrometer used for the investigations was a VISION 2000 laser desorption reflectron time-of-flight instrument (Finnigan MAT, Bremen, Germany). Ions were formed using a pulsed nitrogen laser (pulse width 3 ns) which operates at 337 nm. Fine attenuation of the laser irradiance is achieved by a dielectric mirror using its angle-dependent reflection-transmission rate. The focal spot size of the laser beam on the target was about 100  $\mu\text{m}$  in diameter. The ions were accelerated to a potential of 6.5 kV in the ion source and post-accelerated by a conversion dynode in front of the detector to a potential of 20 kV. The effective drift length of the instrument is 1.7 m. Ions were detected by a secondary electron multiplier and the signal was amplified and digitized by a high speed transient recorder linked to a 486 personal computer. All spectra shown represent unprocessed data either accumulated from ten single-shot or one single-shot spectra without any filtering or background subtraction.

### *Picoliter vials*

The picoliter vials were fabricated as described earlier [11], by micromachining of a monocrystalline silicon wafer with a  $\langle 100 \rangle$  surface orientation. Arrays of  $100 \times 100 \mu\text{m}$  vials, with a  $200 \mu\text{m}$  spacing between each vial were defined by UV photolithography. A subsequent anisotropic chemical etching of the wafer resulted in square, pyramidally shaped cavities with sharply defined rims. The volume of the individual vials is 250 pL, since the angle between the  $\langle 100 \rangle$  and the  $\langle 111 \rangle$  crystal planes of the silicon wafer is 54.74 degrees (Figure 1). The silicon wafer was covered with a sputtered film of chromium and gold. This was needed to establish an electrical contact between the sample holder and the surface of the wafer.

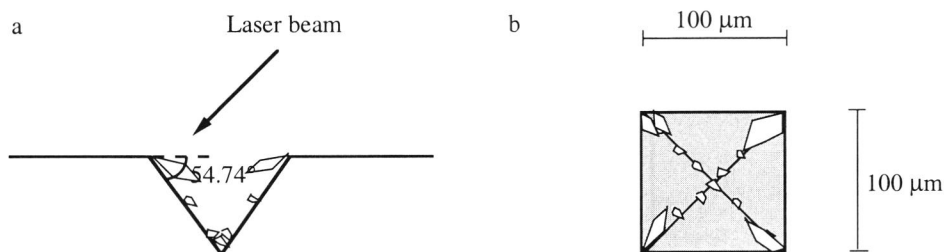


**Figure 1.** Schematic drawing of a 250 picoliter vial, showing the position of the micro-crystal (a) cross sectional view of the vial, (b) top view of the vial

*Sample preparation*

Dilution series were produced from 1 mg/ml aqueous stock solutions for human bradykinin ( $M_r = 1060$  Da) and horse heart cytochrome c ( $M_r = 12360$  Da) (Sigma Chemical Co., St. Louis, MO, USA) with concentrations as indicated in Table 1. A 10 mg/ml aqueous solution of 2,5-dihydroxybenzoic acid (Aldrich Chemie, Steinheim, Germany) was used as matrix. Analyte and matrix solution were mixed in a 1:1 (v/v) ratio. The picoliter vials were filled manually under an optical microscope using laboratory-made glass micro-pipettes. The latter were pulled with a Model P-87 Flaming-Brown micro-pipette puller (Sutter instruments), resulting in pipettes with an outer tip diameter smaller than 100  $\mu\text{m}$ . A part (ca 8 x 8 mm) of the silicon wafer with the picoliter vials was glued on to a MALDI stainless steel target. Electrical contact with the gold coated surface of the chip and the target was obtained by interconnection of the surfaces with a small strip of aluminium foil. This target arrangement was mounted on an x, y movable sample support. The irradiation of selected sample vials was monitored with a high resolution camera during operation.

**Table 1.** Sample concentration and absolute sample amount in one microliter and in 250 picoliter for bradykinin and horse cytochrome c.

Analyte	sample concentration (fmol/ $\mu\text{l}$ )	absolute amount in a standard sample preparation spot (fmol)	absolute amount in one picoliter vial (amol)
bradykinin	8000	4000	1000
	800	400	100
	80	40	10
	40	20	5
	20	10	2.5
cytochrome c	8000	4000	1000
	4000	2000	500
	2000	1000	250
	800	400	100
	400	200	50
	200	100	25

**Results and discussion**

A characteristic feature of DHB is its crystallization into extended needles on solvent evaporation. In the standard sample preparation these crystalline needles nucleate at the rim of the matrix-analyte droplet and protrude into the inner part of the preparation [10]. In the 250 picoliter vials evaporation of the solvent takes place in a few seconds.

This was observed under the microscope as a smoothly declining solvent meniscus. Crystals, only a few  $\mu\text{m}$  in size, are formed randomly at all eight edges of the vial pyramid (Figure 1).

The target with the picoliter vials were loaded into the mass spectrometer and ten single spectra were accumulated from a single vial for each concentration. Figure 2 shows the spectra obtained for bradykinin at quantities of 100, 10, 5 and 2.5 amol. Spectra obtained for cytochrome c at quantities of 1 fmol, 100, 50 and 25 amol are shown in Figure 3. A decline in signal intensities at threshold irradiation was observed with decreasing analyte amounts. A stepwise increase of the irradiation with decreasing analyte amounts was applied to increase the intensities of the ion signal. However, the increase in irradiance also caused an increase in intensity of the matrix signals in the low mass range and an increase in the width of the analyte ion peak and thereby a decrease in mass resolution. Going from the highest to the lowest concentration, the irradiation was increased by approximately a factor of 3 for both bradykinin and cytochrome c. The resolution was decreased by approximately a factor of 5 for bradykinin (at absolute amount of 100 amol,  $R \sim 2500$ ) and a factor of 3 for cytochrome c (at absolute amount of 1 fmol,  $R \sim 240$ ).

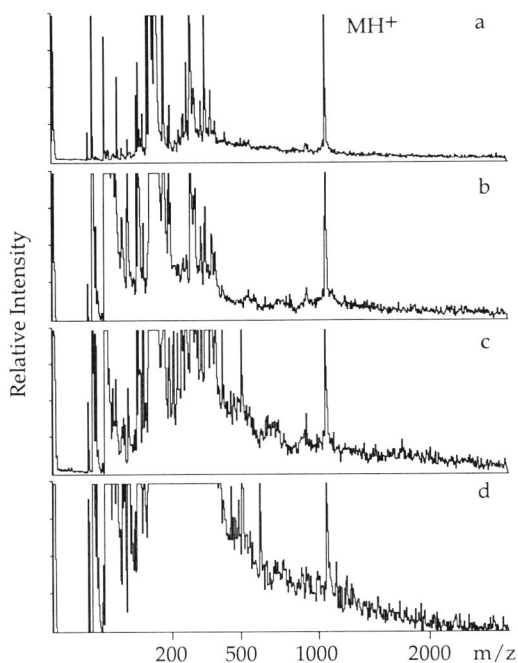


**Figure 2.** MALDI spectra of bradykinin obtained from the 250 picoliter vials containing absolute amount of (a) 100 amol (b) 10 amol, (c) 5 amol and (d) 2.5 amol.

Even though the signal is decreasing with decreasing sample amount, analyte ion signals for 2.5 amol of bradykinin and 25 amol of cytochrome c are still quite pronounced. Attempts to obtain spectra from smaller amounts of sample were not successful.

The ability to reduce the applied volume and thereby the absolute sample amount from 1 microliter to 250 picoliter has improved the detection limits from the fmol range to the low amol range. At the lowest absolute amount, 2.5 amol of bradykinin and 25 amol of horse cytochrome c, approximately ten spectra could be accumulated from the same vial, resulting in a detection limit of 250 zeptomol ( $10^{-21}$  mol) for bradykinin and 2.5 amol for cytochrome c per single spectrum. This is slightly lower than the sample consumption of 10 amol per single spectrum as estimated by Karas *et al.* [9]. Figure 4 shows single-shot spectra obtained from the picoliter vials at an absolute amount of 2.5 amol for bradykinin (Figure 4a) and 25 amol for cytochrome c (Figure 4b).

Since analyte ions could be desorbed with higher intensities from the vials with a larger number of micro-crystals, improvements in the sample preparation may lead to further improvements in the detection limits. The results presented are currently the lowest amount of protein and the smallest volumes analyzed by MALDI-MS.

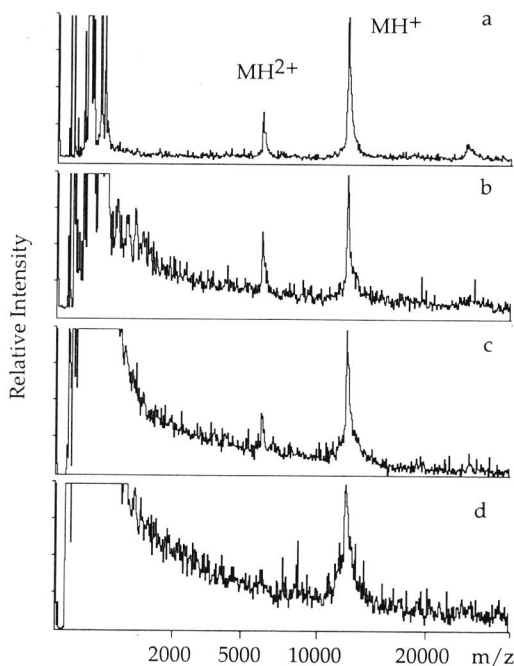


**Figure 3.** MALDI spectra of horse cytochrome c obtained from the 250 picoliter vials containing absolute amount of (a) 1 fmol (b) 100 amol (c) 50 amol and (d) 25 amol.

The combination of picoliter vials and MALDI-MS may prove to be extremely useful for sample volume limited applications. The matrix tolerance to impurities make MALDI-MS very suitable for direct analysis of biological extracts and cells [12] without any further purification. The potential of transferring single cells to the picoliter vials, followed by the addition of the matrix solution, offers the possibility of following cell-specific processing of proteins, post-translational modifications and peptide sorting and targeting to different intracellular sites. In addition, the possibility to investigate very small sample spots, could provide a convenient mean for coupling capillary electrophoresis separation systems to MALDI-MS.

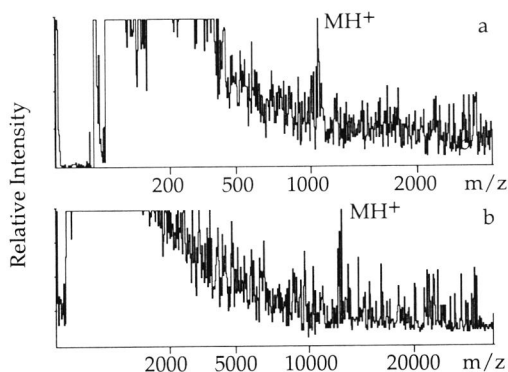


**Figure 4.** Single-shot MALDI spectra obtained from the 250 picoliter vials containing (a) 2.5 amol of bradykinin and (b) 25 amol of horse cytochrome c

### Acknowledgement

Sonja Jespersen is grateful to the Danish Research Academy for the financial support of these investigations. The group of the Royal Institute of Technology gratefully acknowledges financial support from the Swedish Natural Science Research Council and the Swedish Board for technical development.

## References

- [1] M. Karas and F. Hillenkamp, *Anal. Chem.*, **1988**, 60, 2299-2301.
- [2] M. Karas, D. Bachmann, U. Bahr and F. Hillenkamp, *Int. J. Mass Spectrom. Ion Processes.*, **1987**, 78, 53-68.
- [3] M. Karas, U. Bahr, A. Ingendoh and F. Hillenkamp, *Angew. Chem. Int. Ed. Engl.*, **1989**, 28, 760-761.
- [4] B. Stahl, M. Steup, M. Karas and F. Hillenkamp, *Anal. Chem.*, **1991**, 63, 1463-1466.
- [5] K. K. Mock, C. W. Sutton and J. S. Cottrell, *Rapid Commun. Mass Spectrom.*, **1992**, 6, 233-238.
- [6] G. J. Currie and J. R. Yates III, *J. Am. Soc. Mass Spectrom.*, **1993**, 4, 955-963.
- [7] K. J. Wu, A. Steding and C. H. Becker, *Rapid Commun. Mass Spectrom.*, **1992**, 7, 142-146.
- [8] U. Bahr, A. Deppe, M. Karas, F. Hillenkamp and U. Giessmann, *Anal. Chem.*, **1992**, 64, 2866-2869.
- [9] M. Karas, U. Bahr and F. Hillenkamp, *Int. J. Mass Spectrom. Ion Processes.*, **1989**, 92, 231-242.
- [10] K. Strupat, M. Karas and F. Hillenkamp, *Int. J. Mass Spectrom. Ion Processes.*, **1991**, 111, 89-102.
- [11] M. Jansson, Å. Emmer, J. Roeraade, U. Lindberg and B. Hök, *J. Chromatogr.*, **1992**, 626, 310-314.
- [12] C. R. Jiménez, P. A. v. Veelen, K. W. Li, W. C. Wildering, P. M. Geraerts, U. R. Tjaden and J. v. d. Greef, *J. Neurochem.*, **1994**, 62, 404-407.



## **Chapter 4**

---

Basic matrices in the analysis of non-covalent  
complexes by MALDI-MS



---

## Basic matrices in the analysis of non-covalent complexes by MALDI-MS

*A number of potential matrix candidates were investigated with regards to the importance of the pH in the matrix-assisted laser desorption/ionization mass spectrometry (MALDI MS) analysis of non-covalently bound protein complexes. The matrices examined were 2,5-dihydroxybenzoic acid (DHB), 4-hydroxy- $\alpha$ -cyanocinnamic acid (HCCA), 2-aminonicotinic acid (ANA), 4-nitroanilin (NA), 2-amino-4-methyl-5-nitropyridine (AMNP) and 3-hydroxypicolinic acid (HPA). In solution these matrix compounds permitted the preparation of MALDI samples at a pH ranging from 2-7. Among the tested matrices, complex formation, formed by specific non-covalent interactions, could only be observed when HPA (pH 3.8) was used as matrix for the MALDI analysis. Under this condition specific non-covalent complex formation of recombinant streptavidin and glutathione-S-transferases were observed but not for human hemoglobin. The MALDI spectra obtained with the more neutral compounds ANA (pH 4.4), NA (pH 6.4) and AMNP (pH 7.1) as matrices, comprises only peaks of the subunit with no signal of the non-covalent bound complexes present. Considering the results obtained in this study with basic and acidified matrix materials, there does not appear to be a strong correlation between pH of the matrix solution and the utility of a matrix for the analysis of non-covalent bound complexes.*

---

### Introduction

Intermolecular non-covalent interactions are responsible for the aggregation of folded polypeptide chains into multimers which determines a protein systems quaternary structure. The strengths of such intermolecular forces, including hydrogen bonding and hydrophobic and ionic interactions, can vary widely and are reflected by the dissociation constants ( $K_D$ ) typically determined for a specific set of solution conditions. Changing the pH, solvent condition and/or temperature, will typically cause a protein in solution to denature and partially or completely unfold.

Although a few techniques exist for the direct observation of non-covalent macromolecular complexes, such as size exclusion chromatography, sedimentation equilibrium ultra-centrifugation and non-denaturing gel electrophoresis, each has significant limitations and can only provide an approximate molecular mass of the complex. With the development of soft ionization techniques, such as electrospray ionization (ESI) [1,2] and matrix assisted laser desorption/ionization (MALDI) [3,4] mass spectrometry (MS) has become an indispensable tool for accurate measurements of molecular mass in biochemistry and biomedical research involving structural analysis of proteins and

peptides. Nevertheless, the detection of non-covalent complexes by MS methods is still a challenging task.

There have been several examples of detection of non-covalently bound complexes by ESI-MS since the initial reports by Ganem and co-workers [5,6]. Applied to aqueous solution conditions close to those of physiological interest non-covalent complexes such as peptide/protein, protein-nucleic acid and protein-ligand, which form structurally specific associations in solution, have been preserved intact by the electrospray process (for review see references 7 and 8).

Whereas MALDI-MS has been successfully applied to determine the molecular mass and primary structure of biopolymers, non-covalently bound complexes almost always dissociate into individual components during the MALDI analysis. Accordingly, there are only a few examples where specific oligomeric complexes have been observed by this technique. The initial MALDI applications reported by Hillenkamp *et al.* included spectra of the undissociated tetrameric forms of glucose isomerase, catalase [9] and streptavidin [10] and the dimeric form of violet phosphatase [11] all obtained with nicotinic acid as matrix, at a desorption wavelength of 266 nm. The dimeric form of yeast alcohol dehydrogenase was observed with sinapinic acid (SA) as matrix at a desorption wavelength of 337nm [12]. Later the non-covalent association of membrane proteins was detected by MALDI-MS. The matrices were ferulic acid (355nm) for the trimeric form of porin [13] and SA (337 nm) for the heptameric form of aerolysin [14]. When ferulic acid was used as matrix, ions corresponding to complex formation were only observed for the first laser shot on a not-yet-irradiated sample spot [13].

Dissociation into subunits is mainly due to the conditions in the matrix-analyte solution. The commonly used matrix compounds (at 337 nm) such as SA, 4-hydroxy- $\alpha$ -cyanocinnamic acid (HCCA) and 2,5-dihydroxybenzoic acid (DHB) are typically dissolved in an aqueous solution containing 30-70 % acetonitrile and/or 0.1% trifluoroacetic acid (TFA). In the presence of the organic solvent [10] and under these highly acidic conditions (pH < 2-3) denaturation of protein structures and dissociation of specific interactions must generally be expected. Sample preparation avoiding acidic conditions has previously been carried out with 6-aza-2-thiothumine (ATT) providing a pH close to 7, for the observation of intact double-stranded oligonucleotides [15] and the specific complexes of enzyme RNase S and leucine zipper dimer by MALDI-MS [16]. More recently Cohen *et al.* [17] described the observation of specific non-covalent complexes of alcohol dehydrogenase, catalase and streptavidin, using the matrix 2,6-dihydroxyacetophenone (pH 4-5) in an organic solvent. Intact streptavidin tetramers were also observed with ferulic acid and other dihydroxyacetophenone derivatives. Similar to Rosinke *et al.* [13] ion signal corresponding to the non-covalent complexes could only be obtained from the first shot at a given sample position.

---

Successful matrix desorption is only possible at pH values determined by the matrix compound itself or in a more acidic medium. When the pH of the matrix solution is increased above the pK value of acid, the matrix molecules are transformed into anions, yielding the respective salts when dried, and matrix desorption is no longer possible [18,19]. In principle, matrices with neutral pH values are required for possible desorption of intact non-covalent complexes and other molecular structures that are pH sensitive in their quaternary structure. A number of new matrices for MALDI-MS analysis that can be crystallized from aqueous solution at pH 2-8 [20] have been investigated as possible matrices. These matrices extend the utility of MALDI-MS to the analysis of acid sensitive species. The goal of this study was to examine the potential of these more basic matrices and the importance of pH in the MALDI-MS analysis of non-covalently bound complexes. Besides the two previously mentioned acidic matrices HCCA and DHB, the tested matrices include 3-hydroxypicolinic acid (HPA), 2-aminonicotinic acid (ANA), 4-nitroanilin (NA) and 2-amino-4-methyl-5-nitropyridine (AMNP). Proteins that are known to form multimers were analyzed, i.e. recombinant streptavidin, human glutathione-S-transferase (GST) A1-1, and human hemoglobin.

## **Experimental**

### *Materials*

The matrices 2,5-dihydroxybenzoic acid (DHB), 2-aminonicotinic acid (ANA), 4-nitroanilin (NA), 2-amino-4-methyl-5-nitropyridine (AMNP) and 3-hydroxypicolinic acid (HPA) were obtained from Aldrich Chemie (Steinheim, Germany) and 4-hydroxy- $\alpha$ -cyanocinnamic acid (HCCA) from SIGMA Chemical Co (St.Louis, MO, USA). Human hemoglobin and  $\alpha$ -chymotrypsinogen A were purchased from SIGMA Chemical Co (St. Louis, MO, USA), recombinant streptavidin from Boehringer Mannheim (Almere, the Netherlands) and human glutathione-S-transferases (GST) A1-1 were kindly provided by J.J.P. Bogaards, TNO Biological Toxicology Institute, (Zeist, The Netherlands). Ultra-high quality water, prepared by Elgastate 4 (Elga Ltd., High Wycombe, Bucks England) was used for the matrix and sample solution preparations. Acids and organic solvents were HPLC grade or better.

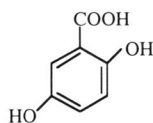
### *Matrices and sample preparation*

The samples were all dissolved in water to yield protein at concentration of 0.1 mg/ml for  $\alpha$ -chymotrypsinogen A and GST A1-1 and of 0.2 mg/ml for recombinant streptavidin and human hemoglobin. The matrix solutions were freshly prepared before use, HCCA was dissolved in 30% acetonitrile, all the other solutions were prepared in water. The concentrations were 10 mg/ml for DHB, HCCA, ANA, NA and AMNP and 30 mg/ml

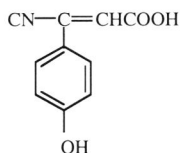
for HPA. The pH measurements of the matrix solutions were performed at room temperature with a Model 5985-50 pH meter (pH Wand, Cole-Parmer Instrument Company, Chicago, IL, USA). An aliquot of the sample and the matrix solution was mixed directly onto the target 1:1 (v/v) and dried under a cold air stream before loading into the mass spectrometer.

### Mass spectrometry

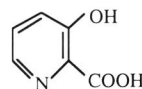
The mass spectrometer used was a VISION 2000 laser desorption reflectron time-of-flight instrument (Finnigan MAT, Bremen, Germany). Ions were formed using a pulsed nitrogen laser, which operates at 337nm. The ions were accelerated to a potential of 6.5 kV in the ion source and post-accelerated by a conversion dynode in front of the detector to a potential of 20 kV. The effective drift length of the instrument was 1.7 m. Ions were detected by a secondary electron multiplier and the signal was amplified and digitized by a high speed transient recorder linked to a 486 personal computer. The laser irradiance was controlled by a variable attenuator and was kept just above the ion generation threshold. All spectra were obtained in positive-ion reflector mode, 20-30 single shot spectra were accumulated in order to obtain a good signal-to-noise ratio.



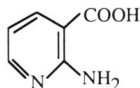
2,5-dihydroxybenzoic acid  
pH 2.0



4-hydroxy- $\alpha$ -cyanocinnamic acid  
pH 2.7



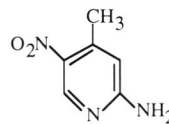
3-hydroxypicolinic acid  
pH 3.8



2-aminonicotinic acid  
pH 4.4



4-nitroanilin  
pH 6.4



2-amino-4-methyl-5-nitropyridine  
pH 7.1

**Figure 1.** The chemical structure of the six matrices investigated with regards to the importance of pH in MALDI analysis of non-covalently bound protein complexes.

## Result and discussion

### *Matrices*

Six matrix compounds (Figure 1) permitting sample preparation at a pH ranging from 2 to 7 were examined with regard to the importance of the pH in MALDI-MS analysis of non-covalently bound complexes. Besides the commonly used acidic matrices 4-hydroxy- $\alpha$ -cyanocinnamic acid (HCCA) and 2,5-dihydroxybenzoic acid (DHB) the matrices investigated include the more basic matrix 3-hydroxypicolinic acid (HPA), first introduced for MALDI-MS analysis of oligonucleotides [21] and three less known matrices, 2-aminonicotinic acid (ANA), 4-nitroaniline (NA) and 2-amino-4-methyl-5-nitropyridine (AMNP) selected from a previously reported screening of a large number of basic matrices [20]. All the matrices were dissolved in water except for HCCA, which needs a proportion of organic solvent and was dissolved in 30 % acetonitrile.

### *$\alpha$ -Chymotrypsinogen (reference conditions)*

Together with the singly charged ion, multiply charged ions and cluster ions are generally observed in a MALDI mass spectrum. The singly charged ion ( $M^+$ ) form the base peak with the doubly charged ion ( $M^{2+}$ ) and the dimer ion ( $M_2^+$ ) at lower intensity [22]. The observation of oligomer cluster ions implies that non-specific non-covalent interactions can survive the desorption event. Therefore a primary consideration in the study of non-covalent associations is determination of their specificity, i.e. establishing whether the species detected in the mass spectrometer are both structurally specific and derived from the species present in solution.  $\alpha$ -Chymotrypsinogen A (25 656 Da) which is known to exist as a monomer only was used to ensure that multimeric forms observed not resulted from the desorption process under the conditions employed. No additional ion signals due to non-specific aggregation of the monomer were observed when  $\alpha$ -chymotrypsinogen A was analysed with neither of the six matrices (results not shown).

### *Recombinant streptavidin*

Recombinant streptavidin was chosen for the initial screening of the six matrices, because the tetrameric species in solution is relatively stable throughout a wide pH range and observation of this protein by MALDI MS might therefore be less sensitive to the acidic conditions. Native streptavidin isolated from the bacterium *Streptomyces avidinii*, exists in its active form as a non-covalent tetramer, which is comprised of four identical subunits each consisting of 159 amino acids. Recombinant streptavidin, which was used in this studies, contains amino acid 13-138 of the native streptavidin (mass 13 271 Da) giving a molecular mass of 53 084 Da for the tetramer complex.

MALDI mass spectra of the recombinant streptavidin prepared with matrices of increased pH are shown in Figure 2a-c. Figure 2a shows the MALDI mass spectrum of recombinant streptavidin obtained under standard MALDI-MS conditions i.e. at pH 2.0 with DHB as matrix. As expected, the spectrum only shows the doubly ( $S^{2+}$ ) and singly ( $S^+$ ) charged ions, together with oligomer cluster ions up to the tetramer form ( $2S^+$ ,  $3S^+$  and  $4S^+$ ) for the dissociated subunits. The singly charged ion at mass 13.3 kDa forms the base peak in the spectrum with the doubly charged ion and the multimeric ions at lower intensity. A comparable spectrum was obtained with HCCA (pH 2.7) as matrix.

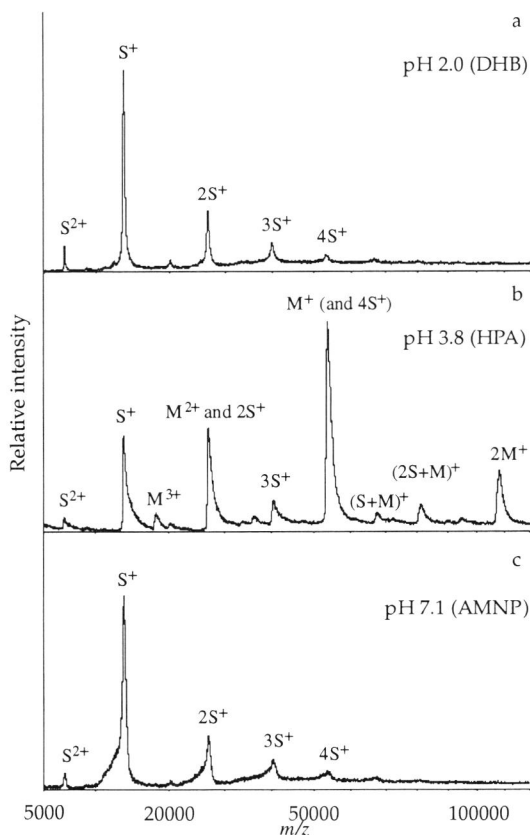


**Figure 2.** Comparison of MALDI mass spectra of recombinant streptavidin (0.2 mg/ml) obtained at different pH with three different matrix compounds (a) DHB in water (pH 2); (b) HPA in water (pH 3.8); and (c) AMNP in water (pH 7.1). All spectra were obtained under subsequent irradiation of the same sample area (sum of 20-30 laser shots). Peaks corresponding to the dissociated and undissociated subunits are denoted by S and M respectively.

In comparison, the ion pattern observed for the recombinant streptavidin at pH 3.8 with HPA as matrix, shown in Figure 2b, differs from that of the dissociated subunits. The interpretation of the intensity distribution indicates the presence of a mixture of the intact non-covalent tetramer and the fully dissociated protein. The non-covalent tetramer at mass 54.0 kDa forms the base peak accompanied by the doubly (26.9 kDa) and triply (18.1 kDa) charged ions as well as a small amount of aggregation of the streptavidin tetramer into octamer (i.e. the dimer of the tetrameric molecular complex) at mass 108.2 kDa. The relatively weak signal of the triply charged tetrameric molecular complex ( $M^{3+}$ ) at mass 18.1 kDa, suggests that the dimer cluster ion ( $2S^+$ ) of the dissociated subunit (13.5 kDa) contributes significantly to the peak at mass 26.9 kDa, besides the doubly charged tetrameric complex ( $M^{2+}$ ). The low intensity of the trimer, pentamer and hexamer species suggests that the MALDI MS data reflect the specific subunit association expected from solution behaviour. In contrast to previous studies [13,17] the observation of non-covalent complexes was not restricted to the first laser shot only. The spectrum shown in Figure 2b was obtained under subsequent irradiation of the same sample area.

When recombinant streptavidin was prepared with one of the more neutral compounds ANA (pH 4.4), NA (pH 6.4) or AMNP (pH 7.1) as matrix, surprising only ion signal corresponding to the subunit and no signal of the intact tetrameric complex were observed. For comparison, the MALDI spectrum of recombinant streptavidin at pH 7.1 with AMNP as matrix is shown in Figure 2c, the mass of the subunit was determined to 13.4 kDa.

The ion signals were significantly broadened under the more neutral pH conditions with either HPA, ANA, NA or AMNP as matrix as compared to the ion signals generated when the acidic DHB or HCCA matrix was used. Similar results were obtained by Fitzgerald *et al.* [20], when screening potential basic matrices for MALDI MS analysis and the loss of mass resolution was explained by the formation of multiple matrix adducts. This accounts for the less accurate molecular mass determination with the more basic matrices.

Since dissociation into subunits is expected to occur with acidification and/or addition of an organic solvent, the stability of the tetrameric complex of recombinant streptavidin was further examined, preparing the HPA matrix with 0.1% trifluoroacetic acid (TFA) pH 2 or with an increasing amount of acetonitrile (0-100%). Figure 3a and b shows the spectra obtained for recombinant streptavidin with HPA dissolved 0.1% TFA and 100% acetonitrile respectively. Contrary to the expected, the obtained spectra show no further dissociation into subunits than with HPA in water as matrix (figure 2b). Dissociation into subunits was only found to be enhanced and completed using a higher concentration of the strong acid TFA (1-10 %) as matrix solution, giving a pH below 1.

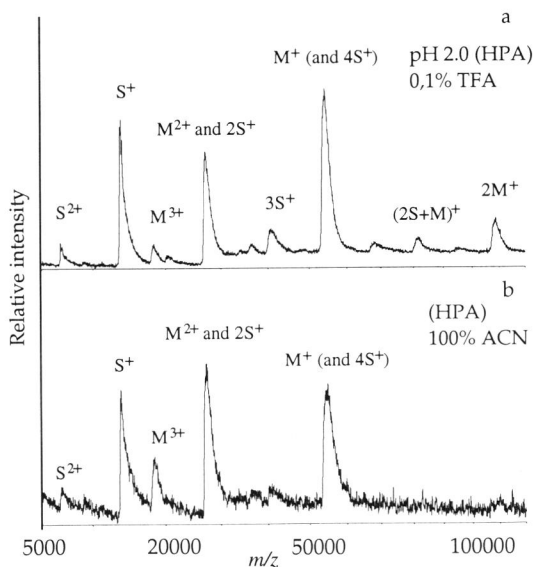


**Figure 3.** MALDI mass spectra of recombinant streptavidin (0.2 mg/ml) obtained from two HPA matrix solutions (a) 0,1 % TFA and (b) 100 % acetonitrile. All spectra were obtained under subsequent irradiation of the same sample area (sum of 20-30 laser shots). Peaks corresponding to the dissociated and undissociated subunits are denoted by S and M respectively.

#### Human glutathione-S-transferase A1-1

Glutathione-S-transferase (GST) A1-1 belongs to the GST alpha family and is a dimeric liver enzyme composed of two identical subunits (A1-1) with an average molecular mass of 25 499 Da.

MALDI mass spectra of GST A1-1 using DHB, HPA and AMNP as matrices are shown in Figure 4a, b and c, respectively. Ions corresponding to the dimer (mass 51.3 kDa) and the monomer (mass 25.6 kDa) could be obtained with equal abundance when HPA was used as matrix (Figure 4b). The doubly and triply charged ions together with the multimeric ions appeared at lower intensity. The relatively weak signal of the tetramer ion (i.e. the dimer of the dimer) at mass 102.9 kDa, suggests that besides the trimeric complex ( $3S^+$  at 77.0 kDa), cluster formation between the mono- and di-meric species ( $SM^+$ ) contributes significantly to the peak at mass 77.0 kDa. As for recombinant streptavidin, dissociation into the subunits could only be enhanced and completed by adding a higher concentration of a strong acid such as TFA to the matrix solution.

When the sample was prepared using either the more acidic DHB (pH 2) or the more basic AMNP (pH 7.1) as matrix the mass spectra (Figure 4a and c) showed peaks indicative of the dissociated monomer only. The mass of the subunit was determined to 25.5 and 26.3 kDa using DHB and AMNP as matrix respectively.

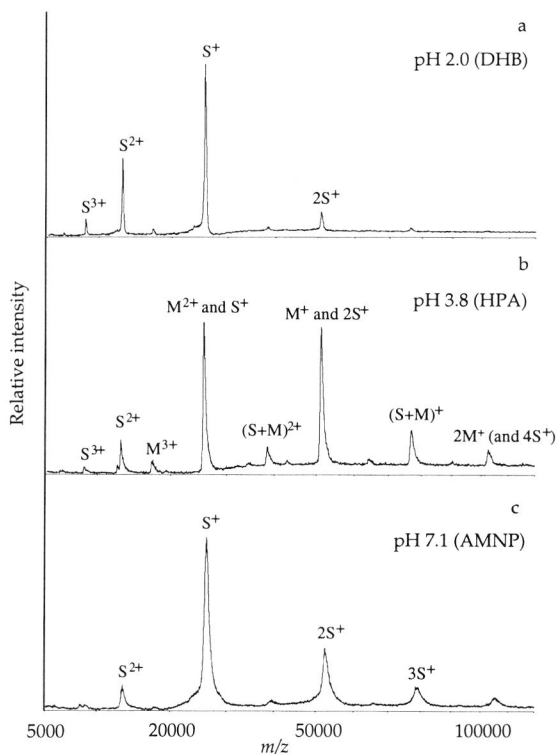


**Figure 4.** Comparison of MALDI mass spectra of glutathione-S-transferase obtained at different pH with three different matrix compounds (a) DHB in water (pH 2); (b) HPA in water (pH 3.8); and (c) AMNP in water (pH 7.1). All spectra were obtained under subsequent irradiation of the same sample area (sum of 20-30 laser shots). Peaks corresponding to the dissociated and undissociated subunits are denoted by S and M respectively.

#### Human hemoglobin

In contrast to the identical subunits composing recombinant streptavidin and GSH transferases A1-1, human hemoglobin is a more complex non-covalent tetrameric protein consisting of two identical  $\alpha$  subunits (141 amino acids, mass 15 125) and two identical  $\beta$  subunits (146 amino acids, mass 15 865) in addition to the heme moiety (616 Da) non-covalently bound to each chain.

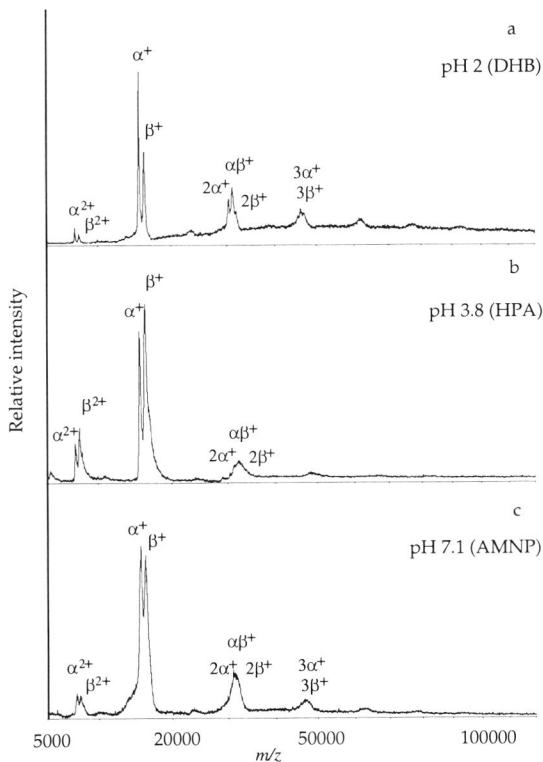


**Figure 5.** Comparison of MALDI mass spectra of human hemoglobin obtained at different pH with three different matrix compounds (a) DHB in water (pH 2); (b) HPA in water (pH 3.8); and (c) AMNP in water (pH 7.1). All spectra were obtained under subsequent irradiation of the same sample area (sum of 20–30 laser shots). Peaks corresponding to the dissociated  $\alpha$  and  $\beta$  chains of human hemoglobin are denoted by  $\alpha$  and  $\beta$  respectively.

When hemoglobin was prepared with either of the three matrices DHB, HPA or AMNP, only ion signals related to the individual  $\alpha$  and  $\beta$ -subunits were obtained (Figure 5a, b and c respectively). With the more acidic matrix DHB (Figure 5a) the three cluster ions obtained just above 30 kDa could be assigned to the homo dimers  $2\alpha$  and  $2\beta$  and the hetero dimer  $\alpha\beta$ , whereas these signals were unresolved when HPA (Figure 5b) or AMNP (Figure 5c) were used as matrices. In contrast to the results obtained for recombinant streptavidin and GSH transferases A1-1, it was not possible to maintain the physiologically significant tetrameric forms of human hemoglobin during MALDI-MS analysis with HPA as matrix (Figure 5b). Previous studies have shown that hemoglobin fully dissociates in solution into predominantly  $\alpha/\beta$  dimers at pH 3.8 [11].

Increasing the HPA matrix solution from pH 3.8 to pH 7, aimed at preventing the dissociation into the  $\alpha$  and  $\beta$  subunits, revealed no significant change in the ion signal pattern (results not shown). Since dissociation of the non-covalent structure can occur not only in solution, or during the transition from solution to solid phase, but also upon desorption/ionization after laser irradiation, photo-dissociation could be the reason for the unsuccessful detection of the  $\alpha_2\beta_2$  complex.

All ions detected represent species without the heme group (apohemoglobin). As found for the quadrupled Nd-YAG laser of 266 nm with nicotinic acid as matrix, the dissociation of the heme group from the protein has been induced by the laser irradiation upon the strong deposition of energy [11].

## **Conclusion**

The ability to detect non-covalent complex ions in MALDI MS was highly dependent on the choice of matrix. Among the six tested matrices, specific non-covalent interactions, could only be observed with HPA as matrix. In the case of recombinant streptavidin and GST A1-1, the non-covalent forces holding the subunits together were sufficiently strong to maintain the physiologically significant complex forms under the conditions employed with HPA as matrix. Whereas for human hemoglobin it was not possible to maintain the tetrameric complex with neither of the matrices tested.

In contrast to previous studies [13,17] the "first laser shot phenomena" was not observed for neither streptavidin nor GST A1-1. The spectra were obtained under subsequent irradiation of the same sample area, indicating that the intact complexes are incorporated equally well at all level within the HPA matrix crystal.

Although the more acidic pH of the commonly used DHB and HCCA matrix solutions may be responsible for the dissociation of the proteins into subunits, unexpectedly dissociation of recombinant streptavidin and GST A1-1 complexes was not induced when lowering the pH of the HPA matrix solution. In addition, when the samples were prepared with more basic matrices ANA (pH 4.4), NA (pH 6.4) and AMNP (pH 7.1) only ion signals corresponding to the individual subunits appeared in the MALDI spectra. Considering these results there does not appear to be a strong correlation between the matrix solution pH and the utility of a matrix for the analysis of non-covalent bound complexes, indicating that the matrix itself appears to be a key factor in the MALDI process. In addition, the unsuccessful detection of the hemoglobin  $\alpha_2\beta_2$  complex indicate that the stability of non-covalent complexes might depend upon the deposition of the energy induced by the laser irradiation. Elucidation of matrix chemistry and desorption mechanism(s) will be of crucial importance for further development in this field.

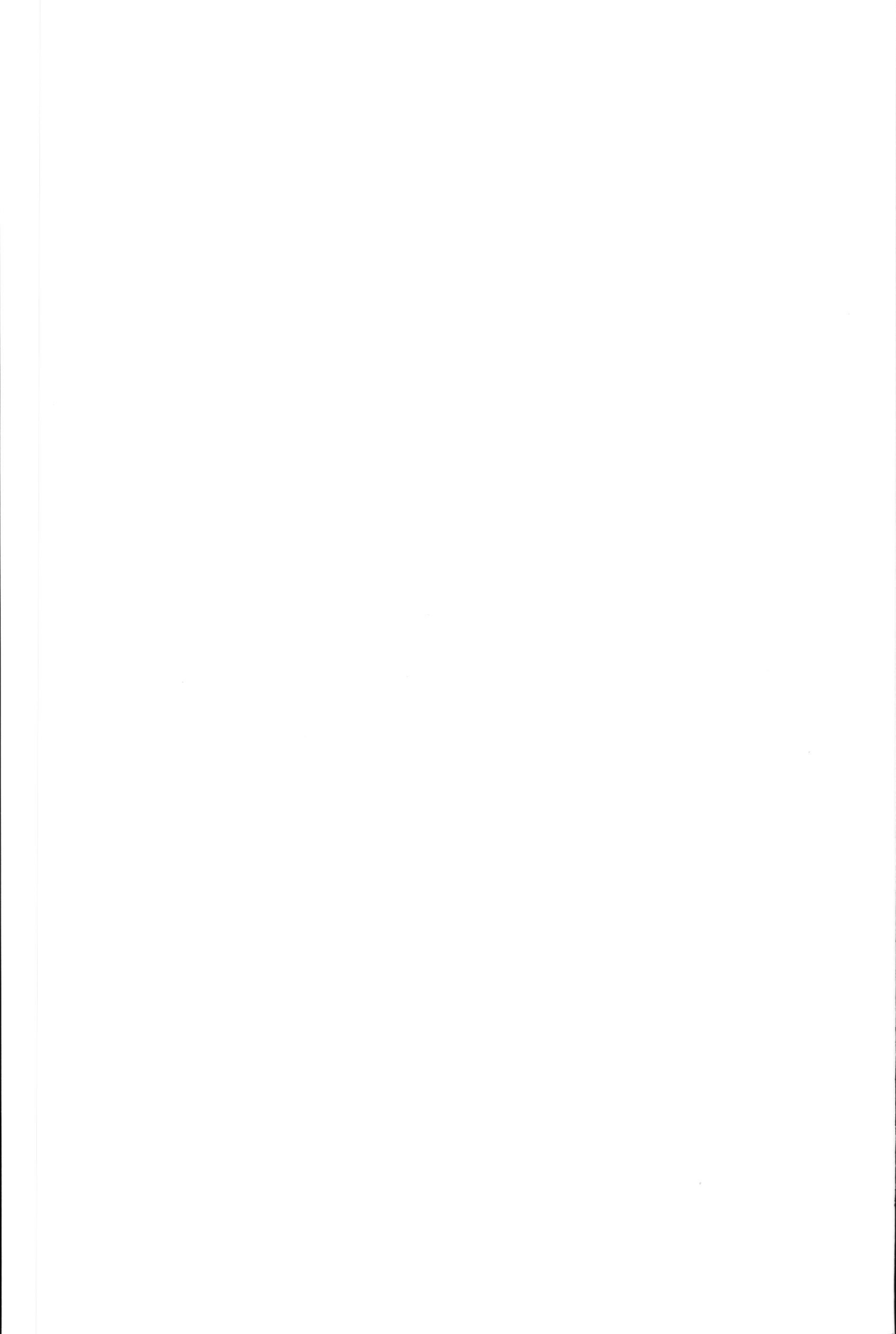
## References

- [1] J. B. Fenn, M. Mann, C. K. Meng, S. F. Wong and C. M. Whitehouse, *Science*, **1989**, 246, 64-71.
- [2] J. B. Fenn, M. Mann, C. K. Meng, S. F. Wong and C. M. Whitehouse, *Mass Spectrom. Rev.*, **1990**, 9, 37-70.
- [3] M. Karas and F. Hillenkamp, *Anal. Chem.*, **1988**, 60, 2299-2301.
- [4] M. Karas, D. Bachmann, U. Bahr and F. Hillenkamp, *Int. J. Mass Spectrom. Ion Processes*, **1987**, 78, 53-68.
- [5] B. Ganem, Y. Li and J. D. Henion, *J. Am. Chem. Soc.*, **1991**, 113, 6294-6296.
- [6] B. Ganem, Y. Li and J. D. Henion, *J. Am. Chem. Soc.*, **1991**, 113, 7818-7819.
- [7] J. A. Loo, *Bioconjugate Chem.*, **1995**, 6, 644-665.
- [8] M. Przybylski and M. O. Glocker, *Angew. Chem. Int. Ed. Engl.*, **1996**, 35, 806-826.
- [9] M. Karas, U. Bahr, A. Ingendoh and F. Hillenkamp, *Angew. Chem. Int. Ed. Engl.*, **1989**, 28, 760-761.
- [10] M. Karas, U. Bahr, A. Ingendoh, E. Nordhoff, B. Stahl, K. Strupat and F. Hillenkamp, *Anal. Chim. Acta*, **1990**, 241, 175-185.
- [11] F. Hillenkamp, M. Karas, A. Ingendoh and B. Stahl, in A. L. Burlingame and J. A. McCloskey (Eds), *Biological Mass Spectrometry*, Amsterdam, Elsevier Science Publishers B. V., **1990**, 49-60.
- [12] M. J.-F. Suter, W. T. Moore, T. B. Farmer, J. S. Cottrell and R. M. Caprioli, in R. H. Angeletti (Eds), *Techniques in Protein Chemistry III*, San Diego, CA, Academic Press, Inc., **1992**, 447-455.
- [13] B. Rosinke, K. Strupat, F. Hillenkamp, J. Rosenbusch, N. Dencher, U. Krüger and H.-J. Galla, *J. Mass Spectrom.*, **1995**, 30, 1462-1468.
- [14] M. Moniatte, F. G. v. d. Goot, J. T. Buckley, F. Pattus and A. v. Dorsselaer, *FEBS Lett.*, **1996**, 384, 269-272.
- [15] P. Lecchi and L. K. Pannell, *J. Am. Soc. Mass Spectrom.*, **1995**, 6, 972-975.
- [16] M. O. Glocker, S. H. J. Bauer, J. Kast, J. Volz and M. Przybylski, *J. Mass Spectrom.*, **1996**, 31, 1221-1227.
- [17] L. R. H. Cohen, K. Strupat and F. Hillenkamp, *J. Am. Soc. Mass Spectrom.*, **1997**, 8, 1046-1052.
- [18] D. Dogruel, R. W. Nelson and P. Williams, *Rapid Commun. Mass Spectrom.*, **1996**, 10, 801-804.
- [19] H. Ehring, M. Karas and F. Hillenkamp, *Org. Mass Spectrom.*, **1992**, 27, 472-480.
- [20] M. C. Fitzgerald, G. R. Parr and L. M. Smith, *Anal. Chem.*, **1993**, 65, 3204-3211.
- [21] K. J. Wu, A. Steding and C. H. Becker, *Rapid Commun. Mass Spectrom.*, **1992**, 7, 142-146.
- [22] F. Hillenkamp and M. Karas, in J. A. McCloskey (Eds), *Mass Spectrometry, Methods in Enzymology*, 193, San Diego, California, USA, Academic Press, Inc., **1990**, 280-294.

## **Chapter 5**

---

Identification of multiple target sites for a glutathione conjugate on glutathione-S-transferase by MALDI-MS



---

# Identification of multiple target sites for a glutathione conjugate on glutathione-S-transferase by MALDI-MS

*A mass spectrometric method providing qualitative site-specific information regarding covalent modification of proteins is described. The method involves comparison of unmodified and modified proteins by matrix-assisted laser desorption/ionization mass spectrometry (MALDI-MS) peptide mapping in combination with site-specific mutagenesis of possible target amino acids. The approach is demonstrated through the mapping of glutathione-S-transferases (GSH transferases) before and after inhibition with the glutathione conjugate 2-(S-glutathionyl)-3,5,6-trichloro-1,4-benzoquinone (GSTCBQ). The results demonstrate the utility of site-specific mutagenesis in combination with MALDI-MS peptide mapping. Evidence is presented that three residues in or near the active site, including the hydroxyl groups of Tyr<sub>6</sub> and Tyr<sub>115</sub> and the sulfhydryl group of Cys<sub>114</sub> are target site for GSTCBQ. Although only one GSTCBQ molecule per active site was detected, it appears to be distributed among all three target sites. In addition, MALDI-MS peptide mapping covered 81% of the cDNA deduced amino acid sequence for GSH transferase and site directed mutagenesis corresponding to a single amino-acid substitution were verified.*

---

## Introduction

Since the introduction of matrix-assisted laser desorption/ionization (MALDI) mass spectrometry (MS) [1,2] numerous studies have demonstrated the large potential of this technique for structural analysis of proteins and peptides. This method allows direct analysis of intact biomolecules up to several 100 kDa [3]. Besides molecular mass information of intact proteins, the ability to analyse complex mixtures in the presence of large molar excesses of ionic contaminants and common buffer components make MALDI-MS a useful technique for mass spectrometric peptide mapping [4-7]. Peptide mapping is a valuable and efficient mean of protein characterisation and/or identification. The basic premise of peptide mapping is to enzymatically or chemically cleave a protein into a number of smaller peptides, directly followed by mass spectrometric analysis. In this way a complete peptide map can be obtained without the need for time and sample-consuming separation procedures. The ability to measure the molecular masses of each peptide permits further examination of the primary structure of the protein allowing post-translational modifications, disulphide bridges and mutated sites to be localised.

---

A strategy designed to reveal site specific information regarding covalent modification of proteins is described in this paper. The approach is demonstrated through the mapping of glutathione-S-transferases (GSH transferases) before and after inhibition with glutathione conjugate 2-(S-glutathionyl)-3,5,6-trichloro-1,4-benzoquinone (GSTCBQ). GSH transferases are a group of isoenzymes that catalyse the addition of the tripeptide glutathione (GSH) to numerous electrophilic compounds. This reaction is considered crucial for the detoxification of endogenous and xenobiotic substances [8-11]. Although GSH transferases serve a detoxification function, inhibitors of the enzymes are of considerable interest as a potential mechanism to overcome the drug resistance of certain tumor cells, encountered in the chemotherapy of cancer. The glutathione conjugate GSTCBQ is an inhibitor designed to resemble a substrate of GSH transferases. The inhibition is due to the covalent binding of this very reactive reagent in the active site of the enzyme, resulting in the modification of a single amino acid [12,13]. The identity of the target residue(s) in the inactivation of GSH transferases with GSTCBQ has not been established.

The strategy includes comparison of unmodified and GSTCBQ-modified proteins by MALDI-MS peptide mapping, allowing the identification of peptide(s) that arise due to the GSTCBQ treatment. Further evidence for the GSTCBQ modified amino acid residue(s) was achieved by site-specific mutagenesis in which the functional groups of three potential target residues in or near the active site have been individually substituted.

## Experimental

### *Materials*

The 2,5-dihydroxybenzoic acid (DHB) and 2-hydroxy-5-methoxybenzoic acid (HMB) was purchased from Aldrich Chemie (Steinheim, Germany). V8 protease from *Staphylococcus aureus* was obtained from Boehringer Mannheim (Mannheim, Germany) and cyanogen bromide from Merck (Darmstadt, Germany). The three calibrants chymotrypsinogen A (molecular mass 25656.1), horse heart cytochrome c (molecular mass 12360.1) and bovine insulin (molecular mass 5733.6) were all from Sigma (St. Louis, MO, USA).

The synthesis of the inhibitor 2-(S-glytathionyl)-3,5,6-trichloro-1,4-benzoquinone (GSTCBQ) was formed as decribed previously [13]. Recombinant isoenzyme 3-3, the cysteine mutant C114S and the tyrosine mutants Y6F and Y115F were prepared as previously described [14-16].

*Covalent incorporation of GSTCBQ.*

A 3.0 ml solution (pH 6.5) of 10  $\mu$ M native or mutant enzyme was incubated with 100  $\mu$ M GSTCBQ for 10 min at 25 °C. The reaction was stopped with ascorbic acid (final concentration 10 mM) and dialyzed three times overnight against three changes of 3 litres of a 0.1% solution of formic acid (v/v). The sample was lyophilized.

*Enzymatic and chemical cleavage*

For the GSTCBQ-modified native and mutant (Y6F, C114S and Y115F) enzymes plus their unmodified controls (in total eight samples), two types of peptide mixtures were generated. Digestion by V8 protease from *Staphylococcus aureus* (w/w 1:20) was carried out in 0.05 M ammonium acetate (pH 4) for 5 hours at 37 °C and cyanogen bromide cleavage was carried out in a 1/50 molar ratio of methionine/cyanogen bromide in 70 % v/v formic acid for 24 hours. The peptide mixtures were lyophilized.

*Sample preparation for mass spectrometry*

Prior to V8 protease digestion a 5-10  $\mu$ l aliquot was withdrawn for MALDI mass spectrometric analysis of intact GSTCBQ-modified and unmodified enzymes. An equivalent volume of matrix was added to give a concentration of 1 pmol/ $\mu$ l.

A 9:1 mixture of a 2,5-dihydroxybenzoic acid (DHB) in 0.1 % trifluoroacetic acid (TFA) and 2-hydroxy-5-methoxybenzoic acid (HMB) in ethanol both at a concentration of 10 mg/ml was used as matrix for the analysis of the intact proteins. This matrix mixture is referred to as super-DHB (sDHB) [17].

The unfractionated peptide mixtures were reconstituted in 0.1% TFA and mixed 1:1 (v/v) with a 10 mg/ml solution of DHB in 0.1% TFA to a concentration of 5 pmol/ $\mu$ l. A 1  $\mu$ l volume of the sample-matrix solution was deposited directly onto a stainless-steel target, air dried and introduced to the mass spectrometer.

*Mass spectrometry*

All spectra were obtained using a VISION 2000 laser desorption reflectron time-of-flight instrument (Finnigan MAT, Bremen, Germany) equipped with a nitrogen laser (337 nm). The laser beam was focused by a quartz lens system onto the sample. The ions were accelerated to a potential of 6.5 kV in the ion source and post-accelerated by a conversion dynode in front of the detector to a potential of 20 kV when analyzing the intact proteins and 10 kV when analyzing the peptide mixtures. The effective drift length of the instrument was 1.7 m. Ions were detected by a secondary electron multiplier and the signal was amplified and digitized by a high speed transient recorder linked to a

486 personal computer. All spectra were obtained in positive-ion reflector mode, 20-30 single shot spectra were accumulated in order to obtain a good signal-to-noise ratio. The MALDI spectra of the intact proteins were externally calibrated using chymotrypsinogen A from a second preparation on the same target. The MALDI peptide map spectra of the unfractionated peptide mixtures were first externally calibrated with horse heart cytochrome c or bovine insulin. A more accurate mass assignment of the peptide mixtures was achieved by using two of the identified peptide fragments together with a matrix-ion as internal calibrants. The analyte peaks employed as internal calibrants did not contain the potential GSTCBQ modification sites.

### *Nomenclature*

Peptides are named by letter codes indicating the cleavage method used, (V for V8 protease and C for cyanogen bromid) followed by a number indicating the position of the peptide relatively to the N-terminal of the intact protein.

The abbreviations used for the three mutant proteins are:

- Y6F        substitution of tyrosine, amino acid number 6, with a phenylalanine residue
- C114S     substitution of cysteine, amino acid number 114, with a serine residue
- Y115F     substitution of tyrosine, amino acid number 115, with a phenylalanine residue

The abbreviations used for the inhibitors are:

- GSTCBQ:    2-(S-glytathionyl)-3,5,6-trichloro-1,4-benzoquinone
- GSTCHQ:    2-(S-glytathionyl)-3,5,6-trichloro-1,4-hydroquinone
- GSDCHQ:    2-(S-glytathionyl)-dichloro-1,4-hydroquinone
- GSMCHQ:    2-(S-glytathionyl)-monochloro-1,4-hydroquinone

## **Results and discussion**

### *Strategy*

The strategy employed for identification of the target residue(s) involved in the inactivation of glutathione-S-transferases (GSH transferases) by 2-(S-glytathionyl)-3,5,6-trichloro-1,4-benzoquinone (GSTCBQ) is outlined in Figure 1. Three mutants GSH transferases, in which the functional groups of three potentially target residues in or near the active site have been individually substituted were used. These include the hydroxyl groups of Tyr<sub>6</sub> (Y6F) and Tyr<sub>115</sub> (Y115F) and the sulfhydryl group of Cys<sub>114</sub> (C114S), substituted with phenylalanine and serine respectively. Initially, the molecular masses of intact rat GSH transferases and mutant proteins were obtained before and

after incubation with GSTCBQ. Subsequently, the unmodified and GSTCBQ-modified proteins were cleaved with both V8 protease and cyanogen bromide. Mass spectrometric peptide maps were established by direct MALDI-MS analysis of the peptide mixtures. The GSTCBQ modified peptides were identified by comparison of the peptide maps of unmodified and GSTCBQ-modified proteins in combination with the cDNA deduced sequence for GSH transferases [10]. The assumption was made that one chlorine atom of GSTCBQ is displaced upon reaction with either cysteine or tyrosine and that the bound adduct was in the hydroquinone oxidation state due to the reduction of quinone with ascorbate, giving an expected mass gain, upon adduct formation, of 482 mass units (2-(S-glythionyl)-dichloro-1,4-hydroquinone, GSDCBQ).

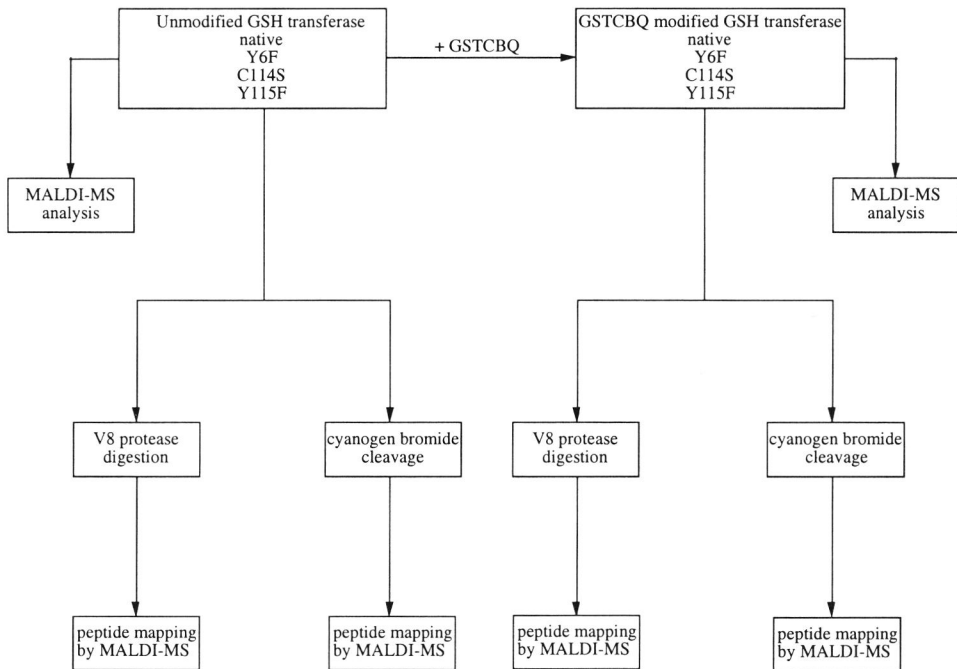


**Figure 1.** Outline of the strategy used to reveal the GSTCBQ modified target residue(s) in rat GSH transferases.

#### MALDI-MS of intact GSH transferases

The calculated molecular masses together with the results obtained by MALDI-MS of intact unmodified and GSTCBQ-modified GSH transferases for the native and the three

mutants are given in Table 1. The determined values for unmodified proteins for both native and the three mutants are in average  $188 \pm 38$  Da above the calculated values. Comparison of the peak width of molecular ion peaks from the GSH transferases and that from the calibrant (chymotrypsinogen A) shows that the sample peaks are extremely broad. The poor mass accuracy is therefore supposed to be due to non-resolved adducts formed between analyte and matrix.

The mass difference of intact unmodified GSH transferases compared with intact GSTCBQ- modified GSH transferases, suggested that approximately one 2-(S-glutathionyl)-dichloro-1,4 hydroquinonyl group (GSDCHQ) was attached to the native enzyme as well as to the three mutants. The average measured increase in molecular mass was  $482 \pm 63$  Da as compared with an expected increase of 482 Da by the incorporation of one GSTCBQ molecule.

These results could lead to the conclusion that none of the three mutated residues is covalently modified by GSTCBQ. Although none of the three mutated residues are crucial in the inactivation of the GSH transferase by GSTCBQ, one or more of the three residues might still participate, substitution of one residue could simply redirect the modification to another target site. The GSTCBQ attachment site(s) to GSH transferase was further examined by comparative peptide mapping of unmodified and modified GSH transferases.

**Table 1** Calculated and MALDI MS measured molecular mass values of intact unmodified and GSTCBQ-modified GSH transferase

Enzyme	Calculated mass unmodified	Measured mass*		Mass difference modified-un modified	Number of GSDCHQ
		unmodified	modified		
native	25783	26012	26483	471	~1
Y6F	25767	25966	26379	413	~1
C114S	25767	25951	26427	476	~1
Y115F	25767	25906	26472	566	~1

\* All masses are an average of two measurements externally calibrated with chymotrypsinogen A

#### *Peptide mapping of unmodified and modified GSH transferases by MALDI-MS*

Peptide mixtures were generated by the cleavage of native and Y6F, C114S and Y115F mutated GSH transferase with V8 protease or cyanogen bromide before and after incubation with GSTCBQ. The resulting peptide mixtures were directly analyzed by MALDI-MS without further purification. The mass axis was internally calibrated using one peak from the matrix and two from the analyte. When the masses of the expected peptides are known the other peptides in the mixture will serve as an internal verification of proper calibration. In this case a mass accuracy better than  $\pm 0.5$  Da was achieved for

most peptides. The calculated molecular masses of the V8 protease (V) and cyanogen bromide (C) peptides and those observed in the corresponding spectra for both native and the three mutant proteins are given in Table 2 and 3, respectively.

**Table 2** Molecular mass values of the peptides derived by digestion of native GSH transferase and its mutants with V8 protease, as determined by MALDI-MS of the peptide mixtures and calculated based on the cDNA deduced sequence.

Peptide	aa position	Calculated mass	native	Observed mass*		
				Y6F	C114S	Y115F
V1	1-21	2493.0	<u>2493.0</u>	<u>2477.0</u>	2492.9	2493.2
V1-4	1-48	5765.5	<u>5765.9</u>	<u>5749.6</u>	5765.7	5764.8
V2+K <sup>+</sup>	22-28	903.7	902.6	903.0	-	903.4
V2-4	22-48	3291.5	3291.8	3291.2	3291.6	3291.6
V3-4	29-48	2445.6	2445.4	2445.8	2445.5	2445.8
V4	30-48	2316.5	2316.6	2316.7	2316.4	2316.4
V5	49-88	4646.5	-	-	-	-
V6-9	89-100	1460.6	1460.4	1460.3	1460.7	1460.5
V7-9	91-100	1230.4	1230.6	1230.4	1230.8	1230.4
V8-9	92-100	1101.3	1101.3	1101.1	1101.6	1101.3
V9	93-100	972.1	972.2	972.3	972.5	972.2
V10	101-120	2475.9	-	-	<u>2460.2</u>	<u>2461.5</u>
V10-11	101-125	3086.6	3086.5	-	<u>3070.4</u>	<u>3070.4</u>
V12	126-132	848.0	848.2	848.1	848.2	848.1
V13	133-139	899.1	899.1	899.3	899.1	899.2
V14	140-180	5875.8	-	-	-	-
V15	189-217	3335.0	3334.5	3335.1	3335.0	3334.9

\* Deviations between measured and calculated masses are underlined

**Table 3** Molecular mass values of peptides derived by cleavage of native GSH transferase and its mutants with cyanogen bromide, as determined by MALDI-MS of the peptide mixtures and calculated based on the cDNA deduced sequence. All the values except the one containing the C-terminal peptide correspond to the homoserine lactone product.

Peptide	aa position	Calculated mass	native	Observed mass*		
				Y6F	C114S	Y115F
C1	1-2	199.2	-	-	-	-
C2	3-34	3841.4	3841.5	<u>3825.2</u>	3841.4	3841.1
C3	35-76	4781.4	4781.3	4781.4	4781.3	4781.4
C4	77-104	3349.7	3350.0	3349.8	3349.8	3350.2
C5	105-108	487.5	487.3	487.7	487.5	487.6
C6 + Na <sup>+</sup>	109-112	478.5	478.3	478.0	478.2	478.9
C7	113-134	2652.1	2652.0	2651.8	<u>2635.9</u>	<u>2636.0</u>
C8	135-197	7440.6	-	-	-	-
C9	198-217	2342.7	2342.6	2342.7	2342.7	2342.8

\* Deviations between measured and calculated masses are underlined

Several peaks in the V8 protease digest spectra indicated incomplete digestion of the proteins, whereas the cyanogen bromide cleavage was completed. The small dipeptide C1 and peptide V5, V14 and C8, being the most hydrophobic peptides, were not observed. Taken together, the two cleavages reveal 81 % of the amino acid sequence, i.e., 176 of 217 amino acid residues were mapped. As expected, peptides from the individually mutated GSH transferases that contain the Y6F (peptide V1 and C1), C114S or Y115F (peptide V10 and C7) mutation sites were observed to be shifted 16 mass units lower than the corresponding peptides from the native protein.

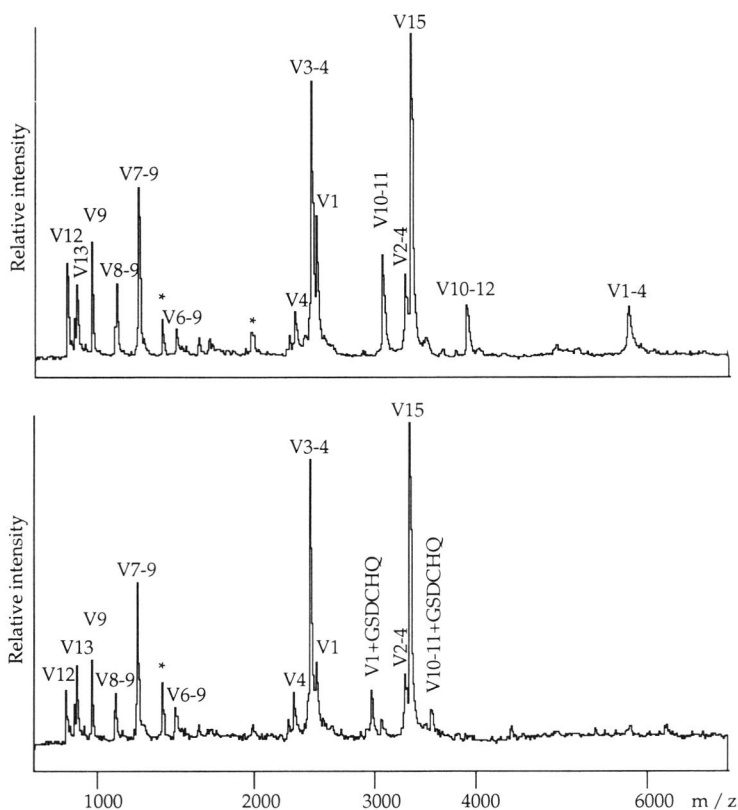


**Figure 2.** Matrix-assisted laser desorption/ionization mass spectra of the peptide mixtures derived by V8 protease cleavage of (A) unmodified and (B) GSTCBQ modified C114S mutated GSH transferase. Peaks corresponding to auto-digestion of V8 protease are labeled with an asterisk.

Peptides that arise as a consequence of GSTCBQ treatment were identified by an individual comparison of the V8 protease or cyanogen bromide generated peptide maps of unmodified and GSTCBQ-modified for native and Y6F, C114S and Y115F mutated GSH transferases. Comparative peptide mapping is illustrated for V8 protease digestion of the C114S mutant in Figure 2 and for cyanogen bromide cleavage of the native protein in Figure 3. Mass differences in the spectra corresponding to 482 mass units (incorporation of GSTCBQ as GSDCBQ) indicate that more than one peptide were covalently modified upon GSTCBQ treatment.

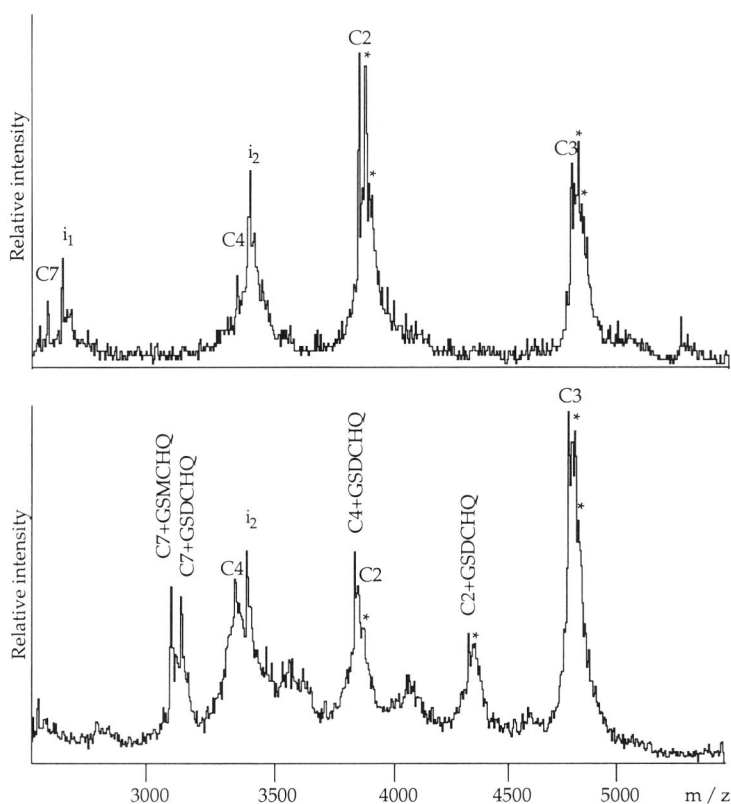


**Figure 3.** Matrix-assisted laser desorption/ionization mass spectra of the peptide mixtures derived by cyanogen bromide cleavage of (A) unmodified and (B) GSTCBQ modified native GSH transferase. The signals except the one containing the C-terminal peptide correspond to the homoserine lactone product. Peaks corresponding to formylation of one or more amino groups (mass shift of 28) are labeled with an asterisk and  $i_1$  and  $i_2$  refer to unidentified peaks.

The predicted molecular masses of the peptide-GSTCBQ adducts and those determined by the two MALDI-MS peptide mappings are summarised in Table 4. For native GSH transferase a mass shift corresponding to the GSTCBQ modification was identified for all peptides that include the three potential target sites, Tyr<sub>6</sub>, Cys<sub>114</sub> and Tyr<sub>115</sub>. Similar results were obtained for the C114S and Y115F mutated GSH transferases, whereas peaks corresponding to GSTCBQ modification of peptides V1 and C2, in which the potential target residue tyrosine had been substituted with phenylalanine, were missing from the peptide maps of Y6F mutated GSH transferase.

**Table 4** Molecular mass values and identification of GSTCBQ modified peptides obtained from V8 protease and cyanogen bromide peptide mapping of native and mutated GSH transferase.

Peptide	aa position	Target site	Calculated mass		Observed mass		
				native	Y6F	C114S	Y115F
V1	1-21	Y6	2493.0	2493.1	2477.2	2493.0	2493.3
V1 + GSDCHQ	1-21	Y6	2973.2	2974.1	-	2974.7	2974.3
V1-4	1-4	Y6	5765.5	5765.2	5749.6	5763.4	5765.5
V1-4 + GSDCHQ	1-4	Y6	6245.7	6246.8	-	-	6245.5
V10-11	101-125	C114/Y115	3086.6	3085.3	-	3070.4	3070.4
V10-11 + GSDCHQ	101-125	C114/Y115	3566.8	3565.9	-	3552.1	3549.9
C2	3-34	Y6	3841.4	3841.5	3825.2	3841.4	3841.1
C2 + GSDCHQ	3-34	Y6	4321.6	4322.7	-	4323.8	4323.1
C4	77-104	C86/Y78	3349.8	3350.0	3349.8	3349.8	3350.2
C4 + GSDCHQ	77-104	C86/Y78	3830.0	3832.4	3830.3	3832.0	3829.5
C7	113-134	C114/Y115	2652.1	2652.0	2651.8	2635.9	2636.0
C7 = GSDCHQ	113-134	C114/Y115	3132.3	3134.1	3135.4	3118.8	3118.1
C7 = GSMCHQ	113-134	C114/Y115	3097.8	3097.5	3098.5	-	-

The results strongly indicate that the side chain of Tyr<sub>6</sub> is the GSTCBQ-attachment site on peptide V1 and C2, this was further supported by Edman degradation [18]. The preserved modification of peptides C7 and V10-11, containing either target site Cys<sub>114</sub> or Tyr<sub>115</sub>, in the C114S and Y115F mutants, suggests that both residues can react with GSTCBQ. The cyanogen bromide mapping of modified native (Figure 3) and Y6F mutated GSH transferase revealed an additional modification of peptide C7 corresponding to the loss of a second chlorine atom (C7 + 2-(S-glytathionyl)-monochloro-1,4-hydroquinone, GSMCHQ), this could arise from an internal cross-linking of Cys<sub>114</sub> and Tyr<sub>115</sub> by GSTCBQ. No peak related to C7-GSMCHQ was found when the functional group of either Cys<sub>114</sub> or Tyr<sub>115</sub> had been substituted. This further supports that both residues are target sites for modification by GSTCBQ. Finally, the cyanogen bromide cleavage gives a GSTCBQ modification of an additional peptide C4, presumably involving either residue Tyr<sub>78</sub> and/or Cys<sub>86</sub>.

Taken together, the two peptide maps clearly reveal multiple target sites of covalent modification of the GSH transferase by GSTCBQ. This is a function of the fact that the trichlorobenzoquinonyl group of GSTCBQ has multiple electrophilic sites of very high reactivity. Molecular modeling studies (for more detail see ref. 18) indicated that the two tyrosyl residues (Tyr<sub>6</sub> and Tyr<sub>115</sub>) are appropriately positioned to participate in the chemical modification of the GSH transferase. Although at least two other residues were modified they seemed more unlikely to be involved in the inactivation of GSH transferase.

### **Conclusion**

Comparative peptide mapping of unmodified and modified proteins allowed the identification of the peptides that arise as a consequence of modification of GSH transferase by GSTCBQ. In addition the precise location of modified residues were explored combining comparative peptide mapping with site-directed mutagenesis of potential target amino acids in the active site of GSH transferase.

GSH transferase was found to be modified by one GSTCBQ molecule per active site, which appears to be distributed among three different GSTCBQ target sites (Tyr<sub>6</sub>, Cys<sub>114</sub> and Tyr<sub>115</sub>) located in the active site of GSH transferase. The reaction of GSTCBQ with other residues than Tyr<sub>6</sub>, Cys<sub>114</sub> and Tyr<sub>115</sub> within the modified peptides can not be ruled out. The exact site of attachment is only inferred from the inability to observe a GSTCBQ modification of the peptides which included a mutated target site in comparison to the observed GSTCBQ modification of the same non-mutated peptides. Here the performance of dual peptide mapping, permitted further confidence in the given results.

The approach combining comparative peptide mapping and site directed mutagenesis is proposed as a general strategy for identification of modification sites in proteins.

### **Acknowledgement**

We thank Professor Richard N. Armstrong, Vanderbilt University, Department of Biochemistry, Nashville Tennessee, U.S.A. for generously providing the cysteine C114S and tyrosine Y6F and Y115 F mutant GSH transferases. Sonja Jespersen is grateful to the Danish Research Academy for financial support of this investigation.

## References

- [1] F. Hillenkamp, M. Karas, R. C. Beavis and B. T. Chait, *Anal. Chem.*, **1991**, 63, 1193-1203.
- [2] M. Karas and F. Hillenkamp, *Anal. Chem.*, **1988**, 60, 2299-2301.
- [3] M. Karas, U. Bahr, A. Ingendoh and F. Hillenkamp, *Angew. Chem. Int. Ed. Engl.*, **1989**, 28, 760-761.
- [4] T. M. Billeci and J. T. Stults, *Anal. Chem.*, **1993**, 65, 1709-1716.
- [5] R. C. Beavis and B. T. Chait, *Proc. Natl. Acad. Sci. USA*, **1990**, 87, 6873-6877.
- [6] A. Tsarbopoulos, M. Karas, K. Strupat, B. N. Pramanik, T. L. Nagabhushan and F. Hillenkamp, *Anal. Chem.*, **1994**, 66, 2062-2070.
- [7] T.-T. Yip and T. W. Hutchens, *FEBS Letters*, **1992**, 308, 149-153.
- [8] R. N. Armstrong, *Chem. Res. Toxicol.*, **1991**, 4, 131-140.
- [9] R. N. Armstrong, *Adv. Enzymol. Relat. Areas Mol. Biol.*, **1994**, 69, 1-44.
- [10] B. Mannervik and U. H. Danielson, *CRC Crit. Rev. Biochem.*, **1988**, 23, 283-337.
- [11] T. H. Rushmore and C. B. Pickett, *J. Biol. Chem.*, **1993**, 268, 11475-11478.
- [12] J. H. T. M. Ploemen, B. van Ommen and P. J. van Bladeren, *Biochem. Pharmacol.*, **1991**, 41, 1665-1669.
- [13] B. van Ommen, C. den Besten, A. L. M. Rutten, J. H. T. M. Ploemen, R. M. E. Vos, F. Müller and P. J. van Bladeren, *J. Biol. Chem.*, **1988**, 263, 12939-12942.
- [14] S. Liu, P. Zhang, X. Ji, W. W. Johnson, G. L. Gilliland and R. N. Armstrong, *J. Biol. Chem.*, **1992**, 267, 4296-4299.
- [15] X. Ji, P. Zhang, R. N. Armstrong and G. L. Gilliland, *Biochem.*, **1992**, 31, 10169-10184.
- [16] W. W. Johnson, S. Liu, X. Ji, G. L. Gilliland and R. N. Armstrong, *J. Biol. Chem.*, **1993**, 268, 11508-11511.
- [17] M. Karas, H. Ehring, E. Nordhoff, B. Stahl, K. Strupat, F. Hillenkamp, M. Grehl and B. Krebs, *Org. Mass Spectrom.*, **1993**, 28, 1476-1481.
- [18] J. H. T. M. Ploemen, W. W. Johnson, S. Jespersen, D. Vanderwall, B. van Ommen, J. van der Greef, P. J. v. Bladeren and R. N. Armstrong, *J. Biol. Chem.*, **1994**, 269, 26890-26897

## **Chapter 6**

---

Characterization of O-glycosylated precursors of  
insulin-like growth factor II by MALDI-MS



---

## Characterization of O-glycosylated precursors of insulin-like growth factor II by MALDI-MS

*High molecular weight precursors of insulin-like growth factor II (IGF II) were isolated from Cohn fraction IV of human plasma by ultrafiltration, affinity chromatography and reversed-phase high performance liquid chromatography (HPLC). Molecular mass determination by matrix-assisted laser desorption/ionization (MALDI) mass spectrometry of two high molecular weight IGF II preparations revealed heterogeneous glycosylation. A combination of enzymatic degradation and MALDI mass spectrometry was applied for further structural characterization of the glycosylated precursors of IGF II. The first step was molecular mass determination of intact high molecular mass IGF IIs prior to and after treatment with neuraminidase and O-glycosidase. This, together with a comparison of molecular mass information available from the cDNA, revealed that both high molecular mass IGF II species contain an identical C-terminal extension of 20 residues but different degree of glycosylation. Second, comparative Endo Glu-C digestion of the preparations prior to and after enzymatic release of carbohydrates and subsequent remeasurement of the molecular weight by MALDI-MS confirmed the primary structure of precursor IGF-II<sup>1-87</sup>. The O-linked carbohydrates were found to be associated with the C-terminal extension and the heterogeneity was identified as varied sialylated forms of one and two HexNAc-Hex groups.*

---

### Introduction

Matrix-assisted laser desorption/ionization (MALDI) [1,2] and electrospray ionization (ESI) [3-5] mass spectrometry have proved to be valuable techniques for precise mass determination of intact biomolecules up to several 100 kDa [6,7].

The accurately determined molecular mass of a protein in comparison with the predicted molecular mass deduced from the cDNA sequence of the corresponding gene, can confirm a predicted structure or differentiate between one or more structural possibilities. If the measured mass of the protein agrees with that calculated from the gene sequence, it is likely that the deduced sequence is correct. Any significant difference implies error in the cDNA-deduced sequence, post-translational modification or proteolytic processing of the protein. More detailed information concerning the nature and site of modification or processing event can be obtained by mass spectrometric peptide mapping. Peptide mapping involves enzymatically or chemically induced degradation of the protein, followed by further mass spectrometric measurement of the resulting

peptide fragments. Comparison of the accurately measured masses of the degradation products with those predicted from the cDNA-deduced sequence yields information on the sites and nature of modification and errors. MALDI MS is preferred for direct analysis of peptide mixtures, because no special sample handling is required, considerable amounts of salts can be tolerated, the sensitivity is high and the spectra are easy to interpret (for reviews see [8-9]).

Insulin-like growth factor II (IGF-II) is a single chain polypeptide of 67 amino acids (MW 7469.4 Da) [10] which occurs in human serum and most tissues of the body. The experimentally determined molecular weight (by mass spectrometry) of plasma-derived mature IGF-II corresponds well with the predicted value [11]. The primary IGF-II translation product contains 180 residues [12,13], including a 24 amino acid N-terminal signal peptide, the 67 residue mature IGF-II and an 89 amino acid extension at the C-terminus (Figure 1). Processing to the mature stage occurs by proteolytic removal of the signal peptide and stepwise cleavage of the C-terminal extension (designated E domain), presumably at mono- and di-basic residues. Incompletely processed higher molecular mass forms (10-15 kDa) of IGF-II have been detected in serum [14-16], cerebrospinal fluid [17] and brain [18]. These forms, also referred to as "big" IGF-II, are elevated in serum from patients with tumors, especially in non-islet cell tumor hypoglycemia [19-21]. Pro-IGF-II has no consensus N-linked glycosylation sites, but O-glycosylation of the E-domain at Thr<sup>75</sup> by sialic acid-containing oligosaccharides has been demonstrated [16]. This post-translational modification of the protein may be necessary for normal peptidase processing of pro-IGF-II [22].

This paper briefly describes the isolation and purification of higher molecular mass forms of IGF-II from human Cohn fraction IV and, in more detail, the extensive use of MALDI-MS for further characterization of the glycosylation and degree of proteolytic processing of human serum-derived IGF-II precursor molecules.

## Experimental

### *Materials*

The 2,5-dihydroxybenzoic acid (DHB) was purchased from Aldrich Chemie (Steinheim, Germany). The enzymes Neuraminidase, O-glycosidase and Endo Glu-C from *Staphylococcus aureus* were obtained from Boehringer Mannheim (Mannheim, Germany). Dithiothreitol (DTT) and the two calibrants, horse heart cytochrome c (molecular mass 12360.1) and bovine insulin (molecular mass 5733.6) were all from Sigma (St. Louis, MO, USA).

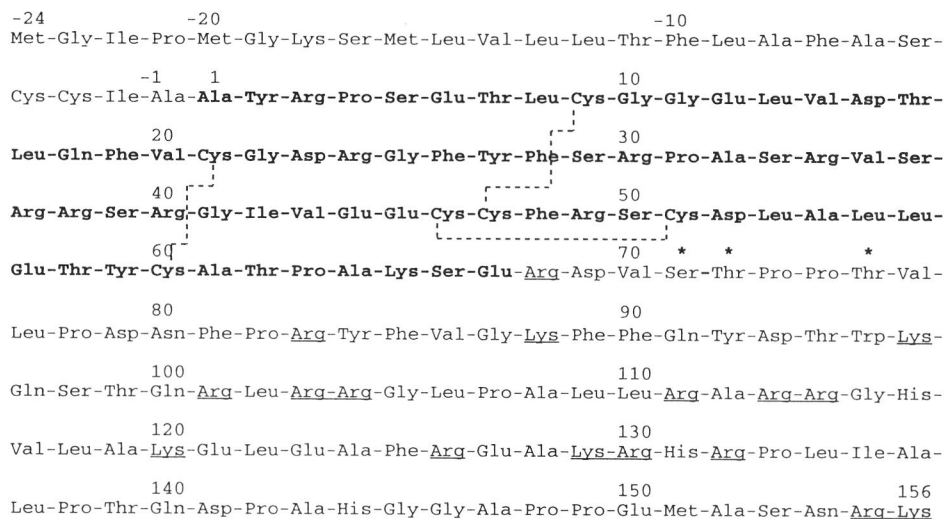


**Figure 1.** The deduced amino acid sequence of human preproIGF II. The amino acids are numbered by designating the first amino acid of mature IGF II (Ala) as 1; amino acids of the signal peptide are given negative numbers. The region corresponding to mature IGF II (residues 1-67) are given with bold letters. Single and pairs of basic residues in the E-domain are underlined and potential O-glycosylation sites in the E-domain are marked by an asterisk.

#### Purification of IGF-II precursors

IGF-II was measured by radioimmunoassay [23] using a monoclonal antibody (Amano Pharmaceutical Co. Ltd, Osaka, Japan).

IGF-II precursor molecules were derived from Cohn fraction IV of human plasma. The initial steps followed the procedure previously described for the isolation of IGF-I and IGF-II [11]. Briefly, The Cohn IV paste was extracted under acidic conditions by ultrafiltration between 30 and 2 kDa, concentrated by SP-Sephadex C-25 cation exchange chromatography and lyophilization, chromatographed on a CM-Sephadex CL-6B cation column and run on Sephadex G-50 under acidic conditions. Fractions with  $K_{av} > 0.42$  were again chromatographed on a neutral Sephadex G-75 column, where IGF-II immunoreactivity eluted between  $K_{av}$  0.04 and 0.3 (between  $M_r$  80 and 30 kDa). Since this preparation also contained IGF binding proteins, as measured by a charcoal binding assay, a further purification was needed. This was obtained by affinity chromatography

on two Affi-Gel 15 (Bio-Rad) columns connected in series to which IGF-II and IGF-binding protein 3 were coupled, respectively (purification of IGFBP-3 to be described elsewhere). The IGFBP-3 column was eluted with 0.3 M acetic acid, yielding IGF-II with no detectable binding protein activity. This preparation was gel-filtered on a Bio-Gel P-60 (Bio-Rad) column under acidic conditions to separate the native IGF-II from the pro-IGF-II precursor forms [24]. Final purification on reverse phase (RP) HPLC was achieved by two consecutive runs on Vydac C18 columns (large and small, respectively) using the neutral system II and one run on the small column using the acidic system I [11]. Finally two preparations were obtained, each consisting of approximately 90 µg protein (by weight), (termed A and B) with slightly different retention times on HPLC. N-terminal amino acid analysis (Institute for Biomembranes, Utrecht University, NL) yielded sequences consistent with IGF-II and indicated that the preparations were > 90% pure.

Preparation C was purified in the same way and had similar properties to preparations A and B.

#### *Release of oligosaccharides*

Untreated-preparations A and B were dissolved in water to a concentration of 0.25 µg/µl.

Neuraminidase treatment - N-Acetylneuraminic acids (sialic acids) were removed from preparations A and B by treatment with neuraminidase. An aliquot of the glycopeptides (10 µl) was incubated with 1 µl of neuraminidase (1 unit/ml) for 3h at 37 °C.

O-glycosidase treatment - Following neuraminidase treatment, O-linked oligosaccharides were removed from preparations A and B by treatment with O-glycosidase. An aliquot of the neuraminidase treated preparations (5.5 µl) was incubated with 0.5 µl of O-Glycosidase (0.5 unit/ml) for 18h at 37 °C.

#### *Proteolytic digestion*

To facilitate the proteolysis of untreated, neuraminidase and O-glycosidase treated preparations A and B, the disulfide bonds were first reduced with DTT. The reduction was carried out by addition of 2 µl of an 50 mM solution of DTT in 40 mM ammonium bicarbonate buffer (pH 8) to 5 µl of each sample solution at 37 °C for 1 hour.

Proteolytic digestion of the reduced preparations was carried out with Endo Glu-C from *Staphylococcus aureus* as enzyme. Approximately 10 µl of 100 mM ammonium acetate (pH 4) was added to the reduced preparations, pH was adjusted to 4 with acetic acid followed by the addition of 1 µl Endo Glu-C (1 µg/µl) giving an enzyme-to-substrate ratio of 1:1 w/w. The incubation was performed at 37 °C for 4 hours.

#### *Sample preparation for mass spectrometry*

Prior to and after Endo Glu-C digestion 1  $\mu$ l aliquots were withdrawn for MALDI mass spectrometric analysis of untreated, neuraminidase and O-glycosidase treated preparations A and B. The matrix 2,5-dihydroxybenzoic acid (DHB) was dissolved in 0.1 % trifluoroacetic acid (TFA) to a concentration of 10 mg/ml. The intact preparations and the peptide digests were diluted with matrix to a concentration of 2-8 pmol/ $\mu$ l, 1  $\mu$ l of this sample-matrix solution was deposited onto the target and dried under a cold air stream before loading into the mass spectrometer.

#### *Mass spectrometry*

All spectra were obtained using a VISION 2000 time-of-flight instrument (Finnigan MAT, Bremen, Germany) equipped with a nitrogen laser operating at a wavelength of 337 nm. The laser beam was focused by a quartz lens system onto the sample. The instrument was operated in either reflector or linear mode. In linear mode the ions were accelerated to a potential of 27 kV, in reflector mode to a potential of 6 kV in the ion source and post-accelerated by a conversion dynode in front of the detector to a potential of 10 kV. The effective drift length of the instrument was 88 cm in the linear mode and 170 cm in the reflector mode. In both modes the ions were detected by a secondary electron multiplier (SEM) and the signal was amplified and digitized by a high speed transient recorder linked to a 486 personal computer. All spectra were obtained in positive-ion mode, 20-30 single shot spectra were accumulated in order to obtain a good signal-to-noise ratio.

The MALDI spectra of the intact proteins were externally calibrated using horse heart cytochrome c from a second preparation on the same target. The MALDI peptide map spectra of the unfractionated peptide mixtures were first externally calibrated with bovine insulin. A more accurate mass assignment of the peptide mixtures was achieved by using two of the identified peptide fragments together with a matrix-ion as internal calibrants. The analyte peaks employed as internal calibrants did not contain any of the glycopeptides.

## **Results**

#### *Untreated*

Preparations A and B obtained from the last RP HPLC steps were analysed by MALDI mass spectrometry. The MALDI mass spectra of both preparations A and B showed the presence of several components (Fig 2A and 3A). A peak corresponding to mature IGF-II (amino acid 1-67) appeared in both preparations although more prominent in

preparations A than B. In addition, three and four distinct signals (designated peak B, C, D and E/F) in the higher mass area were obtained for preparations B and A, respectively. Mass differences ranging from 235 to 330 between adjacent signals suggested the presence of carbohydrates including sialic acids.

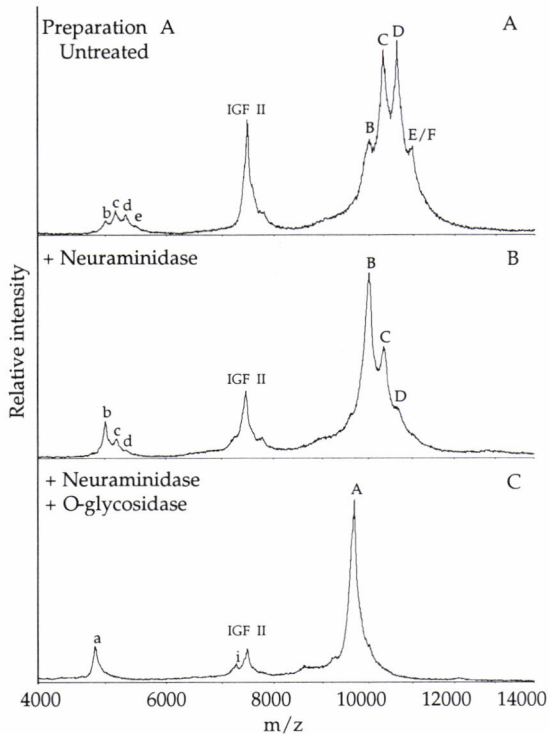


**Figure 2.** MALDI mass spectra of the molecular ion region of (A) untreated intact preparation A which was sequentially treated with (B) neuraminidase and (C) O-glycosidase. The singly and doubly charged ions are designated with upper and lower case letters respectively. The peak designated IGF-II refers to mature IGF-II (aa 1-67) and i to peptide<sup>1-65</sup>. Assignments for peaks A to F are given in Table 1

#### Neuraminidase and O-glycosidase treated

A portion of the two preparations was first treated with neuraminidase to uncover the degree of sialylation. This was followed by O-glycosidase treatment to give the naked precursor IGF-II. O-glycosidase was chosen over N-glycosidase since there are no N-linked glycosylation sites in the deduced sequence of pro-IGF-II. The desialylated and deglycosylated preparations were remeasured by MALDI-MS. Table 1 summarizes the MALDI mass values measured before and after treatment with neuraminidase and O-glycosidase for preparations A and B.

The MALDI mass spectra obtained for preparations A and B after treatment with neuraminidase are shown in Figure 2B and 3B. The number of major peaks was reduced from four (peak B, C, D and E/F) to two (peak B and C) for preparation A and from three (peak B, C and D) to two (peak B and C) for preparation B indicating the release of

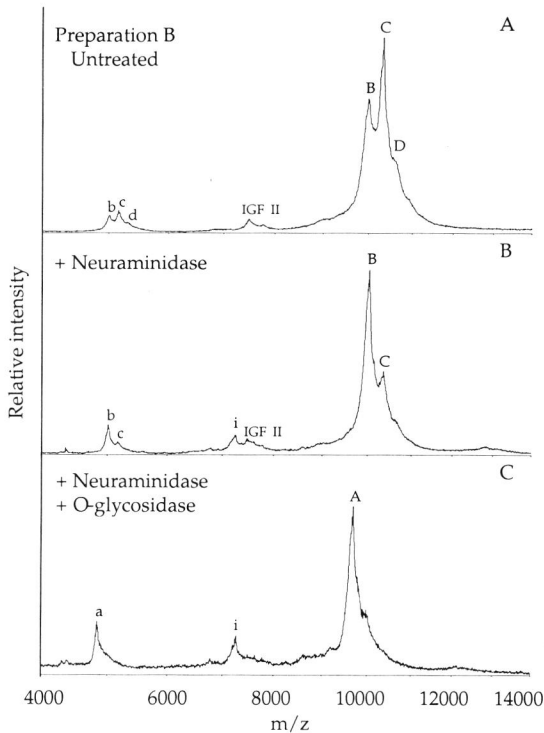


**Figure 3.** MALDI mass spectra of the molecular ion region of (A) untreated intact preparation B which was sequentially treated with (B) neuraminidase and (C) O-glycosidase. The singly and doubly charged ions are designated with upper and lower case letters respectively. The peak designated IGF-II refers to mature IGF-II (aa 1-67) and *i* to peptide<sup>1-65</sup>. Assignments for peaks A to D are given in Table 1

two and one sialic acid respectively. Figures 2C and 3C show the MALDI mass spectra obtained after treatment of preparations A and B with neuraminidase and O-glycosidase. A new molecular ion signal (peak A) slightly shifted to a smaller mass appeared in the spectrum for both preparations A and B, representing the deglycosylated precursor IGF-II molecule. The molecular mass of peak A was determined to 9679 and 9675 for preparations A and B respectively, corresponding to precursor IGF-II<sup>1-87</sup>, containing a C-terminal extension of 20 amino acids. The average masses of the carbohydrates attached to precursor IGF-II<sup>1-87</sup> were calculated from the mass differences between peak

B and A and peak C and B. These suggested the presence of one or two HexNAc-Hex groups and one or more sialic acids. The limited mass resolution at this mass range and the possibility of confusion due to heterogeneity (*e.g.* see peak E/F) made it difficult to proceed further on the intact material. Further evaluation of the type of glycosylation and identification of the modified peptide(s) was carried out by mass spectrometric peptide mapping. To avoid excessive duplication only the detailed results of the more complex preparation A are presented in the following section.

**Table 1** Calculated and MALDI MS observed molecular mass values of intact preparations A and B prior and after neuraminidase and O-glycosidase treatment. The peak designations refer to the denoted peaks in Figures 2 and 3.

peak	assignment	mass calc	mass observed		
			untreated	+ neuraminidase	+ neuraminidase + O-glycosidase
Preparation A					
	aa 66-87	2444.7	-	-	2445.0
	aa 66-87+HexNAc <sub>1</sub> -Hex <sub>1</sub>	2810.0	-	2808.9	-
	aa 66-87+HexNAc <sub>2</sub> -Hex <sub>2</sub>	3175.4	-	3173.6	-
i	aa 1-65	7254.2	-	-	7264.9
IGF II	aa 1-67	7470.4	7478.8	7465.9	7479.9
A	aa 1-87	9679.9	-	-	9679.2
B	aa 1-87+HexNAc <sub>1</sub> -Hex <sub>1</sub>	10044.2	10006.3	10015.6	-
C	aa 1-87+HexNAc <sub>1</sub> -Hex <sub>1</sub> -SA <sub>1</sub>	10335.5	10310.7	10347.1	-
D	aa 1-87+HexNAc <sub>1</sub> -Hex <sub>1</sub> -SA <sub>2</sub>	10626.7	10627.6	10633.8	-
E	aa 1-87+HexNAc <sub>1</sub> -Hex <sub>1</sub> -SA <sub>3</sub>	10917.8	10957.2	-	-
F	aa 1-87+HexNAc <sub>2</sub> -Hex <sub>2</sub> -SA <sub>2</sub>	10992.1	-	-	-
Preparation B					
	aa 66-87	2444.7	-	-	2444.4
	aa 66-87+HexNAc <sub>1</sub> -Hex <sub>1</sub>	2810.0	-	2802.7	-
	aa 66-87+HexNAc <sub>2</sub> -Hex <sub>2</sub>	3175.4	-	3173.2	-
i	aa 1-65	7260.3	-	7242.1	7254.0
IGF II	aa 1-67	7470.4	7489.8	7476.1	-
A	aa 1-87	9679.9	-	-	9674.7
B	aa 1-87+HexNAc <sub>1</sub> -Hex <sub>1</sub>	10044.2	10007.6	10027.5	-
C	aa 1-87+HexNAc <sub>1</sub> -Hex <sub>1</sub> -SA <sub>1</sub>	10335.5	10335.8	10340.7	-
D	aa 1-87+HexNAc <sub>1</sub> -Hex <sub>1</sub> -SA <sub>2</sub>	10626.7	10570.8	-	-

### Peptide Mapping

The remaining portions of untreated, neuraminidase and O-glycosidase treated samples were separately reduced by DTT and cleaved with Endo Glu-C. Mass spectrometric peptide maps were established by MALDI MS analysis of the unfractionated peptide mixtures. The calculated molecular masses of the Endo Glu-C (termed V) peptides and those observed in the corresponding spectra for untreated, neuraminidase and O-

glycosidase treated preparation A and B are given in Table 2. The glycosylated peptide(s) were identified by comparing the Endo Glu-C peptide maps of untreated neuraminidase and O-glycosidase treated preparations as illustrated for preparation A in Figure 4A, B and C.

**Table 2** Calculated and MALDI-MS observed molecular mass values of peptide derived by Endo Glu-C cleavage of untreated, neuraminidase and O-glycosidase treated preparations A and B.

assignment	mass calc	mass observed		
		untreated	+ neuraminidase	+ neuraminidase + O-glycosidase
Preparation A				
aa 1-45 (V1-4)*	5069.7	5069.4	5069.3	5069.4
aa 46-57 (V5)	1373.7	1374.1	1374.2	1374.1
aa 68-87	2228.5	-	-	2228.5
aa 66-87	2444.7	-	-	2445.0
aa 58-87	3280.7	-	-	3280.9
aa 58-87-HexNAc <sub>1</sub> -Hex <sub>1</sub>	3646.0	3647.3	3647.3	-
aa 58-87-HexNAc <sub>1</sub> -Hex <sub>1</sub> -SA <sub>1</sub>	3937.3	3937.8	-	-
aa 58-87-HexNAc <sub>1</sub> -Hex <sub>1</sub> -SA <sub>2</sub>	4228.5	4229.6	-	-
aa 58-87-HexNAc <sub>2</sub> -Hex <sub>2</sub>	4011.3	4010.7	4011.9	-
aa 58-87-HexNAc <sub>2</sub> -Hex <sub>2</sub> -SA <sub>1</sub>	4302.6	4302.6	-	-
aa 58-87-HexNAc <sub>2</sub> -Hex <sub>2</sub> -SA <sub>2</sub>	4593.9	(4592.9)	-	-
Preparation B				
aa 1-45 (V1-4)	5069.7	5069.8	5069.4	5068.9
aa 46-57 (V5)	1373.7	1374.0	1374.9	1374.8
aa 68-87	2228.5	-	-	2229.6
aa 66-87	2444.7	-	-	2445.2
aa 58-87	3280.7	-	-	3280.8
aa 58-87-HexNAc <sub>1</sub> -Hex <sub>1</sub>	3646.0	3645.5	3646.4	-
aa 58-87-HexNAc <sub>1</sub> -Hex <sub>1</sub> -SA <sub>1</sub>	3937.3	3937.5	-	-
aa 58-87-HexNAc <sub>2</sub> -Hex <sub>2</sub>	4011.3	4010.7	4011.5	-
aa 58-87-HexNAc <sub>2</sub> -Hex <sub>2</sub> -SA <sub>1</sub>	4302.6	(4301.8)	-	-

\* Endo Glu-C peptides are named V, followed by a number indicating the position of the peptide relative to the N-terminus.

Endo Glu-C cleavage of untreated preparation A, followed by MALDI peptide mapping, revealed peaks at masses corresponding to peptide V1-4 (aa 1-45) and peptide V5 (aa 46-57) and a complex distribution of unknown peaks in the mass range from 3500 to 4500 daltons (Figure 4A). In this mass area the two most abundant peaks  $m/z$  3647 (peak 1) and 3938 (peak 2) differed by 291 Da, indicating the presence of sialic acid. A similar mass difference was observed between  $m/z$  3938 (peak 2) and 4230 (peak 4) and  $m/z$  4011 (peak 3) and 4303 (peak 5). In comparison, the Endo Glu-C peptide map of the

neuraminidase treated preparation A (Figure 4B) only revealed the two peaks at  $m/z$  3647 and 4012. The observed mass difference between these two peaks was 365 Da which corresponds to the carbohydrate composition HexNAc-Hex. Finally, a major peak at  $m/z$  3281 and a minor at  $m/z$  2445 was observed in the Endo Glu-C peptide map of the neuraminidase and *O*-glycosidase treated preparation A (Figure 4C). In combination with the deduced amino acid sequence for pro-IGF-II the two deglycosylated peptides were identified as the precursor IGF-II peptide<sup>58-87</sup> and the precursor IGF-II peptide<sup>66-87</sup>, confirming the C-terminal extension of 20 amino acids. The mass difference between the major peak in figure 4C and the two peaks observed in figure 4B is consistent with the removal of one and two HexNAc-Hex residues. These data, in association with the linkage specificity of *O*-glycosidase treatment, indicate that precursor IGF-II peptide<sup>58-87</sup> contains a heterogeneous complex-type of *O*-linked mono and disialylated oligosaccharides (Table 2).

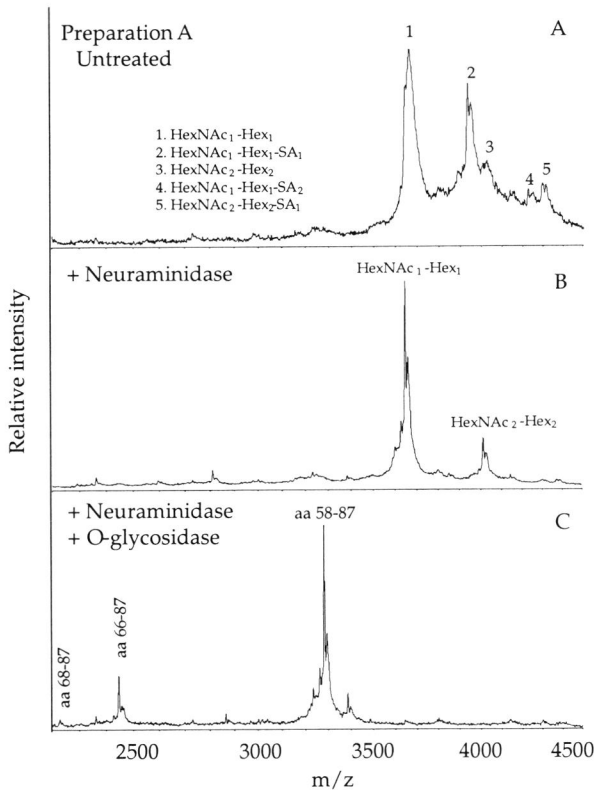


**Figure 4.** MALDI mass spectra of the molecular ion regions of Endo Glu-C precursor IGF-II peptide<sup>58-87</sup> containing *O*-linked oligosaccharides. Endo Glu-C precursor IGF-II glyco-peptide<sup>58-87</sup> from (A) untreated followed by (B) neuraminidase and (C) *O*-glycosidase treated preparation A. The corresponding type of mass values are given in Table 2.

The second peak corresponding to precursor IGF-II peptide<sup>66-87</sup> observed after neuraminidase and *O*-glycosidase treatment, arose from a cleavage at the C-terminal side of Lys<sup>65</sup>. Two precursor IGF-II peptides, peptide<sup>1-65</sup> (designated *i* in figures 2 and 3) and peptide<sup>66-87</sup>, derived as a result of the cleavage at Lys<sup>65</sup>, were already observed in the spectra of the intact preparations after neuraminidase and after *O*-glycosidase treatment (Figures 2-5 and Table 1). This suggest that the cleavage at Lys<sup>65</sup> occurred during neuraminidase treatment and prior to the Endo Glu-C digestion. Incubation of recombinant mature IGF-II with the neuraminidase reagent resulted in the appearance of degradation products, supporting the presence of a contaminating protease (result not shown).

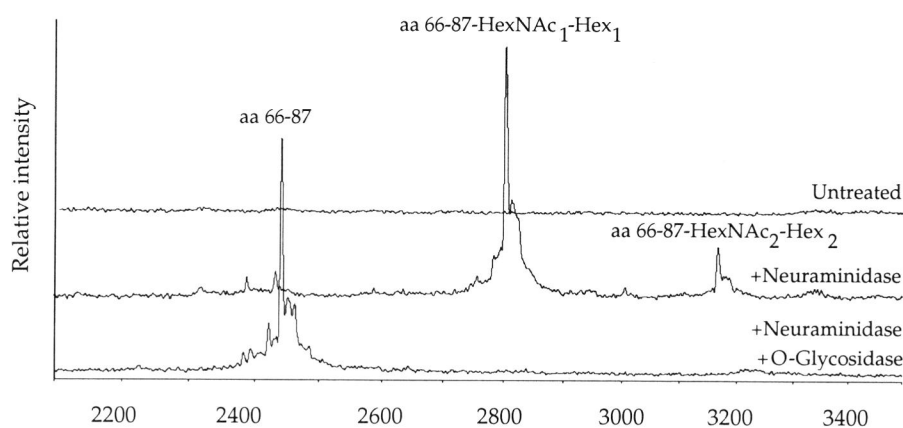


**Figure 5.** MALDI mass spectra of the lower mass region of intact preparation A (Figure 2). The carbohydrate attached to precursor IGF-II peptide<sup>66-87</sup> as determined from the observed mass differences are shown for each step (untreated, neuraminidase and *O*-glycosidase treatment).

#### Linear mode measurement

Recently, loss of sialic acid in glycopeptides has been observed under MALDI conditions. This fragmentation has been shown to be a post source decay (PSD) process that may be detected by comparing the results for linear and reflector time-of-flight analysis [25]. When the linear mode became available in our laboratory, the comparison with reflector mode was made for a third pro-IGF-II preparation, preparation C (preparations A and B were no longer available). In reflector mode the mass spectrum (Figure 6A) was identical to that of preparation B (Figure 3A). Similarly, the linear mass spectrum (Figure 6B) acquired immediately after the reflector mass spectrum (Figure 6A) using the same sample spot, showed several peaks in the molecular region. Both mono- and disialylated species were present (peaks C and D), together with a third signal (peak E) at  $m/z$  10901.2, corresponding to the trisialylated species (Table 3).

The non-sialylated form (peak B) obtained in the reflector mode mass spectrum was poorly presented in the linear mode mass spectrum, indicating that this signal was derived from the metastable loss of sialic acid(s). The occurrence of metastable fragmentation is further confirmed by the presence of peak E in the linear mode mass spectrum, but not in the reflector mode mass spectrum. Taken together, this indicates that only the sialylated forms of pro-IGF-II are present in the preparations.

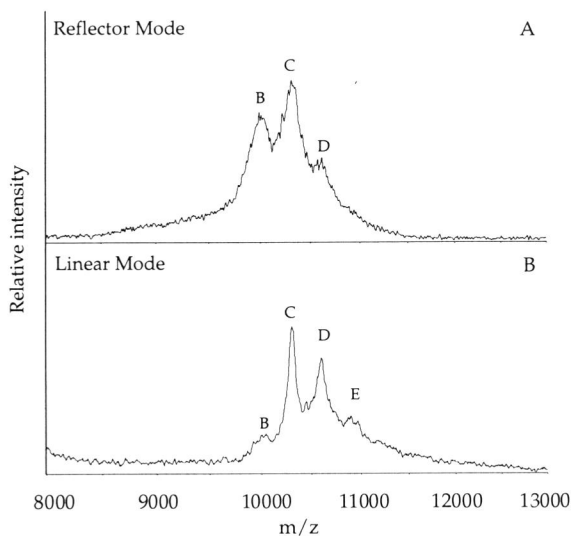


**Figure 6.** Comparison of the (A) reflector and (B) linear mode MALDI mass spectra of the molecular ion region of untreated intact preparation C. Assignments for the peaks are given in Table 3.

**Table 3** Calculated and MALDI-MS observed molecular mass values of intact preparations C in reflector and linear mode. The peak designations refer to the denoted peaks in Figure 6

peak	assignment	mass calc	mass observed	
			reflectron mode	linear mode
Preparation C				
B	aa 1-87+HexNAc <sub>1</sub> -Hex <sub>1</sub>	10044.2	10009.9	(10019.9)
C	aa 1-87+HexNAc <sub>1</sub> -Hex <sub>1</sub> -SA <sub>1</sub>	10335.5	10315.2	10332.1
D	aa 1-87+HexNAc <sub>1</sub> -Hex <sub>1</sub> -SA <sub>2</sub>	10626.7	10591.0	10619.5
E	aa 1-87+HexNAc <sub>1</sub> -Hex <sub>1</sub> -SA <sub>3</sub>	10917.8	-	10901.2

## Discussion

Treatment of preparations A and B with neuraminidase and O-glycosidase and subsequent remeasurement of the molecular mass by MALDI-MS revealed a heterogeneous mixture of glycosylated IGF-II precursor molecules, whose main glycoforms are sialylated O-linked oligosaccharides. The heterogeneity of the carbohydrate component together with the metastable loss of neuraminic acid and/or small neutral molecules (such as  $\text{NH}_3$  and  $\text{H}_2\text{O}$ ) resulted in significant peak broadening. Therefore, the individual glycoform signals could not always be differentiated unambiguously. More accurate information concerning the degree of sialylation, type of glycosylation and the exact processing site of precursor IGF-II was obtained by mass spectrometric analysis of Endo Glu-C generated peptide mixtures of the untreated, neuraminidase and O-glycosidase treated preparations.

A comparison of the peptide maps obtained from Endo Glu-C digestion of untreated, neuraminidase and O-glycosidase treated preparations, revealed the carbohydrate compositions  $\text{HexNAc}_1\text{-Hex}_1$  and  $\text{HexNAc}_2\text{-Hex}_2$  together with their mono- and disialylated components. Although metastable loss of sialic acid from sialylated glycopeptides has been observed under MALDI conditions [25], the linear mode analysis of preparation C confirmed the presence of both the mono-, di- and trisialylated components.

All preparations were found to contain a C-terminal extension of 20 amino acids giving the precursor IGF-II<sup>1-87</sup>. The majority of cleavages in precursors take place at paired basic residues (Figure 1) and occasionally at single basic residues (Lys or Arg). Surprisingly, human IGF II precursors obtained from preparations A and B were found to terminate at the non- basic amino acid Gly<sup>87</sup> and not at the more likely basic residue Lys<sup>88</sup>. Amino acid compositional analysis of Endo Lys-C digest indicated that the C-terminus could be either Gly<sup>87</sup> or Lys<sup>88</sup> [16]. Zumstein *et al.* [14] found that their variant pro-form ended at Lys<sup>88</sup>. The results presented in this paper can only be explained by assuming Gly<sup>87</sup> as the C-terminal residue. The precursor IGF-II<sup>1-87</sup> form is most likely generated from a cleavage at Lys<sup>88</sup> followed by the action of a carboxypeptidase of the type A or Y. These enzymes catalyze the release of unspecific amino acids from the C-terminal position in peptides, while the cleavage of Gly is considerably retarded. Alternatively, a basic carboxypeptidases in plasma could specifically remove Lys and Arg from peptide [26]. The Cys-Gly-Asp/Ser<sup>33</sup> variant reported by Zumstein *et al.* [14] and the Arg-Leu-Pro-Gly/Ser<sup>29</sup> variant reported by others [13,16,27] were not observed. The O-glycosylation was associated with precursor IGF-II peptide<sup>58-87</sup>. This precursor, arising from an incomplete cleavage at Glu<sup>67</sup>, contains six potential O-glycosylation

sites (Thr<sup>58</sup>, Thr<sup>62</sup>, Ser<sup>66</sup>, Ser<sup>71</sup>, Thr<sup>72</sup> and Thr<sup>75</sup>) but only three within the E-domain, Ser<sup>71</sup>, Thr<sup>72</sup> and Thr<sup>75</sup>. Complete Endo Glu-C cleavage of the peptide at Glu<sup>67</sup> would result in two peptides (peptide<sup>58-67</sup> and peptide<sup>68-87</sup>) each including three O-glycosylation sites. The Endo Glu-C cleavage site at Glu<sup>67</sup> was still preserved after prolonged digestion time and further addition of Endo Glu-C. However, a peak corresponding to precursor IGF-II peptide<sup>68-87</sup>, obtained as a result of the cleavage at Glu<sup>67</sup>, was observed in the peptide map after removal of the oligosaccharides by neuraminidase and O-glycosidase (Figure 4C), indicating that Glu<sup>67</sup> may be inaccessible for Endo Glu-C cleavage in the presence of oligosaccharides.

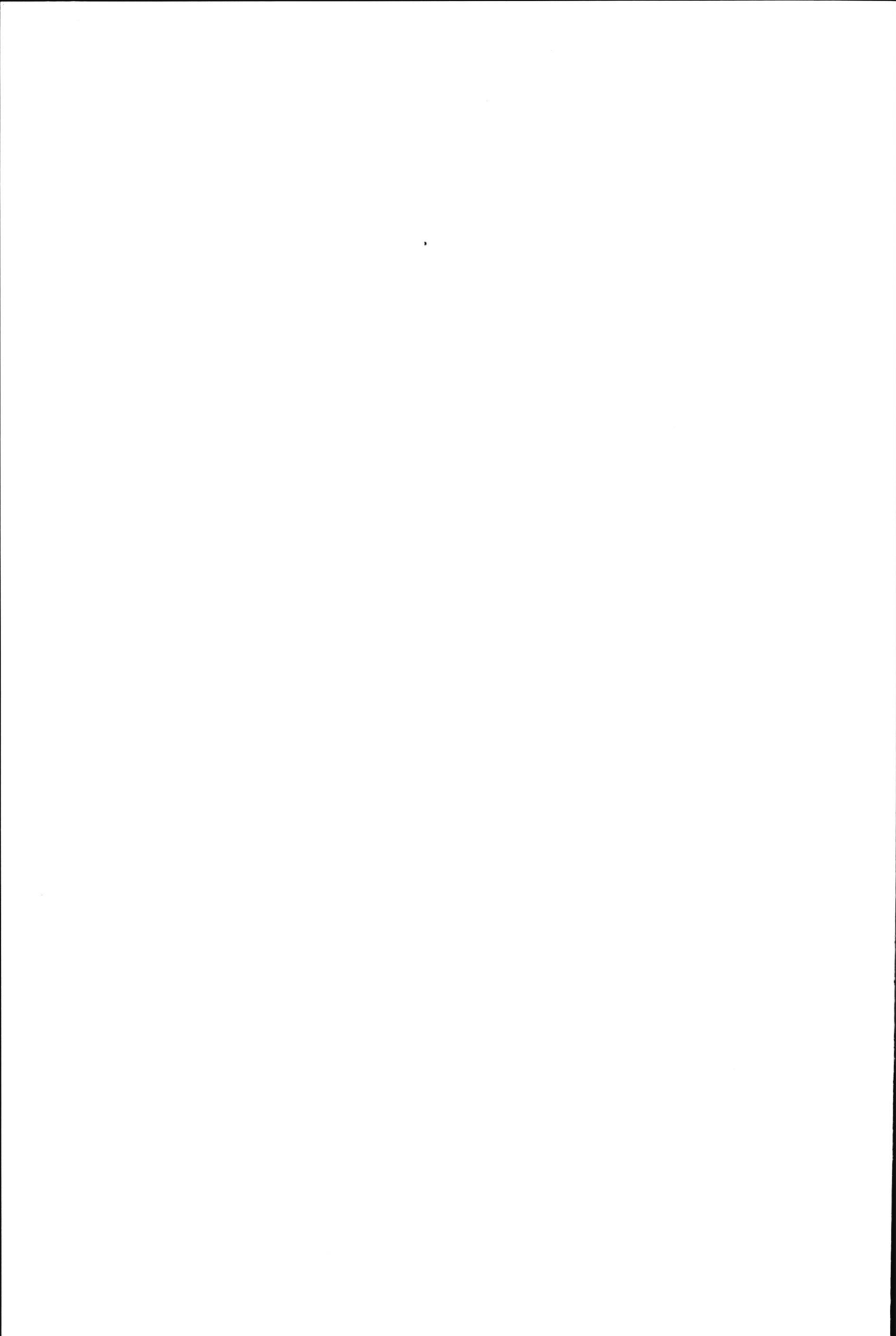
A comparison of the spectra obtained from intact IGF II preparations prior to and after O-glycosidase treatment (Figure 5), revealed the release of O-linked oligosaccharides from peptide<sup>66-87</sup> of the same type as identified for peptide<sup>58-87</sup> (Figure 4). This observation eliminates Thr<sup>58</sup> and Thr<sup>62</sup> as potential O-glycosylation sites. Since enzymatic or chemical means of cleaving peptides at any selected residue are not available, the three potential O-glycosylation sites within the E-domain could not be further distinguished by this method.

Recently Hudgins *et al.* [16] purified high molecular mass precursors of IGF-II from human serum Cohn fraction IV<sub>1</sub>, with apparent molecular masses of 15,000 and 11,500 obtained by SDS-PAGE (sodium dodesyl sulfate-polyacrylamide gel electrophoresis). The C-terminus of these precursors were found to be near or at Lys<sup>88</sup> and to be post translationally modified by O-glycosylation at Thr<sup>75</sup>.

Although SDS-PAGE is an efficient protein separation technique, its accuracy of molecular mass determination is currently limited to 5-10%. Furthermore, glycoproteins show anomalous migration patterns and do not exhibit linear relationship to the molecular mass of protein standard. The processing site, degree of sialylation and type of O-linked carbohydrate could not be established by SDS-PAGE. The obtained mass accuracy in the present study using MALDI MS was approximately 0.1-0.5% at the intact level and 0.01-0.05% at the peptide mixture level. This improved accuracy is of considerable value for the primary characterization of the glycosylated IGF-II precursor molecules. The tolerance to buffer components which is a characteristic feature of MALDI-MS allowed treatment of glycosylated IGF-II precursor with neuraminidase and O-glycosidase followed by DTT reduction and Endo Glu-C digestion and subsequent remeasurement of the molecular weight without removal of the different incubation buffers. In addition, the method provided excellent sensitivity: less than 0.1 µg was required for a MALDI spectrum of the enzymatic digest.

## References

- [1] F. Hillenkamp, M. Karas, R. C. Beavis and B. T. Chait, *Anal. Chem.*, **1991**, 63, 1193-1203.
- [2] M. Karas and F. Hillenkamp, *Anal. Chem.*, **1988**, 60, 2299-2301.
- [3] C. M. Whitehouse, R. N. Dreyer, M. Yamashita and J. B. Fenn, *Anal. Chem.*, **1985**, 57, 675-679.
- [4] J. B. Fenn, M. Mann, C. K. Meng, S. F. Wong and C. M. Whitehouse, *Mass Spectrom. Rev.*, **1990**, 9, 37-70.
- [5] A. P. Bruins, T. R. Covey and J. D. Henion, *Anal. Chem.*, **1987**, 59, 2642-2646.
- [6] M. Karas, U. Bahr, A. Ingendoh and F. Hillenkamp, *Angew. Chem. Int. Ed. Engl.*, **1989**, 28, 760-761.
- [7] J. A. Loo, H. R. Udseth and R. D. Smith, *Anal. Biochem.*, **1989**, 179, 404-412.
- [8] U. Bahr, M. Karas and F. Hillenkamp, *Fresenius J. Anal. Chem.*, **1994**, 348, 783-791.
- [9] E. J. Zaluzec, D. A. Gage and J. T. Watson, *Protein Expression and Purification*, **1995**, 6, 109-123.
- [10] E. Rinderknecht and R. E. Humbel, *FEBS Letters*, **1978**, 89, 283-286.
- [11] J. L. Van den Brande, C. M. Hoogerbrugge, K. Beyreuther, P. Roepstorff, J. Jansen and S. C. v. Buul-Offers, *Acta Endocrinol (Copenh)*, **1990**, 122, 683-695.
- [12] G. I. Bell, J. P. Merryweather, R. Sanchez-Pescador, M. M. Stempien, L. Priestley, J. Scott and L. B. Rall, *Nature*, **1984**, 310, 775-777.
- [13] M. Jansen, F. M. A. v. Schaik, H. v. Tol, J. L. Van den Brande and J. S. Sussenbach, *FEBS Letters*, **1985**, 179, 243-246.
- [14] P. P. Zumstein, C. Lüthi and R. Humbel, *Proc. Natl. Acad. Sci. USA*, **1985**, 82, 3169-3172.
- [15] L.K. Gowan, B. Hampton, D.J. Hill, R.J. Schlueter and J.F. Perdue, *Endocrinology*, **1987**, 121, 449-458.
- [16] W. R. Hudgins, B. Hampton, W. H. Burgess and J. F. Perdue, *J. Biol. Chem.*, **1992**, 267, 8153-8160.
- [17] G. K. Haselbacher and R. Humbel, *Endocrinology*, **1982**, 110, 1822-1824.
- [18] G. K. Haselbacher, M. E. Schwab, A. Pasi and R. E. Humbel, *Proc. Natl. Acad. Sci. USA*, **1985**, 82, 2153-2157.
- [19] W. H. Daughaday, M. A. Emanuele, M. H. Brooks, A. L. Barbato, M. Kapadia and P. Rotwein, *New Engl. J. Med.*, **1988**, 319, 1434-1440.
- [20] E. T. Shapiro, G. I. Bell, K. S. Polonsky, A. H. Rubenstein, M. C. Kew and H. S. Tager, *J. Clin. Invest.*, **1990**, 85, 1672-1680.
- [21] K. Hoekman, J. v. Doorn, T. Gloudemans, O. S. Hoekstra, J. A. Maassen, J. B. Vermorken, J. Wagstaff and H. M. Pinedo, *Annals of Oncology*, **1994**, 5, 277-281.
- [22] W. H. Daughaday, B. Trivedi and R. C. Baxter, *Proc. Natl. Acad. Sci. USA*, **1993**, 90, 5823-5827.
- [23] J. Jansen, S. C. v. Buul-Offers, C. M. Hoogerbrugge and J. L. van den Brande, *Biochem. J.*, **1990**, 266, 513-520.
- [24] W. H. Daughaday, R. H. Starkey, S. Saltman, J. R. Gavin, B. Mills-Dunlap and E. H. Heath-Monnig, *J. Clin. Endocrinol. Metab.*, **1987**, 65, 617-623.
- [25] M. C. Huberty, J. E. Vath, W. Yu and S. A. Martin, *Anal. Chem.*, **1993**, 65, 2791-2800.
- [26] R. A. Skidgel, *Trends Pharmacol. Sci*, **1988**, 9, 299-304.
- [27] B. Hampton, W. H. Burgess, D. R. Marshak, K. J. Cullen and J. F. Perdue, *J. Biol. Chem.*, **1989**, 264, 19255-19160.



## **Chapter 7**

---

Identification of POMC processing products in single  
melanotrope cells by MALDI-MS



---

## Identification of POMC processing products in single melanotrope cells by MALDI-MS

*The use of matrix-assisted laser desorption/ionization mass spectrometry (MALDI-MS) in identifying proopiomelanocortin (POMC) processing products in melanotrope cells of the pituitary intermediate lobe of *Xenopus laevis* was explored. Mass spectra were obtained with such a high sensitivity of detection that the peptides could be identified in a single melanotrope cell. In addition to known POMC processing products of the *Xenopus* melanotrope cell, the presence of previously unidentified POMC-derived peptides was demonstrated. Together these POMC processing products account for the entire length of the POMC precursor. Furthermore, *Xenopus* possesses two genes for POMC and the sensitivity and accuracy of the MALDI-MS technique allowed identification of processing products of both the POMC<sub>A</sub> and POMC<sub>B</sub> gene. In addition, differences were obtained between the mass spectra of melanotrope cells from *Xenopus laevis* adapted to different conditions of background illumination. These results show that MALDI-MS is a valuable tool in the study of the expression of peptides in single (neuroendocrine) cells.*

---

### Introduction

In amphibians, the melanotrope cells of the intermediate lobe of the pituitary gland secrete a melanotropic peptide,  $\alpha$ -melanocyte-stimulating-hormone ( $\alpha$ -MSH), which causes pigment dispersion in dermal melanophores. Thus, the pituitary melanotropes play a pivotal role in the process of skin colour adaptation. In lower vertebrates, as in mammals,  $\alpha$ -MSH originates from a high molecular mass precursor protein, proopiomelanocortin (POMC). Based on the cDNA nucleotide sequence, the complete amino acid sequence of POMC has been determined in various mammalian [1-6] and non-mammalian vertebrates [7-10]. Through tissue-specific processing POMC can generate a number of bioactive peptides including adrenocorticotrophic hormone (ACTH),  $\alpha$ -,  $\beta$ -, and  $\gamma$ -MSH,  $\beta$ -lipotropin ( $\beta$ -LPH) and  $\beta$ -endorphin [11].

The melanotrope cells of the amphibian *Xenopus laevis* are specialized in producing and secreting POMC-derived products. Although in some studies MSH peptides and endorphin end products [12-14] have been identified, little is known about the complete profile of POMC processing products within the melanotrope cell. The complexity of the POMC precursor makes identification of all processing end products using traditional biochemical methods extremely difficult. The common practice of analysing neuropeptides by radioimmunoassay becomes arduous when applied to entire profiles. Moreover, this method can only be used for known peptide families.

---

In recent years, mass spectrometry has developed into an important analytical tool in the biological sciences. The introduction of ionization techniques such as electrospray ionization (ESI)[15,16] and matrix-assisted laser desorption/ionization (MALDI) [17,18] has resulted in new strategies in the characterization of biopolymers. MALDI mass spectrometry (MS) in particular enables the measurement of direct peptide profiles in biological cells and tissues without prior peptide purification [19-21]. For proteins where the sequence is (largely) known, mass spectrometry permits a rapid, detailed confirmation of the sequence and the identification of possible protein modifications, e.g., acetylation, amidation, glycosylation and phosphorylation [22].

In the case of the *Xenopus* melanotrope cell, the majority of the peptides produced are derived from POMC [23]. The complete amino acid sequence of this precursor has been deduced from its nucleotide sequence [7]. *Xenopus* possesses two different POMC genes, named POMC<sub>A</sub> and POMC<sub>B</sub>, which are similar (but not identical) in their amino acid sequences [24]. Furthermore, melanotrope cells of black background-adapted *Xenopus laevis* are very active in synthesizing and processing of POMC whereas melanotrope cells from white-adapted *Xenopus* serve as storage cells with an inactive biosynthetic apparatus [25,26]. The purpose of this study was (1) to identify the different POMC (POMC<sub>A</sub> and POMC<sub>B</sub>) processing products and (2) to elucidate possible differences in the contents of melanotrope cells from animals adapted to different environmental light conditions. This was done by MALDI-MS, using single *Xenopus* melanotrope cells to prevent interference with other cell types present in the pituitary gland.

## Experimental

### *Animals*

Adult *Xenopus laevis* with a weight of approximately 35 g were obtained from the Nijmegen institute for Neurosciences (University of Nijmegen, the Netherlands) laboratory stock. Toads were kept under constant illumination on a black or a white background for at least 3 weeks at 22°C. They were fed trout pellets (Trouvit, Trouw, Putten, The Netherlands) once a week.

### *Preparation of single cells*

The melanotrope cells of 8 animals were isolated from the pituitary neurointermediate lobe as described previously [27], with minor changes. In short, animals were anaesthetized for 15 min in a solution containing 0.1 % MS222 (Sigma; St. Louis, MO, USA) and 0.15% NaHCO<sub>3</sub> (pH 6.8). After perfusing the animal with *Xenopus* Ringer's solution, containing 112 mM NaCl, 2 mM KCl, 2 mM CaCl<sub>2</sub> and 15 mM HEPES

(Calbiochem; La Jolla, CA, USA; pH 7.4) to remove blood cells, lobes were dissected and incubated for 45 min in Ringer's solution without  $\text{CaCl}_2$  to which 0.25% (w/v) trypsin (Gibco, Renfrewshore, UK) had been added. Cells were subsequently dispersed in Ringer's solution by gentle trituration of the lobes with a siliconized Pasteur's pipette. The cells were readily identified on the basis of their characteristic round shape and used immediately for mass spectrometry.

#### *Sample preparation*

Before MALDI-MS only minimal sample preparation was necessary. The matrix used was 2,5-dihydroxybenzoic acid (DHB; Aldrich Chemie, Steinheim, Germany) dissolved at a concentration of 10 mg/ml in 0.1 % trifluoroacetic acid (TFA; Merck, Darmstadt, Germany). After deposition of 1  $\mu\text{l}$  of the matrix on a stainless steel target, the cells were placed in the matrix solution. The sample was dried in a cold air stream before loading into the mass spectrometer. Calibration was performed using a mixture of bovine insulin and horse cytochrome c (Sigma).

#### *Mass spectrometry*

The mass spectrometer used was a VISION 2000 (Finnigan MAT, Bremen, Germany). This is a reflectron time-of-flight (TOF) laser desorption instrument equipped with a nitrogen laser at 337 nm. The laser beam was focused by a quartz lens system to a spot size of 70 mm in diameter. The ions generated were accelerated to a potential of 5 kV in the ion source and post-accelerated by a conversion dynode to a potential of 20 kV. The effective drift length of the instrument is 1.7 m. Ions were detected by a secondary electron multiplier and the signal was amplified and digitized by a high speed transient recorder linked to a 486 personal computer. Molecular mass data were collected and compared with computer-analysed POMC precursor fragments with known or predicted molecular mass, using the "find mass" program (MacProMass, Beckman Research Institute of the City of Hope, Duarte, CA, USA).

### **Results and discussion**

This study is based on the rationale that molecular mass information is sufficiently specific to tentatively identify all peptides that are either known to be present or can be predicted to occur in a given cell or tissue. This approach reduces the number of peptides that have to be analyzed by more rigorous, but also more laborious and time-consuming methods. Prediction is on the basis of "classical" precursor processing through cleavage at consecutive basic amino acids or by processing at "consensus" sequence sites that

are present around monobasic cleavage sites [28-30]. With single cells, especially with a homogeneous cell suspension such as the melanotrope cells of *Xenopus laevis*, that only express one major type of precursor molecule, mass accuracy becomes less important.

#### Mass profiles of melanotrope cells

The mass spectra of a single melanotrope cell from both white- and black-background adapted *Xenopus laevis* revealed 20 to 25 significant ion signals (Figure 1). Reproducible mass spectra were obtained in the 500 -10 000 Da mass range. The mass error was in most cases better than  $\pm 1$  Da. Increased peak broadening at higher mass slightly decreases the mass accuracy.

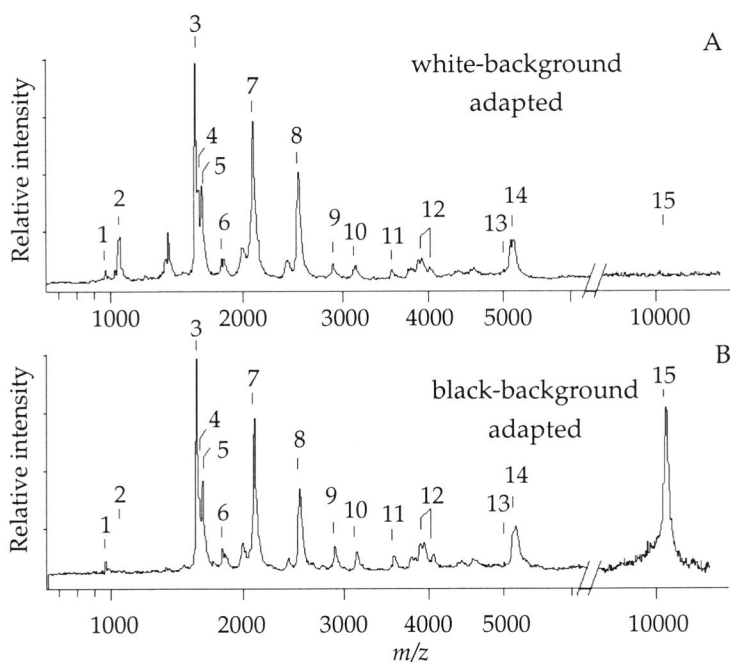


**Figure 1.** Representative example of MALDI mass spectra from freshly isolated, single melanotrope cells of *Xenopus laevis*. The number indicate the position of identified POMC processing products is (see Table 1). (A) Spectrum from a melanotrope cell derived from a white background-adapted animal. (B) Spectrum from a melanotrope cell of a black background-adapted animal. Peak 4 was present as a small peak partially overlapping with peak 3 and peak 13 was not always detected in the spectrum.

Several of the obtained mass values could immediately be assigned to a number of the previous reported processing products of *Xenopus* POMC [12,13,31], ultimately accounting for the entire length of the POMC precursor (see Table 1 and Figure 2). Both desacetyl- $\alpha$ -MSH and  $\alpha$ -MSH as well as  $\beta$ -MSH and lys- $\gamma_1$ -MSH could readily be identified. However, the  $\alpha$ -MSH peak was small compared to the desacetyl- $\alpha$ -MSH peak. This abundance of the desacetyl- $\alpha$ -MSH peak over the  $\alpha$ -MSH peak is in line with results obtained using radioimmunoassay for  $\alpha$ -MSH [14,32,33].

**Table 1** Calculated and observed mass values (M+H<sup>+</sup>) of identified POMC<sub>A</sub> and POMC<sub>B</sub> processing products obtained from *Xenopus* melanotrope cells. Peak numbers are related to the peaks shown in Figure 1. The amino acid position of the peptides within the precursor is given. Amino acids 1-25 of the POMC precursor, form the signal peptide, which is generally not found. The complete POMC<sub>A</sub> precursor comprises 259 amino acids (260 for POMC<sub>B</sub>; [24]).  $\delta m$  is the difference between calculated and observed mass values. Ac=acetyl, AJP=acidic joining peptide, NF=not found, ST=see text.

Peptide	Peak N <sup>o</sup>	POMC <sub>A</sub> (POMC <sub>B</sub> )	calculated mass	observed mass	$\delta m$
N-terminus <sup>1</sup>	2	26-34	1070.2	1069.4	-0.8
N-terminus <sup>2</sup>	14	26-73	5139.7 (5183.9)	5139.1 (5182.7)	-0.6 (-1.2)
N-terminus <sup>3</sup>	15	26-101	ST	>10,000	
lys- $\gamma_1$ -MSH	5	75-86NH <sub>2</sub>	1657.0	1656.0	-1.0
lys- $\gamma_3$ -MSH	13	75-101	ST	5006.8 (5050.2)	+0.2(+0.4)
AJP	12	104-137 (104-138)	3885.1 (4042.2)	3882.7 (4041.5)	-0.1 (-0.7)
Des-Ac- $\alpha$ -MSH	3	140-152NH <sub>2</sub> (141-153NH <sub>2</sub> )	1607.9	1607.0	-0.9
$\alpha$ -MSH	4	140-152NH <sub>2</sub> (141-153NH <sub>2</sub> )	1649.9	1648.9	-1.0
CLIP-fragment	6	157-172 (158-173)	1818.0	1817.2	-0.8
CLIP	8	157-178 (158-179)	2538.8 (2522.8)	2537.9 (2522.4)	-0.9 (-0.4)
N-fragment	9	181-205 (182-206)	2895.1 (2965.1)	2897.2 (NF)	+2.1
$\beta$ -MSH	7	210-226 (211-227)	2100.3	2099.7	-0.6
Ac- $\beta$ -Ep{1-8}	1	229-236 (230-237)	966.1	966.4 (+Na)	+0.3
Ac- $\beta$ -Ep{1-27}	10	229-255 (230-256)	3125.6 (3139.6)	3123.6 (3139.1)	-2.0 (-0.5)
Ac- $\beta$ -Ep{1-31}	11	229-259 (230-260)	3567.2 (3566.2)	3566.8 (3564.8)	-0.4 (-1.4)

The  $\alpha$ ,N-acetylated- $\beta$ -endorphin (1-8) (POMC 229-236) was present as sodium and potassium ion signals, resulting in a mass shift of 22 Da and 38 Da for the sodium and potassium ion, respectively. This result was confirmed by analysing synthetic  $\alpha$ ,N-acetylated- $\beta$ -endorphin (1-8) under the same conditions which resulted in the appearance of the sodium (966.1 Da) and potassium (982.2 Da) ion adducts, but no protonated ion signal (944.1 Da).

Though it is known that the *Xenopus* melanotrope cells contain high amounts of  $\alpha$ ,N-acetyl- $\beta$ -endorphin (1-8)(POMC 229-236) [13] only relatively low signal intensities were obtained for the acetylated endorphins;  $\alpha$ ,N-acetyl- $\beta$ -endorphin (1-8), (1-27) and (1-31). The complexity of the peptide contents of the melanotrope cell could account for a possible signal suppression of the  $\alpha$ ,N-acetyl- $\beta$ -endorphins.

Although the absence of a signal does not prove that a peptide is not there, the absence of nonacetylated endorphins in the melanotrope cells confirms previous findings [14,34]. These results support the observations concerning the spatial difference in acetylation of  $\alpha$ -MSH and endorphins, while the endorphins are rapidly acetylated after synthesis (so, no nonacetylated endorphins can be found within the cell), acetylation of desacetyl- $\alpha$ -MSH occurs at the moment of secretion, which explains the small amount of  $\alpha$ -MSH present within the cell [31-33,34].

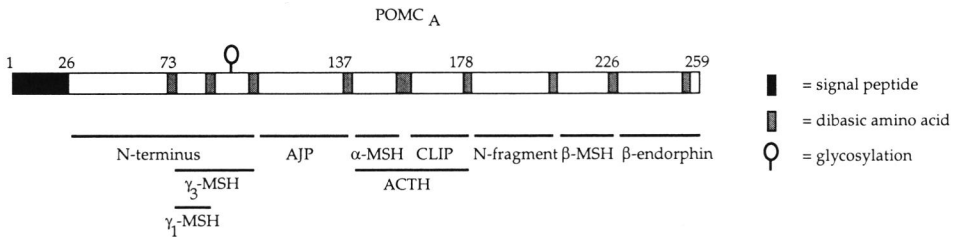


**Figure 2.** Schematic representation of the POMC<sub>A</sub> precursor of the amphibian *Xenopus laevis*. The structure of the POMC gene was deduced from nucleotide sequence analysis [7]. The position of the glycosylation is shown by the open circle. Sites where two or more basic amino acids occur are indicated by filled boxes. Processing products formed via processing at dibasic amino acids are indicated by horizontal lines.

#### *Different POMC<sub>A</sub> and POMC<sub>B</sub> processing end products*

Several peptide products, unique to either the POMC<sub>A</sub> or the POMC<sub>B</sub> gene, were found. Only small differences in the intensity of the POMC<sub>A</sub> and POMC<sub>B</sub> end products signals were visible, indicating similar amounts of POMC<sub>A</sub> and POMC<sub>B</sub> end products and similar processing. This is in agreement with the biosynthesis and the level of expression of the two POMC genes [35]. The corticotropin-like intermediate peptides (CLIPs) derived from POMC<sub>A</sub> and POMC<sub>B</sub> have a difference in mass of only 18 Da, both peptides were clearly present (Figure 3A). Interestingly, no evidence for posttranslational modification of this product in *Xenopus laevis* melanotropes could be obtained, although it has been shown that both rat and human CLIP can be phosphorylated as well as glycosylated [36,37]. Two different peaks were also observed to match the N-terminal 26-73 peptide of the two POMC genes (N-terminus<sup>2</sup>, Figure 3B). Recent biosynthesis studies have shown that this N-terminal peptide is a secretory product rapidly formed from a larger  $\gamma$ -MSH-containing POMC product [38].

#### *$\gamma$ -MSH peptides in *Xenopus melanotropes**

The POMC precursor protein of *Xenopus laevis* contains only one glycosylation site, which is present in the  $\gamma$ -MSH region (Figure 2) [24]. However cleavage near this site results in several glycosylated products (lys- $\gamma_3$ -MSH and the N-terminal peptides containing this  $\gamma$ -MSH). Since the carbohydrate structures of the intermediate glycopeptides are not known, the identification of these peptides is not straightforward. Nevertheless, both POMC<sub>A</sub> lys- $\gamma_3$ -MSH and POMC<sub>B</sub> lys- $\gamma_3$ -MSH have been isolated and their molecular weights identified by electrospray mass spectrometry [38]. Although only low intensity ion signals were obtained for the melanotrope cells, the molecular masses for the lys- $\gamma_3$ -MSH peptides are here confirmed by MALDI-MS. Consistent with earlier reports [39-41] lys- $\gamma$ -MSH and not  $\gamma$ -MSH was observed. Apparently, the dibasic arg-lys is used as a monobasic processing site. It remains an unanswered question as to why the cleavage procedure for lys- $\gamma$ -MSH is different from that occurring at other dibasic sites.

#### *Unexpected POMC peptides*

The usefulness of the "find mass" program for the recognition of unexpected peptides was demonstrated for C-terminally shortened forms of CLIP, of the so called N-fragment (POMC 181-207), and of the N-terminal peptide (POMC 26-73, N-terminus<sup>2</sup>). On the basis of the computer analysis the ion signal at  $m/z$  1817.2 (peak 6) corresponds to the C-terminally truncated CLIP peptide (POMC 157-172). Furthermore, the ion signals at

$m/z$  1069.4 and 2897.2 could be assigned to the C-terminally shortened products of the N-terminal(N-terminus<sup>1</sup>) and the N-fragment respectively (peak 2 and 9). CLIP, the N-terminal peptide and the N-fragment are both acidic and contain high molecular percentages of proline, glutamic acid, aspartic acid and threonine. This has been linked to fast proteolytic degradation in vivo [42] and explains the presence of the truncated forms of the N-fragment, the N-terminal and CLIP in this study.

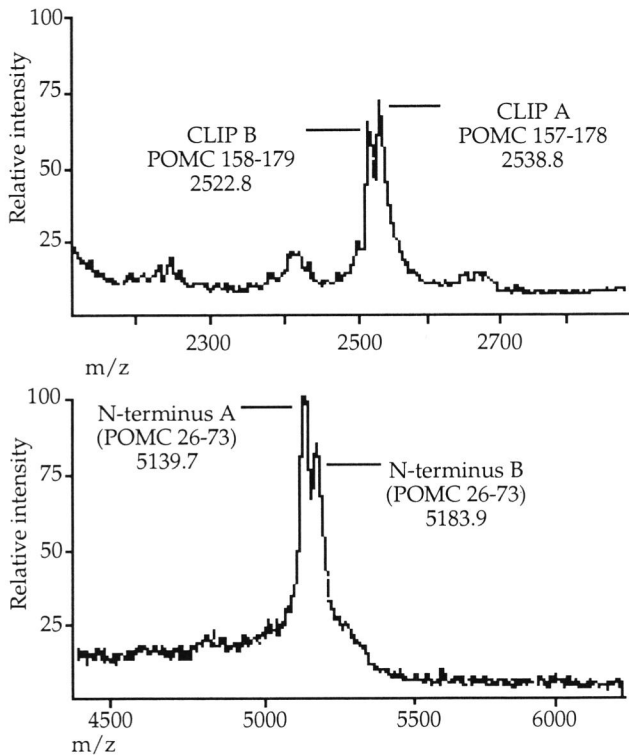


**Figure 3** MALDI mass spectrum obtained from a single melanotrope cell confirming the presence of both  $POMC_A$  and  $POMC_B$  gene products. (A) Corticotropin-like intermediate peptide (CLIP) derived from  $POMC_A$  ( $[M+H]^+_c = 2538.8$ ) and from  $POMC_B$  ( $[M+H]^+_c = 2522.8$ ). (B) The N-terminal peptide (POMC 26-73) derived from  $POMC_A$  ( $[M+H]^+_c = 5139.7$ ) and  $POMC_B$  ( $[M+H]^+_c = 5183.9$ ).

### *Unidentified products*

Some peaks could not be identified as POMC processing products by MALDI-MS ( $M_r$  1388.9, 2002.2, 2422.3). Possibly, these peaks represent posttranslationally modified POMC end products (e.g., by amidation, acetylation, phosphorylation or glycosylation). Alternately, they may be non-POMC peptides produced by the *Xenopus* melanotrope cell. The post source decay technique, which is currently in a developmental stage, will probably allow the extraction of sequence information from these products [43]. Other POMC peptides deduced by computer analysis matching ions present in the spectrum were judged to be poor candidates either because they (1) contain dibasic cleavage sites not expected to survive in the intermediate pituitary or (2) their processing would require the unlikely cleavage of a dibasic cleavage site next to a proline [44].

### *Background adaptation*

Although the MALDI-MS profiles of cells derived from black background- adapted animals (Figure 1A) and those of white background- adapted animals (Figure 1B) showed little qualitative difference, the relative intensity of several peaks was quite different. Major differences were found, for instance, in the higher molecular mass region, where the 10 kDa product (peak 15, N-terminus<sup>3</sup>) was more pronounced in cells derived from black-adapted animals compared to the peak in cells of white-adapted animals. This ion signal might be identified as a POMC processing product. The N-terminal processing product of POMC (POMC 26-101, N-terminus<sup>3</sup>) contains the lys- $\gamma_3$ -MSH and has a molecular mass of 10 kDa. Previous findings have reported the existence of large intermediates in the processing of POMC to its end products in melanotrope cells from black background-adapted *Xenopus* [23] and such a N-terminal product has been identified as a major processing product on SDS gel electrophoresis [39]. It seems likely that the 10 kDa ion (N-terminus<sup>3</sup>) is this product. Some other products in the mass profile with lower molecular mass (peak 2 and an unidentified ion signal at  $m/z$  1388.9) were more pronounced in melanotrope cells of white-adapted than in cells of black-adapted animals. The physiological significance of this difference in processing end products is not known. However, these findings are in agreement with the idea that melanotropes of black background-adapted animals are very active in the biosynthesis and processing of POMC and thus will contain larger intermediates, while melanotropes of white background-adapted animals serve as storage cells, containing completely processed POMC end products [14,26,45].

---

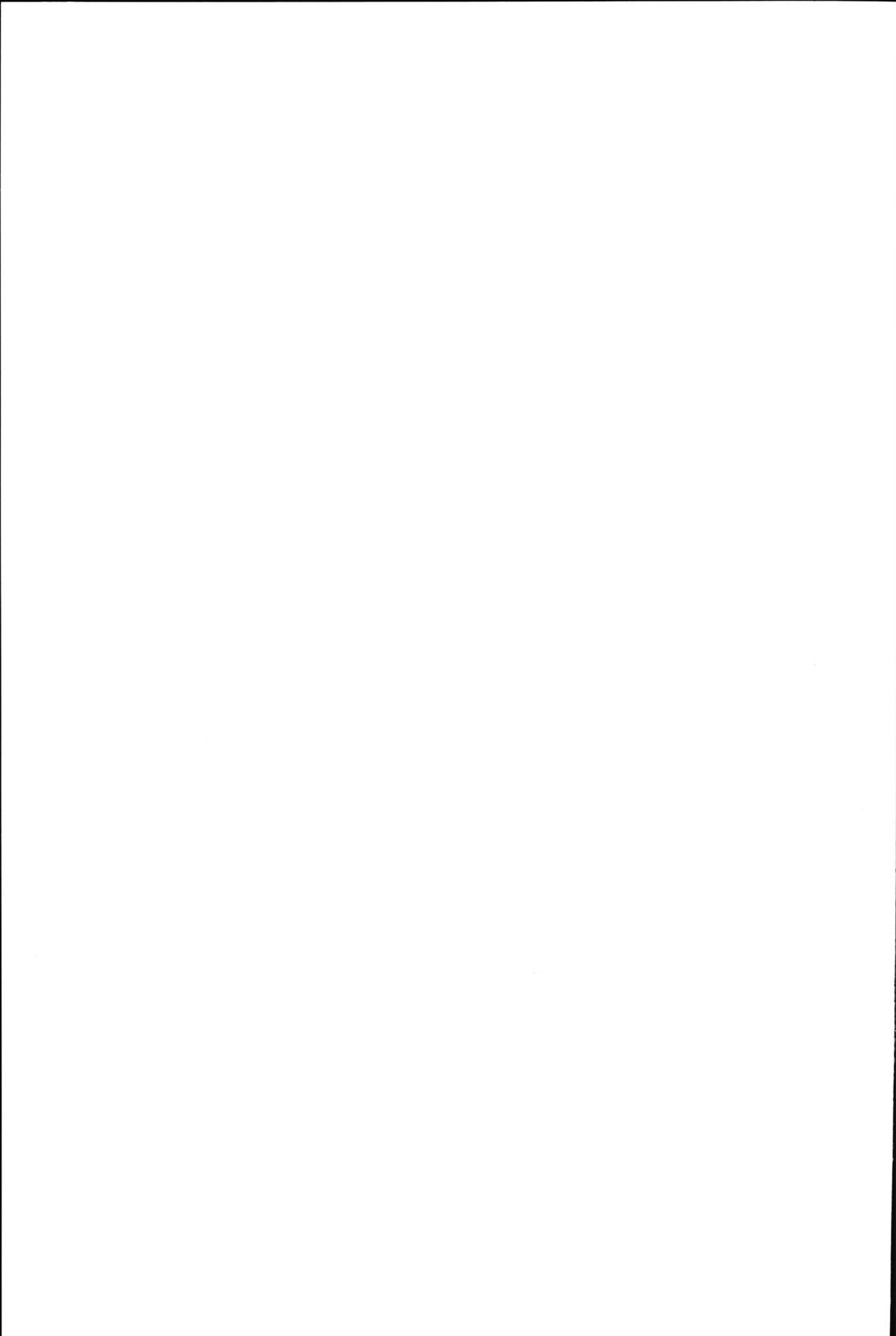
**Conclusion**

Single pituitary melanotrope cells can be efficiently charted by MALDI-MS and reveal a complete profile of the POMC-derived peptides. Although the samples are in physiological environment, neither sample pretreatment nor separation steps are necessary. This offers a fast screening which is minimizing artifacts caused by extraction or separation procedures of conventional methodologies, and offers the possibility to directly mass analyse proteins present in naturally occurring biological fluids. All previously identified and several new POMC end products in melanotrope cells of *Xenopus laevis* were identified by MALDI-MS. In addition, the differences in processing end products of POMC<sub>A</sub> and POMC<sub>B</sub> could be resolved. While little can be said of the absolute quantity of the peptides in the profiles, clear differences between the relative intensities of the peaks show that MALDI-MS can be used to demonstrate different peptide contents in melanotrope cells from animals under different physiological conditions.

**References**

- [1] S. Nakanishi, I. A. T. Kita, M. Nakamura, A. C. Y. Chang, S. N. C. and S. Numa, *Nature*, **1979**, 278, 423-427.
- [2] J. Drouin and H. M. Goodman, *Nature*, **1980**, 288, 610613.
- [3] H. Takahashi, Y. Teranishi, S. Nakanishi and S. Muma, *FEBS Lett.*, **1981**, 135, 97-102.
- [4] M. Uhler and E. Hebert, *J. Biol. Chem.*, **1983**, 258, 257-261.
- [5] G. Boileau, C. Barbeau, L. Jeanotte, M. Chrétien and J. Drouin, *Nucl. Acids Res.*, **1983**, 11, 8063-8071.
- [6] P. D. Patel, T. G. Sherman and S. Watson, *DNA*, **1988**, 7, .
- [7] G. J. M. Martens, O. Civelli and E. Herbert, *J. Biol. Chem.*, **1985**, 260, 13685-13689.
- [8] N. Kitahara, T. Nishizawa, K. Iida, H. Okazaki, T. Andoh and G. I. Soma, *Comp. Biochem. Physiol.*, **1988**, 91B, 365-370.
- [9] E. Hilario, I. Lihrmann and Y. Vaudry, *Biochem. Biophys. Res. Commun.*, **1990**, 173, 653-659.
- [10] G. Salbert, I. Chauveau, G. Bonnet, Y. Valotaire and P. Jego, *Mol. Endocrinol.*, **1992**, 6, 1605-1613.
- [11] B. A. Eipper and R. E. Mains, *Endocrine Rev.*, **1980**, 1, 1-27.
- [12] Y. Rouillé, G. Michel, M. T. Chauvet, J. Chauvet and R. Acher, *Proc. Natl. Acad. Sci. USA*, **1989**, 86, 5272-5275.
- [13] F. J. C. van Strien, B. G. Jenks, W. Heerma, C. Versluis, H. Kawauchi and E. W. Roubos, *Biochem. Biophys. Res. Commun.*, **1993**, 191, 262-268.
- [14] F. J. C. van Strien, L. Galas, B. G. Jenks and E. W. Roubos, *J. Endocrinol.*, **1995**, 146, 146-157.
- [15] C. M. Whitehouse, R. N. Dreyer, M. Yamashita and J. B. Fenn, *Anal. Chem.*, **1985**, 57, 675-679.
- [16] J. B. Fenn, M. Mann, C. K. Meng, S. F. Wong and C. M. Whitehouse, *Mass Spectrom. Rev.*, **1990**, 9, 37-70.

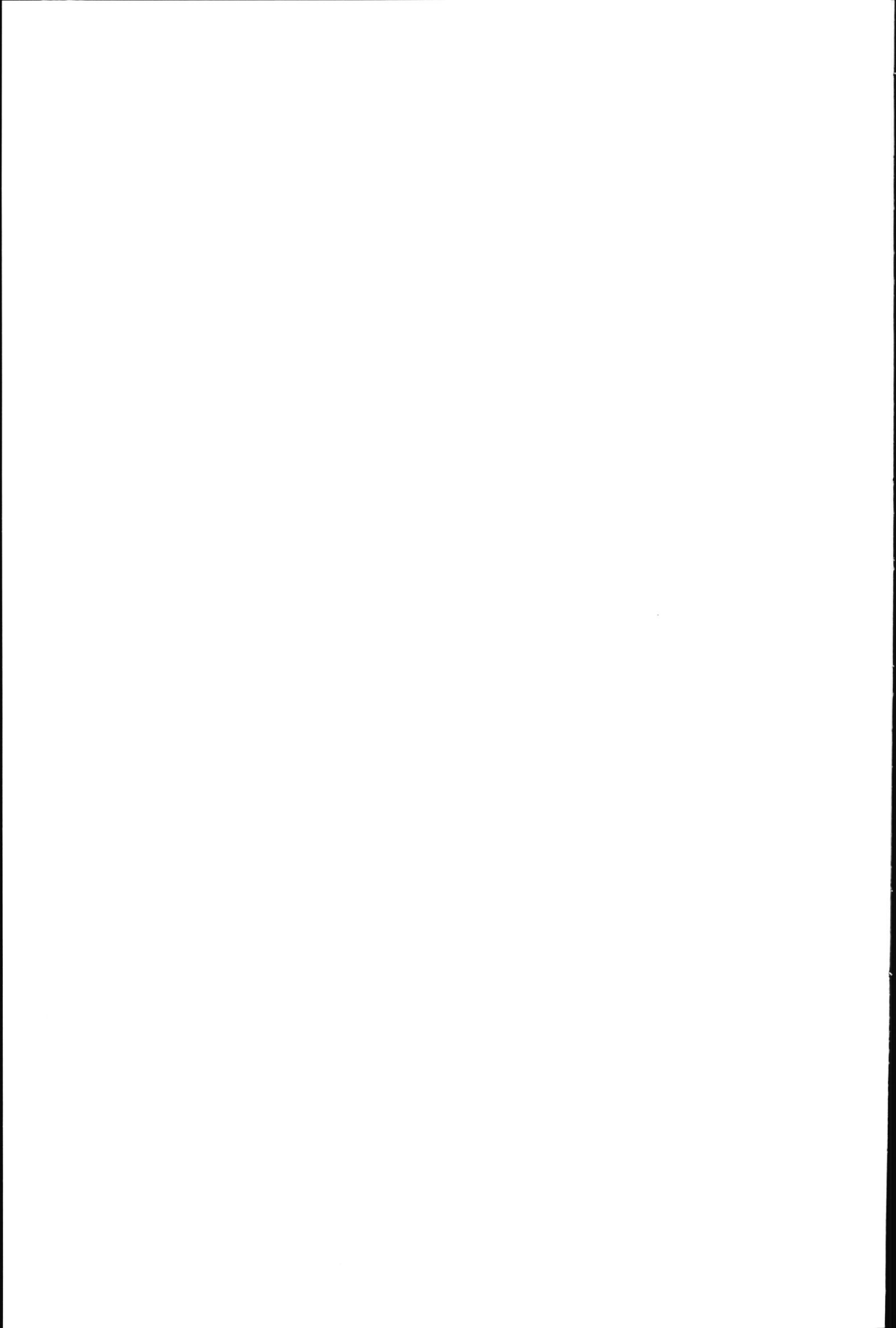
- [17] M. Karas and F. Hillenkamp, *Anal. Chem.*, **1988**, 60, 2299-2301.
- [18] F. Hillenkamp, M. Karas, R. C. Beavis and B. T. Chait, *Anal. Chem.*, **1991**, 63, 1193A-1203A.
- [19] P. A. v. Veelen, C. R. Jiménez, K. W. Li, W. C. Wildering, P. M. Geraerts, U. R. Tjaden and J. v. d. Greef, *Org. Mass Spectrom.*, **1993**, 28, 1542-1546.
- [20] K. W. Li, C. R. Jiménez, P. A. v. Veelen and W. P. M. Geraerts, *Endocrinology*, **1994**, 134, 1812-1819.
- [21] C. R. Jiménez, P. A. v. Veelen, K. W. Li, W. C. Wildering, P. M. Geraerts, U. R. Tjaden and J. v. d. Greef, *J. Neurochem.*, **1994**, 62, 404-407.
- [22] G. J. Feister, P. Højrup, C. J. Evans, D. F. Barofsky, K. F. Faull and P. Roepstorff, *Proc. Natl. Acad. Sci. USA*, **1989**, 86, 5013-6017.
- [23] G. J. M. Martens, K. A. P. Weterings, I. D. v. Zoest and B. G. Jenks, *Biochem. Biophys. Res. Commun.*, **1987**, 143, 678-684.
- [24] G. J. M. Martens, *Nucl. Acids Res.*, **1986**, 14, 3791-3798.
- [25] B. Weatherhead, V. Navaratnam and R. J. Harrison (Eds), *Progress in Anatomy*, Cambridge, University Press, **1983**, 1-32.
- [26] E. P. C. T. de Rijk, B. G. Jenks and S. E. W. Bonga, *Gen. Comp. Endocrinol.*, **1990**, 79, 74-82.
- [27] W. J. J. M. Scheenen, B. G. Jenks, P. H. G. M. Willems and E. W. Roubus, *Pflügers Arch.*, **1994**, 427, 244-251.
- [28] T. W. Schwartz, *FEBS Lett.* **1986**, 200, 1-10.
- [29] R. Benoit, N. Ling and F. Esch, *Science*, **1987**, 238, 1126-1129.
- [30] P. Gluschkof and P. Cohen, *Neurochem. Res.*, **1987**, 12, 951-958.
- [31] B. G. Jenks, B. M. L. V. v. Kemenade and G. J. M. Martens, M. E. Hadley (Eds), *The Melanotropic Peptides*, Florida, CRC Press. **1988**, Vol 1, 103-125.
- [32] B. M. L. V.-v. Kemenade, B. G. Jenks and R. J. M. Smits, *Neuroendocrinology*, **1987**, 46, 289-296.
- [33] R. M. Does, T. C. Steveson and K. Lopez, *Neuroendocrinology*, **1991**, 53, 54-62.
- [34] G. J. M. Martens, B. G. Jenks and A. P. v. Overbeeke, *Nature*, **1981**, 294, 558-560.
- [35] G. J. M. Martens, M. E. Hadley (Eds), *The Melanotropic Peptides*, 1, Florida, CRC Press., **1988**, Vol 1 67-83.
- [36] H. P. J. Bennett, C. A. Browne and S. Solomon, *J. Biol. Chem.*, **1982**, 257, 10096-10102.
- [37] H. P. J. Bennett, P. L. Brubaker, M. A. Seger and S. Solomon, *J. Biol. Chem.*, **1983**, 258, 8108-8112.
- [38] F. J. C. v. Strien, B. Devreese, J. v. Beeumen, E. W. Roubos and B. G. Jenks, *J. Neuroendocrinol.*, **1995**, 7, 807-815.
- [39] P. Böhlen, F. Esch, T. Shibasaki, A. Baird, N. Ling and R. Guillemin, *FEBS Lett.*, **1981**, 128, 67-70.
- [40] G. L. Hammon, D. Chung and C. H. Li, *Biochem. Biophys. Res. Commun.*, **1982**, 109, 118-123.
- [41] R. E. Mains, B. A. Eipper, C. C. Glembotski and R. M. Does, *Trends Neurosci.*, **1983**, 6, 229-235.
- [42] S. Rogers, R. Wells and M. Rechsteiner, *Science*, **1986**, 234, 364-368.
- [43] B. Spengler, D. Kirsch, R. Kaufmann and E. Jaeger, *Rapid Commun. Mass Spectrom.*, **1992**, 6, 105-108.
- [44] J. Martinez and P. Potier, *Trends Pharmacol. Sci.*, **1986**, 7, 139-147.
- [45] R. W. Nelson, M. A. McLean and T. W. Hutchens, *Anal. Chem.*, **1994**, 66, 1408-1415
-



## **Chapter 8**

---

Direct sequencing of neuropeptides in biological tissue  
by MALDI-PSD mass spectrometry



---

## Direct sequencing of neuropeptides in biological tissue by MALDI-PSD mass spectrometry

*Dissected tissue pieces of the pituitary pars intermedia from the amphibian Xenopus laevis was directly subjected to matrix-assisted laser desorption/ionization (MALDI) mass analysis. The obtained MALDI peptide profile revealed both, previously known as well as unexpected processing products of the proopiomelanocortin (POMC) gene. Mass spectrometric peptide sequencing of a few of these neuropeptides was performed by employing MALDI combined with post-source decay (PSD) fragment ion mass analysis. The potential of MALDI-PSD for sequence analysis of peptides directly from unfractionated tissue samples was examined for the first time for the known desacetyl- $\alpha$ -MSH-NH<sub>2</sub> and the presumed vasotocin neuropeptide. In addition the sequence of an unknown peptide which was present in the pars intermedia tissue sample at molecular mass 1392.7 Da was determined. The MALDI-PSD mass spectrum of precursor ion 1392.7 Da contained sufficient structural information to uniquely identify the sequence by searching protein sequence databases. The determined amino acid sequence corresponds to the vasotocin peptide with a C-terminal extension of Gly-Lys-Arg ("vasotocinyl-GKR") indicating incomplete processing of the vasotocin precursor protein in the pituitary pars intermediate of Xenopus laevis. Both vasotocin and vasotocinyl-GKR are non-linear peptides containing a disulfide (S-S) bridge between two cysteine residues. Interpretation of the spectra of these two peptides reveal three different forms of characteristic fragment ions of the cysteine side chain which are: peptide-CH<sub>2</sub>-SH (regular mass of Cys-containing fragment ions), peptide-CH<sub>2</sub>-S-SH (regular mass +32 Da) and peptide=CH<sub>2</sub> (regular mass -34 Da) due to cleavage on either side of the sulfur atoms.*

---

Until recently matrix-assisted laser desorption/ionization time-of-flight mass spectrometry (MALDI TOF MS) was thought to produce little fragmentation which could be used for structural analysis. Although only limited prompt fragmentation has been observed in the MALDI process [1-3] Spengler *et al.* have demonstrated that analyte ions formed by MALDI undergo extensive spontaneous decomposition in the first field free region (called "post source decay") and that the resulting fragments can be detected and analysed using a reflectron instrument [4-6]. Since its introduction MALDI post source decay (PSD) has gained interest as a very promising tool for sequencing peptides and successful applications in this area have appeared in recent years. Confirmation of the primary structure of several linear peptides [4,5,7-13] has been demonstrated. In addition the practical use of this approach provide valuable sequence information and/or confirms additional structural features of peptide in enzymatic digests [14-18].

---

Amongst the more complex samples examined by MALDI MS is the successful analysis of neuropeptides directly from intact biological cells and tissue samples dissected from animal brains, initially demonstrated for neurons from the freshwater snail *Lymnaea stagnalis*. [19,20]. In a recent study MALDI MS was used for the identification of proopiomelanocortin (POMC) processing products in melanotrope cells of the pituitary pars intermedia of *Xenopus laevis* [21]. Peptides were defined by their mass and their identities assigned to the predicted masses of peptides deduced from the cDNA nucleotide sequence of the POMC gene [21-23]. The presence of known POMC-processing products, as well as of previously unexpected POMC-derived peptides were demonstrated. Moreover, the peptide profile spectra revealed the presence of mass peaks which could not be directly identified as POMC processing products. The classic approach towards the structural identification of such unidentified neuropeptides requires pooling and extraction of large numbers of cells from the region of interest, followed by several separation steps and subsequent identification and sequencing by mass spectrometry and Edman degradation.

In the present study, pars intermedia of the pituitary of *Xenopus laevis* were used to show the feasibility of obtaining sequence information of neuropeptides directly from tissue samples using MALDI MS combined with PSD fragment ion mass analysis. Initially the sequence of the known peptide desacetyl- $\alpha$ -MSH (1606.8 Da) and an unknown but suspected vasotocin peptide (1050.5 Da) were verified by comparing the MALDI-PSD spectra with the theoretical fragment patterns. Finally the sequence of an unknown peptide at mass 1392.7 Da was determined, using partial sequence informations, obtained from the MALDI PSD spectrum, as the "peptide sequence tag" [24] for screening protein databases.

## Experimental

### *Animals*

Adult *Xenopus laevis* with a weight of approximately 35 g were obtained from the Nijmegen institute for Neurosciences (University of Nijmegen, the Netherlands) laboratory stock. Toads were kept under constant illumination on a green background for at least three weeks at 22 °C. They were feed trout pellets (Trouvit, Trouw, Putten, The Netherlands) once a week.

### *Sample preparation*

Animals were decapitated and pituitary neurointermediate lobes were rapidly dissected. Small pieces of the pars intermedia (containing melanotrope cells, folliculo stellate cells and nerve endings) were cut from the pituitary neurointermediate lobe and placed in

small vials containing 10-20  $\mu$ l of matrix. The matrix used was 2,5-dihydroxybenzoic acid (DHB; Aldrich Chemie, Steinheim, Germany) dissolved at a concentration of 10 mg/ml in 0.1% trifluoroacetic acid (TFA; Merck, Darmstadt, Germany). Approximately 1  $\mu$ l of the sample-matrix solution was deposited on a stainless steel target and allowed to dry before loading into the mass spectrometer.

#### *MALDI-PSD, instrumentation and method*

MALDI-PSD time-of-flight mass spectrometry measurements were performed on a new home built reflector instrument (Institute of Laser Medicine, Duesseldorf) especially optimised for post-source decay (PSD) analysis [8,9]. The mass spectrometer was operated under delayed extraction conditions [25] and the attainable mass resolution (FWHM definition) was close to 7000 on the molecular ions which provides a unit mass resolution across the entire PSD ion mass range for precursor ions up to 3000 Da. Under these experimental conditions and in the considered mass range, the mass accuracy on the molecular ion is in the order of 30 ppm and the maximum error on the mass assignment of the PSD ions was of  $\pm 0.3$  Da. PSD ion data acquisition was performed by PC-based software ("ULISSES" version 7.5, Chips at Work GmbH, Bonn, Germany). Approximately 200 spectra were accumulated per PSD ion spectrum. The PSD ion spectra were compiled and edited by home built software ("PepSeq", F. Lützenkirchen, Institute of Laser Medicine, Duesseldorf).

#### *Protein data base analysis*

EMBL's (European Molecular Biology Laboratory) non-redundant protein database (nrdb) was used in the interpretation of the PSD spectra for the precursor ion at 1392.7 Da. The database was searched by the "PeptideSearch" software available at: <http://www.mann.embl-heidelberg.de/Service/PeptideSearchPeptideSearchIntro.html>. The search parameters were as follows: The protein mass range was set from 0 to 300 kDa, monoisotopic (neutral) peptide mass = 1391.7 with a mass accuracy: of 3 Da, peptide sequence tag, b type sequence ions (723) PRGGK/QR (1374.5), peptide mass cysteine is Cys, isoleucine equals leucine and glutamine equals lysine.

#### *Nomenclature.*

The peptide fragment ion nomenclature is as proposed by Roepstorff and Folhman [26] and by Johnson and Biemann [27]. Small letters denote dissociation sites and subscript numbers specify the number of the amino acid residues on the ion. For internal ions formed by cleavages from both ends of the peptide chain the ions are indicated by standard one letter symbols for their amino acid residues. Immonium fragment ions are characteristic signatures of the presence of a certain amino acid.

## Results and discussion

### Peptide profiling of *pars intermedia* tissue

Dissected *pars intermedia* tissue from the amphibian *Xenopus laevis* was directly subjected to MALDI mass analysis. The obtained mass spectrum, shown in Figure 1, revealed the presence of peaks with masses corresponding to the previously identified peptides, desacetyl- $\alpha$ -MSH-NH<sub>2</sub>, Lys- $\gamma$ <sub>1</sub>-MSH-NH<sub>2</sub>,  $\beta$ -MSH, CLIP POMC<sub>B</sub> and CLIP POMC<sub>A</sub> [21] which are derived from the two related proopiomelanocortin POMC<sub>A</sub> and POMC<sub>B</sub> precursors [22,23]. In addition, two unidentified putative peptide peaks, at mass 1050.4 Da and 1392.7 Da, were obtained as the most prominent signals in the spectrum. In contrast to the previously obtained MALDI MS peptide profiles of melanotrope cells from *Xenopus laevis* [21] the spectrum in Figure 1 was obtained using a reflectron instrument equipped with delayed extraction (DE) of ions. DE provides substantially improved mass resolving power and signal-to-noise ratio over that obtained from electrostatic operation [28]. The obtained mass resolving power in the range of 7000 (FWHM definition), provided for the assignment of monoisotopic masses throughout

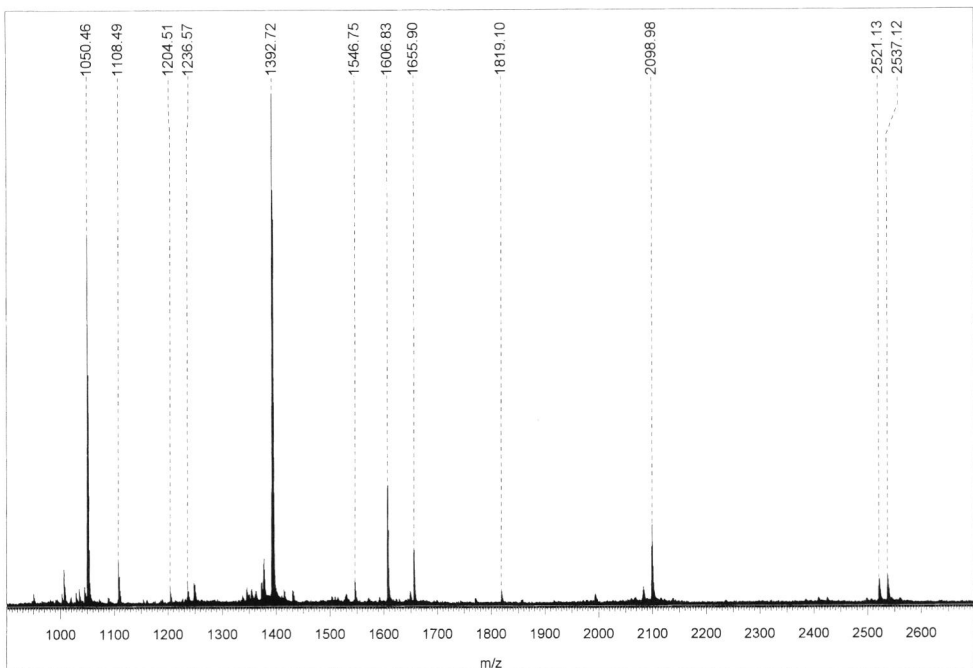


**Figure 1.** Mass profile of peptides in *pars intermedia* tissue from the amphibian *Xenopus laevis*, obtained by direct MALDI-TOF-MS analysis under delayed extraction conditions. The spectrum is confirming the presence of previously known POMC-processing products, as well as unexpected POMC-derived peptides (see Table 1).

the whole mass range (up to 3000 Da). With the use of internal calibration the mass accuracy was in the range 20-70 ppm, which is a factor of 10 better than the mass accuracy obtained previously [21] with electrostatic extraction (Table 1).

The abundances of mass peaks at  $m/z$  1050.4 and  $m/z$  1392.7 (Figure 1) are different from the peptide profiles obtained previously [21], in which the identified POMC derived peptides dominated the spectra. This is most probably due to differences in sample preparation. In the previous study, 95% of the cells were POMC producing melanotrope cells, the remaining were biosynthetically inactive folliculo stellate cells. The pars intermedia tissue used in the present investigation, though mainly consisting of melanotrope cells (and folliculo stellate cells) also included nerve endings. These nerve endings are known to contain a number of different neurotransmitters, which might explain the differences in the two peptide profile spectra. The observed mass peak at  $m/z$  1050.5 corresponds to the calculated mass of one such widely distributed neurotransmitter in amphibians, vasotocin [29,30], whereas the mass peak at  $m/z$  1392.7 could not be directly assigned to any well-known neurotransmitters.

Amino acid sequence informations of both the presumed vasotocin peptide and the unknown peptide at  $m/z$  1392.7 were obtained by employing MALDI TOF MS with post-source-decay (PSD) fragment mass analysis. The performance of MALDI-PSD for sequence analysis of peptides directly from unfractionated tissue samples was initially tested for the known desacetyl- $\alpha$ -MSH-NH<sub>2</sub> peptide (1606.8 Da). A pulsed ion gate with a selectivity  $m/dm$  of about 150 allowed preselection of the precursor ions of interest directly from the unfractionated tissue sample spot.

**Table 1.** Observed and calculated masses for identified neuropeptides obtained from pars intermedia tissue in *Xenopus laevis*. The absolute and relative mass deviations are given in Da and ppm, respectively. The corresponding delayed-extraction MALDI mass spectrum is shown in Figure 1.

observed mass	calculated mass (iso)	$\delta m$ (Da)	accuracy (ppm)	assignment
1050.4	1050.48	0.08	76	CYIQNCPRG-NH <sub>2</sub>
1108.4	1108.48	0.08	72	CYIQNCPRGG
1236.5	1236.58	0.08	65	CYIQNCPRGGK
1392.7	1392.68	0.02	14	CYIQNCPRGGKR
1606.8	1606.77	0.03	19	desacetyl- $\alpha$ -MSH-NH <sub>2</sub>
1655.9	1655.84	0.06	36	Lys-g1-MSH-NH <sub>2</sub>
2099.1	2098.97	0.13	62	b-MSH
2521.1	2521.22	0.12	48	CLIP POMC <sub>B</sub>
2537.1	2537.22	0.12	47	CLIP POMC <sub>A</sub>

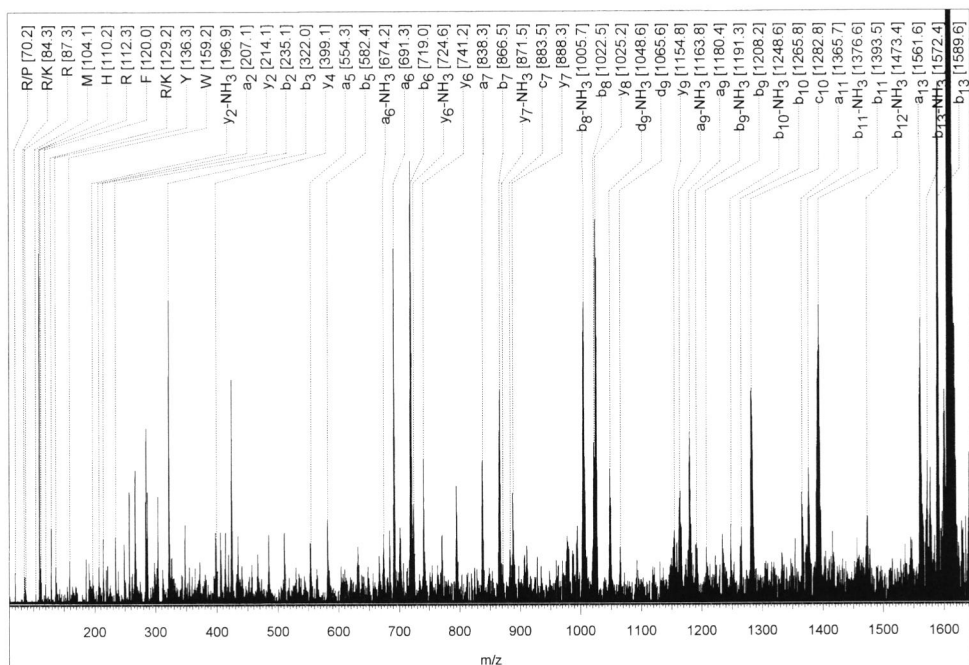


**Figure 2.** MALDI-PSD fragment ion spectrum of precursor ion 1606.8 Da from Figure 1, confirming the structure of the desacetyl- $\alpha$ -MSH-NH<sub>2</sub> peptide. Labeled are the ion signals assigned as N-terminal and C-terminal ions.

### Desacetyl- $\alpha$ -MSH-NH<sub>2</sub>

The fragment mass spectrum obtained by MALDI-PSD analysis of the precursor ion 1606.8 Da is shown in Figure 2. In the low mass range ( $m/z$  50-150) of the PSD spectrum, immonium ions formed from amino acids with large side chains, indicate the presence or absence of specific residues in the peptide stretch. Eight of the thirteen amino acid residues present in the desacetyl- $\alpha$ -MSH-NH<sub>2</sub> peptide (AYSMEHFRWGKPV-NH<sub>2</sub>) can be identified. Besides the immonium ions, the N-terminal fragment ions predominate the PSD spectrum forming an almost complete series of b-type ions. C-terminal fragment ions were observed as y-type ions. The fragment ions containing the Arg residue are accompanied by satellites due to loss of ammonia (-17 Da). The majority of the remaining fragment ions appear to originate from internal fragmentations. The obtained masses are in good agreement with the calculated masses for the theoretical fragment ions, confirming the structure of the desacetyl- $\alpha$ -MSH-NH<sub>2</sub> peptide.

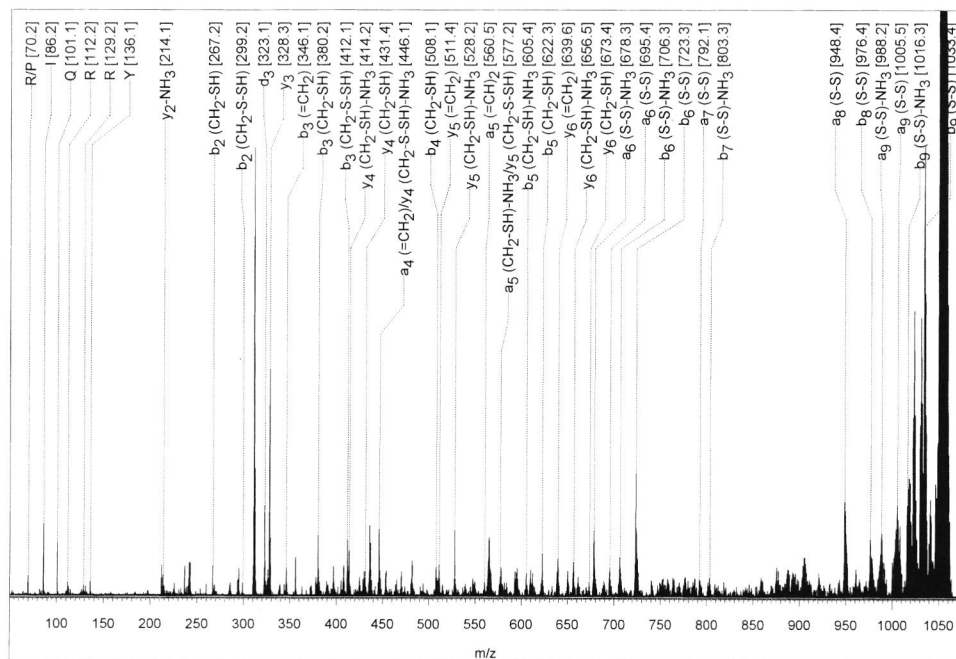


**Figure 3.** MALDI-PSD fragment ion spectrum of precursor ion 1050.4 Da from Figure 1, confirming the structure of the presumed vasotocin peptide, CYIQNCPRG-NH<sub>2</sub> including an intrinsic disulfide (S-S) bridge between the two cysteine residues. Labeled are the ion signals assigned as N-terminal and C-terminal ions (see Figure 4)

#### Precursor ion 1050.4 Da

The MALDI-PSD spectrum of the 1050.4 Da precursor ion is shown in Figure 3 and the identified fragment ions are summarized in Figure 4. The occurrence of immonium ions at  $m/z$  70, 86, 101, 112, 129, 136 indicate the presence of amino acid residues Pro, Ile/Leu, Gln, Arg and Tyr respectively. This is in agreement with the amino acid sequence for vasotocin, CYIQNCPRG-NH<sub>2</sub>. Vasotocin is a non-linear peptide, with a disulfide (S-S) bridge between the two cysteine residues, making interpretation of the spectrum more difficult. A specific pattern of fragment ion peaks, however, was observed for the disulfide-bridged peptides investigated, which was found to be useful for interpretation of such non-linear peptides. Three different forms of characteristic fragment ions of the cysteine side chain were observed: peptide-CH<sub>2</sub>-SH (regular mass of Cys-containing fragment ions), peptide-CH<sub>2</sub>-S-SH (regular mass +32 Da) and peptide=CH<sub>2</sub> (regular

mass -34 Da) due to cleavage on either side of the sulfur atoms. All fragment ions that contained one of the two Cys residues were found to express this fragmentation pattern more or less completely (see Figure 4). All fragment ions which include both cysteine residues, on the other hand, were observed in the non-reduced form (S-S) only.

Except for the  $b_1$  ion, the complete series of  $b_n$  ions ( $n=2-9$ ) and five of the  $a_n$  ions ( $n=5-9$ ) could be assigned to the vasotocin sequence (Figure 4). Again the only C-terminal fragment ions observed were the  $y_n$  ions ( $n=2-6$ ). From these data the sequence of vasotocin from position 3 (Ile/Leu) to position 9 (Gly-NH<sub>2</sub>) could be confirmed. The sequence of residues one and two (CY) could only be clarified by the help of the internal fragment ions. The most pronounced internal fragmentation corresponded to ions extending in the C-terminal direction from proline and internal ions derived from the residues located between the two cysteines.

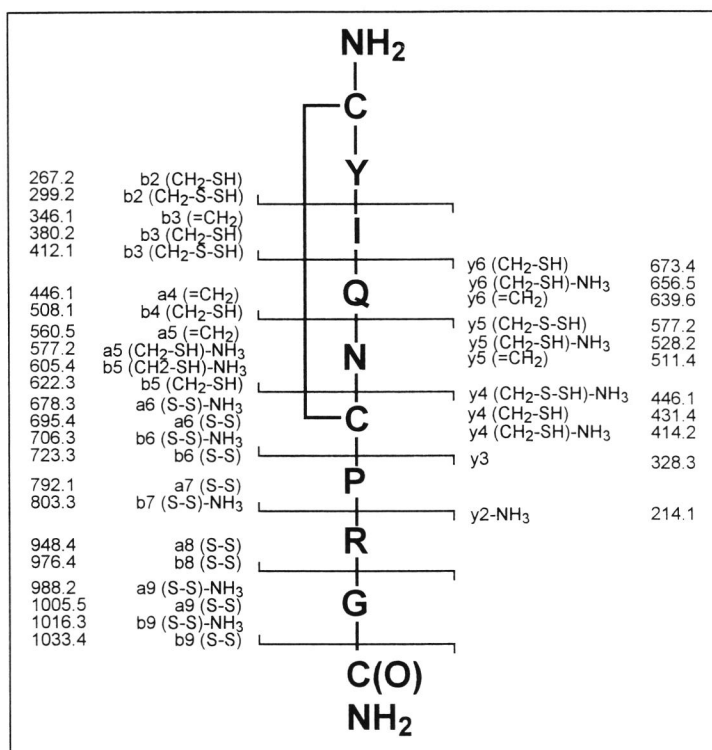


**Figure 4** Known sequence of the vasotocin peptide (N-terminal end on top) including an intrinsic disulfide (S-S) bridge between the two cysteine residues. Indicated are the a, b and y typed ions observed in the MALDI-PSD fragment spectrum shown in Figure 3.

*Precursor ion 1392.7 Da*

Figure 5 show the PSD spectrum obtained from the unknown precursor ion at  $m/z$  1392.7. Immonium ions in the low mass range of the spectrum indicate the presence of the amino acids Pro (70 Da), Ile/Leu (86 Da), Lys/Gln (101 Da), Arg (112 Da and 129 Da) and Tyr (136 Da). Corresponding fragment ions  $b_n$  and  $y_{j-n}$  (both arise from the cleavage of the  $n_{th}$  peptidic bond C(O)-NH-,  $n=0$  being the N-terminus,  $j$  being the number of amino acids of the peptide) can be identified using the formula:

$$m(b) + m(y) = m(\text{precursor}) + 1$$

where  $m(b)$ ,  $m(y)$  and  $m(\text{precursor})$  are the masses of the b- and y-type fragment ions and the protonated precursor peptide, respectively. Correspondences between N- and C-terminal ions were found for mass signal pairs at  $m/z$  174.9/1218.2, 303.1/1090.5, 360.0/1033.4, 417.0/976.2 and 670.2/723.0. Except for the first ion pair, a-type ions at  $m-28$  Da were found for mass signals 1090.5, 1033.4, 976.2 and 723.0 Da, which were therefore assumed to be of fragment ion type "b". The corresponding mass peaks at 303.1, 360.0, 417.0 and 670.2 u were assumed to be y-type ions accordingly. Furthermore, the fragment ion at  $m/z$  174.9 was accompanied by a mass peak due to loss of ammonia (-17 Da) suggesting arginine as the C-terminal  $y_1$  ion. The second C-terminal residue could be determined from the mass difference  $303.1-174.9 = 128$  Da, corresponding to either a lysine or a glutamine residue. The third and fourth  $\Delta m = 57$  Da were found to correspond to two glycine residues. The following  $\Delta m = 253$  Da is too large for any of the 20 amino acid residues and must therefore represent the sum of two amino acid residues. With proline present in the sequence usually no intense signals of N- or C-terminal fragment ions are observed starting from this residue. Proline (increment mass of 97 Da) at the N-terminal side of the amino acid doublet leaves a mass difference of 156 Da, which corresponds to arginine. In summary, the above data suggest that the last six residues of the peptide are PRGGK/QR. This sequence proposition is further confirmed by five proline-directed internal fragments PR (254 Da), PRG (311 Da), PRGG (368 Da), PRGGK/Q (496 Da) and PRGGK/QR (652 Da).

Since no further sequence information could directly be assigned to the remaining abundant signals, the partial sequence PRGGK/QR was used as a sequence tag to search the protein database. Database search utilizing this sequence tag in combination with the mass of the precursor ion resulted in the same sequence CYIQNCPRGGKR derived from the vasotocin precursor found in fourteen different species. The observed PSD fragment ions matched the calculated fragment ions for CYIQNCPRGGKR, containing a disulfide bridge between the two cysteine residues and a free carboxylic acid (COOH)

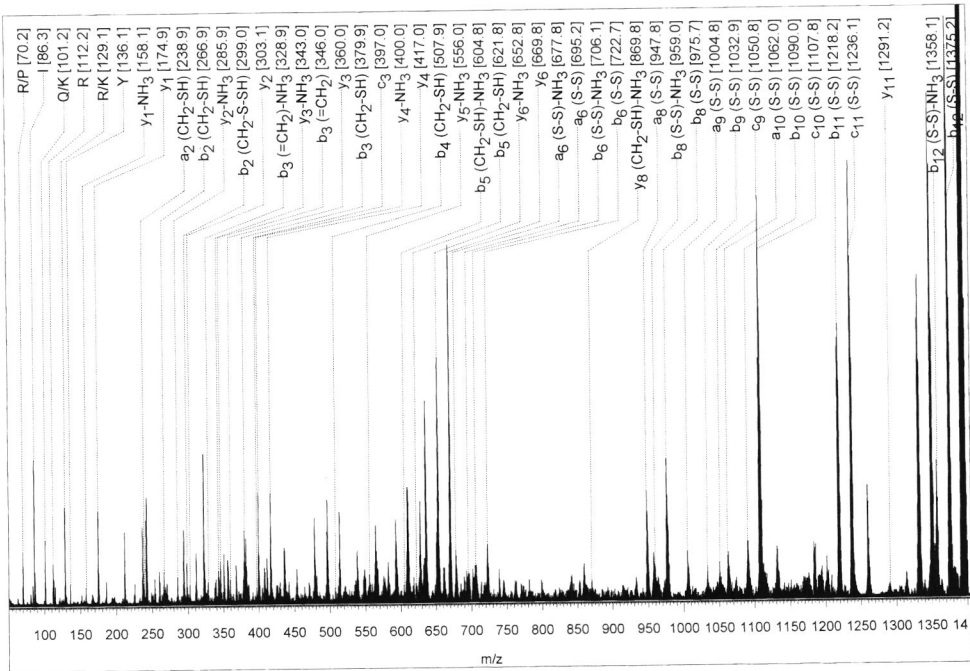
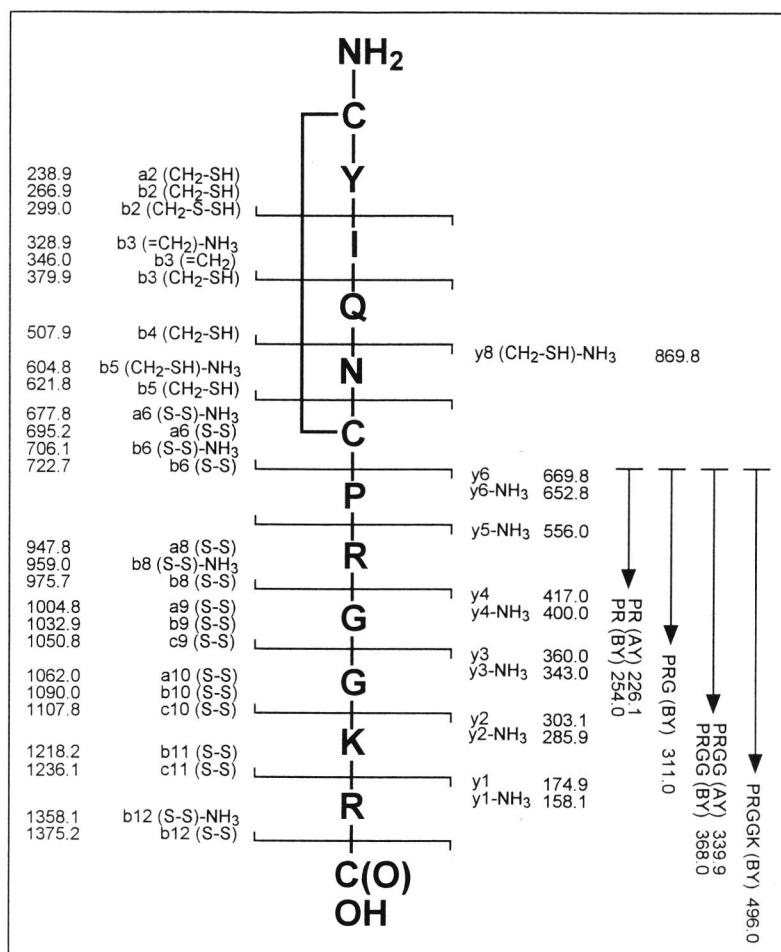


Figure 5. MALDI-PSD fragment ion spectrum of precursor ion 1392.7 Da from Figure 1. The obtained partial sequence PRGGK/QR was used to perform a protein databases search, resulting in the unique sequence CYIQNCPGGKR containing an intrinsic disulfide (S-S) bridge between the two cysteine residues. Labeled are the ion signals assigned as N-terminal and C-terminal ions (see text and Figure 6)

at the C-terminal end (Figure 6). Though the presence of the disulfide bridge made the interpretation of the spectrum more difficult, fragment ions containing either of the cysteine residue could be assigned to the same type of (S-S) fragmentation pattern as described above for vasotocin. As for vasotocin, fragment ions which include both cysteine residues were only observed in the non-reduced form (S-S).

The found sequence corresponds to the above identified vasotocin peptide with the C-terminal extension Gly-Lys-Arg. Vasotocin is linked in its precursor-protein to a neurophysin peptide (MSEL-neurophysin) through the processing signal sequence Gly-Lys-Arg. Complete processing involves endopeptidase cleavage at the carboxylic side of the arginine, removal of arginine and lysine by carboxypeptidase, followed by  $\alpha$ -

amidation and dismutation of the glycine[31]. In previously published results this peptide, vasotocinyl-GKR, was isolated from the neurointermediate lobe in *Xenopus laevis* together with vasotocinyl-GK and vasotocinyl-G [31,32]. The peptide profile spectrum shown in Figure 1 revealed in addition to vasotocinyl-GKR precursor ion, signal with mass values corresponding to the calculated mass for vasotocinyl-GK and vasotocinyl-G (Table 1) indicating incomplete processing of the vasotocin precursor protein.



**Figure 6.** Final sequence determined for precursor peptide ion at 1392.7 Da (N-terminal end on top) including an intrinsic disulfide (S-S) bridge between the two cysteine residues. Indicated are the a, b and y typed ions plus the proline-directed internal fragments ions observed in the MALDI-PSD fragment spectrum shown in Figure 5.

## Conclusion

The mapping and sequencing of peptides directly from tissue samples was performed by MALDI-TOF mass spectrometry and MALDI post source decay fragment ion analysis. Although the peptides were in physiological environment, neither sample pretreatment nor separation steps were necessary.

Delayed extraction MALDI-TOF MS provides substantial improvement in resolution and mass accuracy over that obtained under electrostatic conditions. With the use of internal calibration the mass accuracy was in the 20-70 ppm range, a factor 10 better than the mass accuracy obtained with electrostatic extraction, allowing confident assignment of the POMC derived peptides.

Confirmation of the complete sequence of desacetyl- $\alpha$ -MSH and the presumed vasotocin peptide was possible by comparing the MALDI-PSD spectra to the predicted fragment ion masses for the two peptides. The average mass accuracy of the fragment determination with delayed extraction was better than  $\pm 0.3$  Da, sufficient to differentiate all common amino acid residues except for Leu versus Ile and Lys versus Gln.

The complete sequence of the unknown precursor ion 1392.7 Da could not be directly interpreted from the MALDI-PSD mass spectrum. However identification of a partial sequence of six amino acids was sufficient to obtain a unique match, when used as sequence tag in screening the protein sequence databases. MALDI-PSD combined with databases searching is shown to be a promising method for rapid structural characterization of specific neuropeptides directly from tissue samples.

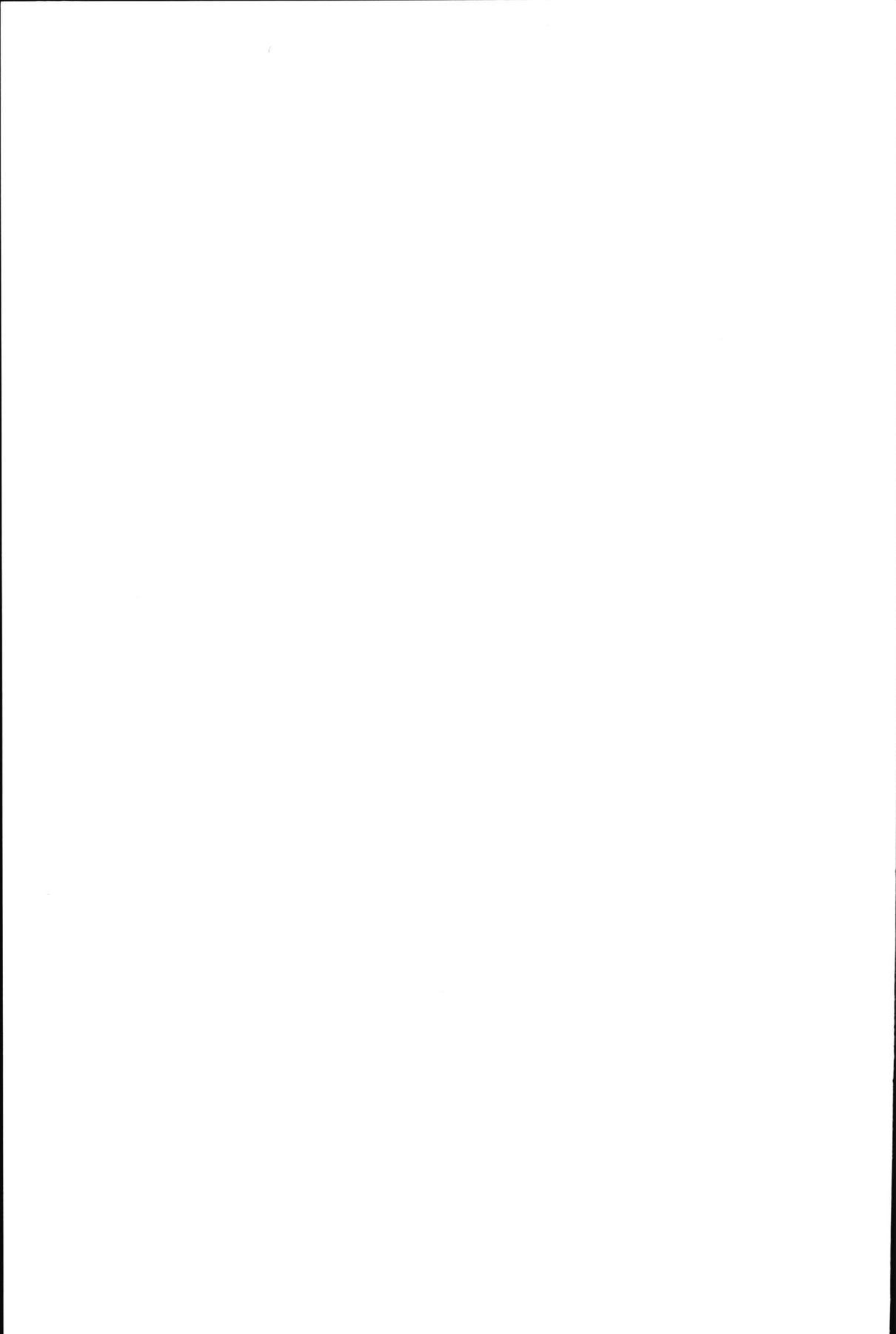
## Acknowledgement

Financial support by the Bundesministerium für Bildung, Wissenschaft, Forschung und Technologie (BMBF, contract No. 0310709), by the European Community (contract No. MAT1-CT94-0034) by the Medical Faculty of the University of Düsseldorf and by Thermo Bioanalysis Ltd., Santa Fee, USA is gratefully acknowledged.

## References

- [1] P. Juhasz and C. E. Costello, *J. Am. Soc. Mass Spectrom.*, **1992**, 3, 785-796.
- [2] G. Talbo and P. Roepstorff, *Rapid Commun. Mass Spectrom.*, **1993**, 7, 201-204.
- [3] S. D. Patterson and V. Katta, *Anal. Chem.*, **1994**, 66, 3727-3732.
- [4] B. Spengler, D. Kirsch and R. Kaufmann, *Rapid Commun. Mass Spectrom.*, **1991**, 5, 198-202.
- [5] B. Spengler, D. Kirsch, R. Kaufmann and E. Jaeger, *Rapid Commun. Mass Spectrom.*, **1992**, 6, 105-108.
- [6] B. Spengler, D. Kirsch and R. Kaufmann, *J. Phys. Chem.*, **1992**, 96, 9678-9684.

- [7] B. Spengler, F. Lützenkirchen and R. Kaufmann, *Org. Mass Spectrom.*, **1993**, 28, 1482-1490.
- [8] R. Kaufmann, B. Spengler and F. Lützenkirchen, *Rapid Commun. Mass Spectrom.*, **1993**, 7, 902-910.
- [9] R. Kaufmann, D. Kirsch and B. Spengler, *Int. J. Mass Spectrom. Ion Processes*, **1994**, 131, 355-385.
- [10] J. S. Cottrell, *Biochemical Society Transactions*, **1995**, 23, 914-917.
- [11] J. A. Castoro, C. L. Wilkins, A. S. Woods and R. J. Cotter, *J. Mass Spectrom.*, **1995**, 30, 94-98.
- [12] J. Jai-Nhuknan and C. J. Cassady, *Rapid Commun. Mass Spectrom.*, **1996**, 10, 1678-1682.
- [13] J. Vinh, D. Loyaux, V. Redeker and J. Rossier, *Anal. Chem.*, **1997**, 69, 3979-3985.
- [14] M. C. Huberty, J. E. Vath, W. Yu and S. A. Martin, *Anal. Chem.*, **1993**, 65, 2791-2800.
- [15] J. Machold, Y. Utkin, D. Kirsch, R. Kaufmann, V. Tsetlin and F. Hucho, *Proc. Natl. Acad. Sci. USA*, **1995**, 92, 7282-7286.
- [16] R. Kaufmann, D. Kirsch, J. L. Tourmann, J. Machold, F. Hucho, Y. Utkin and V. Tsetlin, *Eur. J. Mass Spectrom.*, **1995**, 1, 313-325.
- [17] S. Goletz, M. Leuck, P. Franke and U. Karsten, *Rapid Commun. Mass Spectrom.*, **1997**, 11, 1387-1398.
- [18] C. L. Nilsson, C. M. Murphy and R. Ekman, *Rapid Commun. Mass Spectrom.*, **1997**, 11, 610-612.
- [19] P. A. v. Veelen, C. R. Jiménez, K. W. Li, W. C. Wildering, P. M. Geraerts, U. R. Tjaden and J. v. d. Greef, *Org. Mass Spectrom.*, **1993**, 28, 1542-1546.
- [20] C. R. Jiménez, P. A. v. Veelen, K. W. Li, W. C. Wildering, P. M. Geraerts, U. R. Tjaden and J. v. d. Greef, *J. Neurochem.*, **1994**, 62, 404-407.
- [21] F. J. C. v. Strien, S. Jespersen, J. v. d. Greef, B. G. Jenks and E. W. Roubos, *FEBS Lett.*, **1996**, 379, 165-170. (Chapter 7)
- [22] G. J. M. Martens, O. Civelli and E. Herbert, *J. Biol. Chem.*, **1985**, 260, 13685-13689.
- [23] G. J. M. Martens, *Nucl. Acids Res.*, **1986**, 14, 3791-3798.
- [24] M. Mann and M. Wilm, *Anal. Chem.*, **1994**, 66, 4390-4399.
- [25] R. Kaufmann, P. Chaurand, D. Kirsch and B. Spengler, *Rapid Commun. Mass Spectrom.*, **1996**, 10, 1199-1208.
- [26] P. Roepstorff and J. Fohlman, *Biomed. Mass Spectrom.*, **1984**, 11, 601.
- [27] R. S. Johnson, S. A. Martin and K. Biemann, *Int. J. Mass Spectrom. Ion Processes*, **1988**, 86, 137-154.
- [28] M. L. Vestal, P. Juhasz and A. S. Martin, *Rapid Commun. Mass Spectrom.*, **1995**, 9, 1044-1050.
- [29] G. Michel, J. Chauvet, M.-T. Chauvet and R. Ancher, *Biochem. Biophys. Res. Commun.*, **1987**, 149, 538-544.
- [30] H. Nojiri, I. Ishida, E. Miyashita, M. Sato, A. Urano and T. Deguchi, *Proc. Natl. Acad. Sci. USA*, **1987**, 84, 3043-3046.
- [31] Y. Rouillé, G. Michel, M. T. Chauvet, J. Chauvet and R. Acher, *Proc. Natl. Acad. Sci. USA*, **1989**, 86, 5272-5275.
- [32] S. Iwamuro, H. Hayashi and S. Kikuyama, *Biochim. Biophys. Acta*, **1993**, 1176, 143-147.

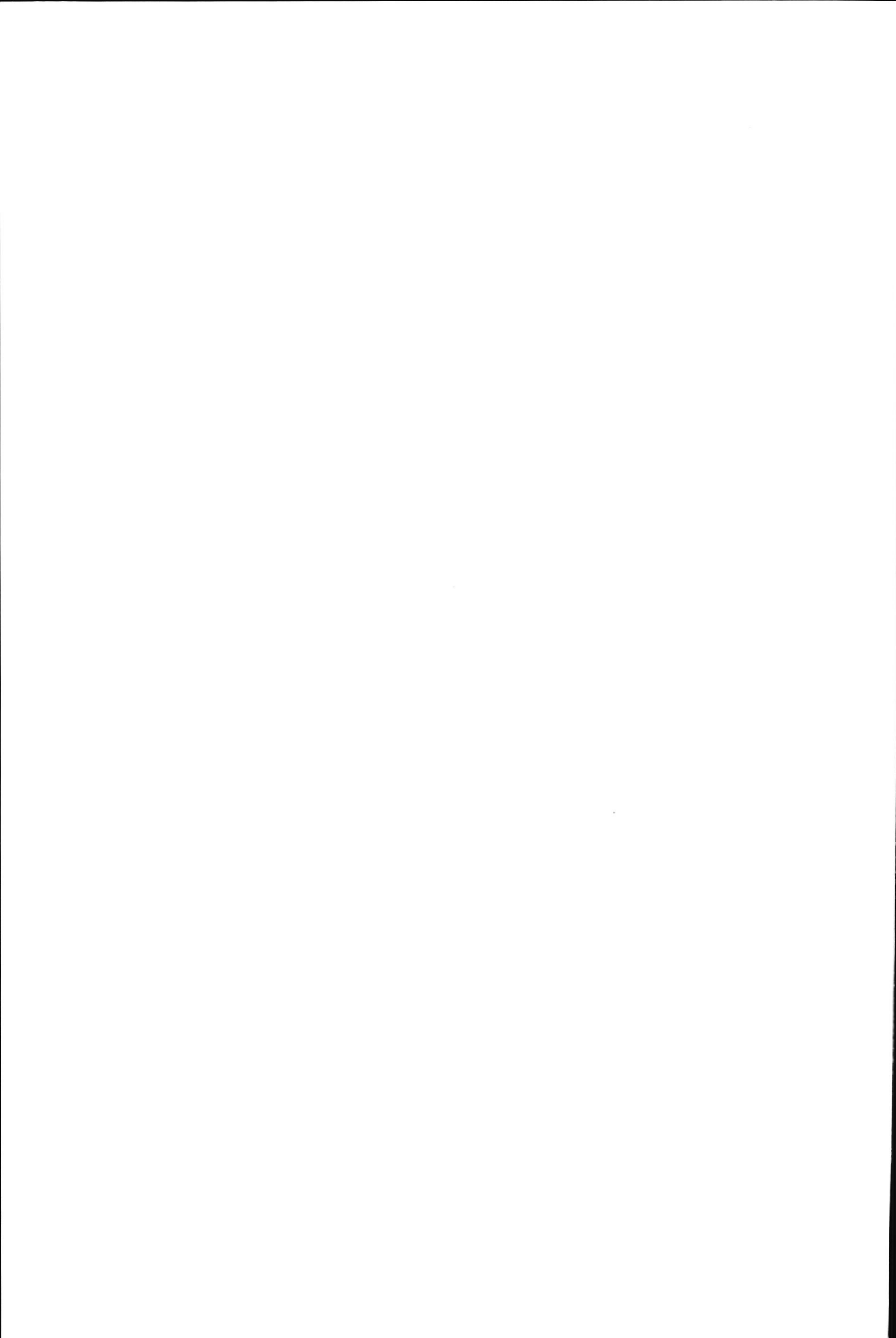


## **Chapter 9**

---

Conclusion and perspectives

Summary



---

## Conclusions and perspectives

Remarkable progress has been made during the first decade of the matrix-assisted laser desorption/ionization (MALDI) mass spectrometry history. It is becoming an indispensable tool in the analysis of a wide range of compounds, with new levels of sensitivity, mass accuracy, mass range and ability for mixture analysis. MALDI has become an important technique in biological science, not only because the molecular mass of the native material at the level of accuracy is in itself very useful information, but also because the changes thereof upon chemical or enzymatic treatment provide further insight into the structure or biological significance of parts of the native molecule. Recent developments, together with ongoing research into protein analytical technology, are fundamentally changing the role and the scope of protein characterization. The exponentially growing contents of sequence databases are resulting in a rapidly increasing fraction of biologically significant proteins for which the complete sequence has been determined at the genetic level. In these cases the task of sequencing a protein is reduced to the task of correlating the sequence of the protein under investigation with the relevant mass entry in a sequence database.

Post source decay fragment-ion mass analysis has largely extended the analytical capabilities of MALDI-TOF-MS so as to make this technique a valuable approach for mass spectrometric based structural elucidations of large analytes, in particular peptides. Routine MALDI PSD application requires; increased knowledge of the type of fragmentation, translated into more comprehensive computer programs, which convert spectral patterns into structural information.

The major disadvantage of MALDI TOF has traditionally been low mass resolution. The latest and superior improvement in TOF resolution has been achieved by incorporating delayed extraction. Delayed extraction has only recently become available in research laboratories and it is reasonable to expect further development. With the success of delay extraction it is likely that this will lead to unit mass resolution in the high mass range (>10 000).

MALDI TOF has greatly contributed to the development of a routine mass spectrometer for the analysis of biomolecules. Because the instrumentation is significantly simpler than conventional mass spectrometers, low cost, user-friendly and commercially available mass spectrometers can now be operated by scientists with no profound training and background in mass spectrometry. Once mass spectrometers are made more accessible to nonspecialists, they could become integral parts of modern biological research laboratories.

Continuation of the efforts aimed at, understanding the desorption/ionization process, improving the sensitive and high resolution analysis of biopolymer as well as sustained progress in sample preparation will not only improve practical aspects, such as the choice of new matrices, but is expected to have direct impact on the instrumental design and its optimization.

In view of development in pharmaceutical science where more focus is on the understanding at the single cell level, the MALDI technique will play an increasingly important role, especially since the technique opens the possibility to study the interaction of bioactive molecules at the protein level as well as profiling the multi-factorial effects. A good example of the latter is the proteomic field, in which this technique enables the simultaneous detection of proteins, providing a monitoring tool for novel drug interactions.

## Summary

Matrix-assisted laser desorption/ionization (MALDI) mass spectrometry has emerged as a highly sensitive and versatile method in biological science. The introduction in Chapter 1 describes the principles of the MALDI technique. The current understanding of the desorption/ionization process is presented, together with the fundamental aspects of post-source decay (PSD) and delayed extraction. Finally a short overview of possible applicability of MALDI focused on the analysis of peptides/proteins is given.

The amount of analyte actually consumed during a MALDI analysis is much less than the amount loaded into the mass spectrometer. The so-called picoliter vials are introduced in Chapter 2 as a new sample handling approach for reduced sample/matrix volume in MALDI mass spectrometry. The absolute detection limit for proteins in MALDI mass spectrometry is shown to be significantly improved by the application of the picoliter vials. When reducing the sample volume from a microliter down to 250 picoliter and simultaneously reducing the sample spot area from a few mm<sup>2</sup> down to 0.01 mm<sup>2</sup>, low attomol detection limits are obtained for bradykinin and cytochrome c. Quantitative aspects of MALDI mass spectrometry are presented in Chapter 3. The method relies on the normalization of the analyte ion signal to that of an internal standard. Best linear response is found between the measured peak height ratio and the applied amount of analyte when an appropriate internal standard was used. The potential of MALDI mass spectrometry as a quantitative tool for biological application is demonstrated with the analysis of amperozide in plasma, using the <sup>13</sup>C<sub>4</sub> stable isotopically labelled amperozide as internal standard.

Whereas MALDI-MS has been successfully applied to determine the molecular mass and primary structure of biopolymers, non-covalently bound complexes almost always dissociate into individual components during the MALDI analysis. A number of potential matrix candidates is investigated with regards to the importance of the pH in the MALDI mass spectrometric analysis of non-covalently bound protein complexes (Chapter 4). The ability to detect non-covalently bound complex ions in MALDI-MS seems to be highly dependent on the choice of matrix rather than the pH of matrix solution.

The second part of this thesis (Chapter 5-8) takes advantage of MALDI-MS ability to analyse complex mixtures in the presence of large molar excesses of ionic contaminants and common buffer.

The valuable and efficient mean of peptide mapping in the characterization of protein is demonstrated in Chapter 5 and 6. The basic premise of peptide mapping is to

enzymatically or chemically cleave a protein into a number of smaller peptides, directly followed by mass spectrometric analysis. The ability to measure the molecular mass of each peptide permits further examination of the primary structure of the protein allowing chemical and post-translational modifications to be localized.

A strategy for identification of modification sites in proteins, combining comparative peptide mapping of unmodified and modified proteins and site directed mutagenesis is described in Chapter 5. This approach is demonstrated through the mapping of glutathione-S-transferases (GSH transferases) before and after inhibition with the glutathione conjugate 2-(S-glutathionyl)-3,5,6-trichloro-1,4-benzoquinone (GSTCBQ). In Chapter 6, structural characterization of the glycosylated precursors of IGF II was obtained by peptide mapping prior to and after enzymatic release of carbohydrates. The sequence and linkage of individual carbohydrates can be obtained by successive digestion of the glycoprotein with specific exoglycosidases, followed by MALDI mass spectrometry. The O-linked carbohydrates were found to be associated with the C-terminal extension and the heterogeneity was identified as varied sialylated forms of one and two HexNAc-Hex groups.

Amongst the more complex samples examined by MALDI MS is the analysis of neuropeptides directly from intact biological cells and tissue samples dissected from animal brains (peptide profiling). Chapter 7 and 8 show the feasibility of profiling and sequencing peptides directly from tissue samples by MALDI TOF mass spectrometry and MALDI post-source decay (PSD) fragment ion analysis. Although the peptides were in physiological environment, neither sample pretreatment nor separation steps were necessary. The sequence of an unknown peptide was determined, using partial sequence information, obtained from the MALDI PSD spectrum, as the "peptide sequence tag" for screening protein databases.

Finally, delayed extraction MALDI-TOF MS provides substantial improvement in resolution and mass accuracy over that obtained under electrostatic conditions. The peptide profile obtained with delayed extraction in Chapter 8 compared to that obtained without delayed extraction (electrostatic extraction) in Chapter 7 resulted in a factor 10 better mass accuracy.

## Samenvatting

Matrix-assisted laser desorption/ionization (MALDI) mass spectrometry heeft zich ontwikkeld tot een zeer gevoelige en veelzijdige methode in bioanalytische massaspectrometrie. In Hoofdstuk 1 worden de principes van de MALDI techniek beschreven. De huidige opvattingen van het desorptie/ionisatie proces worden, samen met de fundamentele aspecten van post-source decay (PSD) en vertraagde extractie behandeld. Tenslotte wordt een kort overzicht gegeven van de toepasbaarheid van MALDI toegespitst op de analyse van peptides/eiwitten.

De hoeveelheid stof die daadwerkelijk gedurende een MALDI analyse wordt verbruikt, is veel minder dan de hoeveelheid stof die geïntroduceerd wordt in de massaspectrometer. De zogenoemde picoliter vials worden in Hoofdstuk 2 geïntroduceerd als een nieuwe benadering in monstervoorbewerking ten behoeve van een verkleind monster/matrix volume in MALDI massa-spectrometrie. Door de toepassing van deze picoliter vials wordt de absolute detectielimiet voor eiwitten in MALDI massaspectrometrie significant verbeterd. Door het monstervolume te verkleinen van een microliter naar 250 picoliter en tegelijkertijd het monsteroppervlak te verkleinen van enkele mm<sup>2</sup> tot 0.01 mm<sup>2</sup>, werden detectielimieten verkregen in het lage attomolgebied voor bradykinine en cytochroom c.

Kwantitatieve aspecten van MALDI massaspectrometrie worden behandeld in Hoofdstuk 3. De methode is gebaseerd op de normering van het monstersignaal ten opzichte van een interne standaard. Het beste lineaire verband tussen het gemeten signaal en de opgebrachte hoeveelheid stof werd verkregen wanneer een geschikte interne standaard werd gebruikt. De kracht van MALDI massaspectrometrie als een kwantitatief gereedschap voor bioanalytische toepassing wordt aangetoond met de bepaling van amperozide in plasma, waarbij <sup>14</sup>C<sub>4</sub> gelabeld amperozide als stabiele isotoop is gebruikt als interne standaard.

Waar MALDI-MS met succes is toegepast op de bepaling van de moleculaire massa en de primaire structuur van biopolymeren, dissociëren niet-covalent gebonden complexen vrijwel altijd in de individuele componenten tijdens de MALDI analyse. Een aantal matrix kandidaten is onderzocht ten aanzien van het belang van de pH in de MALDI massaspectrometrische analyse van niet-covalent gebonden complexen (Hoofdstuk 4). De mogelijkheid niet-covalent gebonden complexen te detecteren in MALDI massaspectrometrie schijnt meer afhankelijk te zijn van de keuze van de matrix dan van de pH van de matrix-oplossing.

In het tweede deel van dit proefschrift (Hoofdstuk 5-8) wordt gebruik gemaakt van het vermogen van MALDI massaspectrometrie complexe mengsels in de aanwezigheid

van een hoge molaire overmaat van ionogene verontreinigingen en van normale buffers. Het waardevolle en efficiënte middel van peptide mapping in de karakterisering van eiwitten wordt gedemonstreerd in Hoofdstuk 5 en 6. De werkwijze van peptide mapping is om enzymatisch of chemisch een eiwit te splitsen in een aantal kleinere peptiden, gevolgd door directe massaspectrometrische analyse. De bepaling van de moleculaire massa's van ieder peptide maakt verder onderzoek naar de primaire structuur van het eiwit mogelijk, waardoor chemische en post-translationele modificaties gelocaliseerd kunnen worden.

Een strategie voor identificatie van modificatie-posities in eiwitten, door de combinatie van vergelijkende peptide mapping van niet-gemodificeerde en gemodificeerde eiwitten en positiegerichte mutagenese wordt beschreven in Hoofdstuk 5. Deze benadering wordt gedemonstreerd met de mapping van glutathion-S-transferases (GSH transferases) voor en na remming met het glutathion-conjugaat 2-(S-glutathionyl)-3,5,6-trichloro-1,4-benzochinon.

In Hoofdstuk 6 werd structuurkarakterisering van de geglycosyleerde precursors van IGF II verkregen door peptide mapping voor en na enzymatische afsplitsing van suikers. De volgorde en de aard van de binding van individuele suikers kan worden verkregen door opeenvolgende splitsing van het glycoproteïne met specifieke exoglycosidases, gevolgd door MALDI massaspectrometrie. De O-gebonden suikers bleken geassocieerd te zijn met het C-terminale uiteinde en de heterogeniteit werd geïdentificeerd als verschillende gesialeerde vormen van een en twee HexNAc-Hex groepen.

Tot de analyse van meer complexe monsters, onderzocht met MALDI massaspectrometrie behoort de succesvolle analyse van van neuropeptiden direct in intacte biologische cellen en weefselmonsters afkomstig van de 'peptide profilering' van dierlijke hersenen. Hoofdstuk 7 en 8 tonen de haalbaarheid van profilering en sequentie-analyse van peptiden, direct van weefselmonsters met behulp van MALDI massaspectrometrie en MALDI post-source decay (PSD) fragment-ionen analyse. Hoewel de peptiden zich bevonden onder fysiologische omstandigheden, waren monstervoorbewerkings- noch scheidings-stappen noodzakelijk. De sequentie van een onbekend peptide werd bepaald, waarbij gebruik gemaakt werd van partiële sequentie informatie, verkregen van het MALDI MS spectrum, als het 'peptide sequentie label' voor de screening van eiwit databases.

Tenslotte levert vertraagde extractie MALDI-TOF MS een substantiële verbetering van de resolutie en massa-nauwkeurigheid op ten opzichte van de resultaten verkregen onder electrostatische omstandigheden. Het peptide-profiel verkregen met vertraagde extractie zoals beschreven in Hoofdstuk 8, vergeleken met dat verkregen zonder vertraagde extractie (electrostatische extractie) (in Hoofdstuk 7) resulteerde in een verbeterde massa-nauwkeurigheid met een factor 10.

## Curriculum Vitae

Sonja Jespersen was born in Hanning sogn, Denmark on January 22nd, 1963. In 1982 she completed her upper secondary school (scientific line) at Holstebro Gymnasium, She started her scientific education at Odense University in 1984 and joined the Laboratory of Mass Spectrometry in Protein Chemistry, (headed by Prof. Peter Roepstorff) Institute of Molecular Biology, in 1989. In April 1992, after finalising her thesis with the title, "The primary structure of an endocuticle protein from two locust species, *Locusta Migratoria* and *Schistocerca Gregaria*" she was awarded her Master Degree in Science (Danish Naturvidenskablig Kandidateksamen). The same year she came to the Netherlands and was enrolled as a Ph.D. student at the Department of Analytical Chemistry, Leiden/Amsterdam Center for Drug Research (LACDR) under the supervision of Prof. Dr. Jan van der Greef. The research presented in this thesis was performed at and carried out in association with TNO Nutrition and Food Research Institute, Department of Bio-Pharmaceutical Analysis, Zeist. She is employed as a "post-doc" at TNO Nutrition and Food Research Institute, Department of Bio-Pharmaceutical Analysis Zeist, since July 1996.



## Acknowledgement

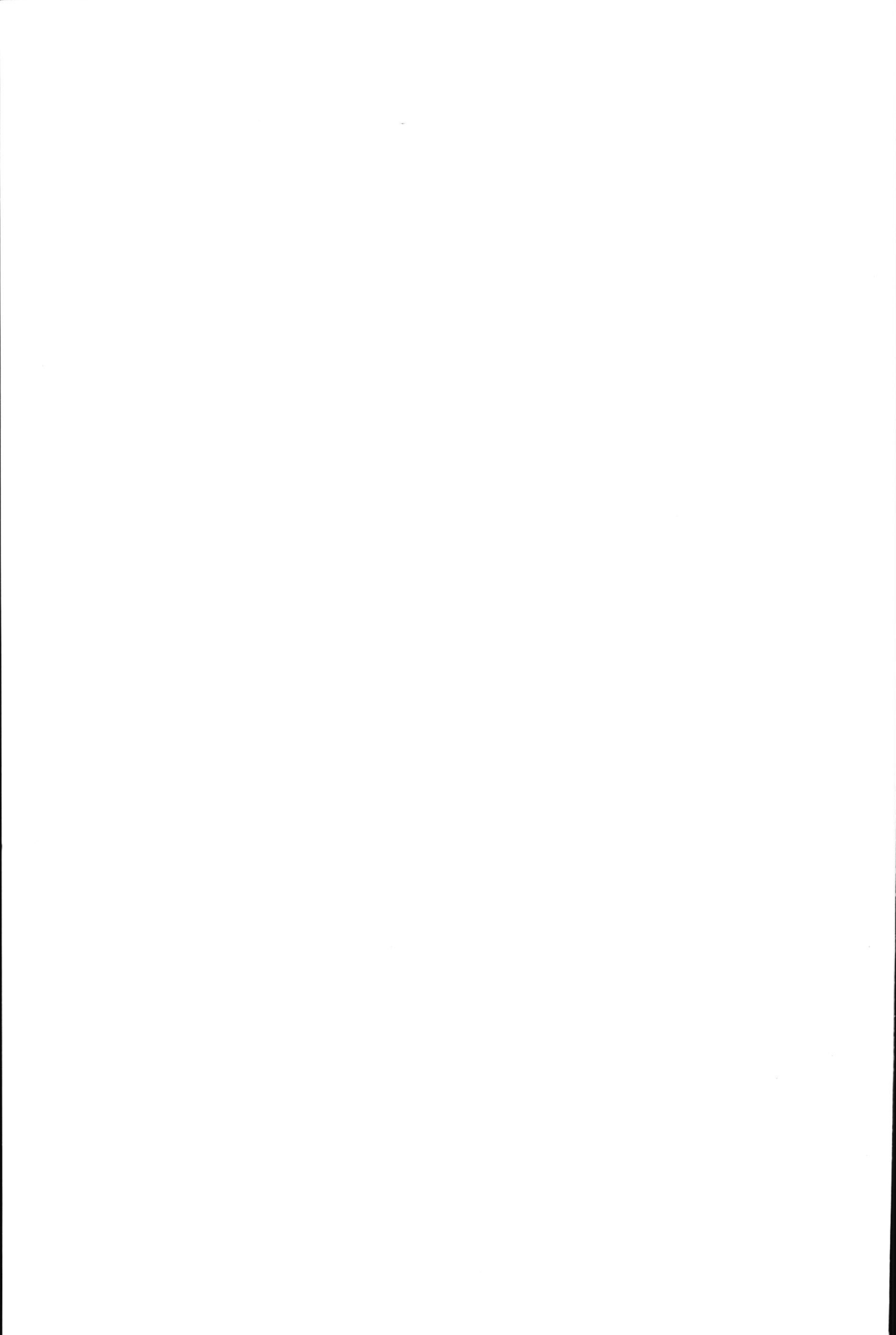
I would like to take this opportunity to acknowledge all those who contributed to the realisation of this thesis.

For the joint projects I have made I would like to acknowledge Dr. J. Roerade and his group for offering me the opportunity to combine microchips with the MALDI technique. Dr. Jan Peter Ploemen - his commitment to the GST project and a pleasant collaboration resulted in several fascinating peptide map puzzles. Dr. J. Koedam is gratefully acknowledged for challenging the MALDI field potential in characterization of a real-life glyco-peptide, presented in a limited amount. I am indebted to Dr. Frank van Strien for continuously providing me with fresh melanotrope cells and to all the toads which were sacrificed in the name of science.

Chapter 8 has been dedicated to Prof. Dr. R. Kaufmann, who was so kind to help me in my desperate attempt to include a PSD (post source decay) part in this thesis. At the same time I would like to acknowledge Dr. Pierre Chaurand for the acquisition and data handling and Prof. Dr. Bernhard Spengler for his editorial work and expertise on this topic.

I wish to express my gratitude to my colleagues at TNO and my friends, who with their understanding and cheerfulness have contributed to a very pleasant atmosphere.

Finally I wish to my thank family for their loving support and constant encouragement.



## List of publications

1. S. Jespersen, G. Talbo and P. Roepstorff.  
Optimization of Sample Recovery from the Nitrocellulose Support Used in Plasma Desorption Mass Spectrometry and its Use for Multiple Analyses of Insulin.  
*Biol. Mass Spectrom.* **22**, 77-83 (1993)
2. S. Jespersen, P. Højrup, S. O Andersen and P. Roepstorff.  
The primary structure of an endocuticular protein from two locust species, *Locusta migratoria* and *Schistocerca gregaria*, determined by a combination of mass spectrometry and automatic Edman degradation.  
*Comp. Biochem. Physiol.* **109B**, 125-138 (1994)
3. S. Jespersen, W. M. A. Niessen, U. R. Tjaden, J. van der Greef, E. Litborn, U. Lindberg and J. Roerade.  
Attomole Detection of Proteins by Matrix-assisted Laser Desorption/Ionization Mass spectrometry with the Use of Picolitre Vials.  
*Rapid Commun. of Mass Spectrom.* **8**, 581-584 (1994)
4. J. H. T. M. Ploemen, W. W. Johnson, S. Jespersen, D. Vanderwall, B. van Ommen, J. van der Greef, P. J. van Bladeren and R. N. Armstrong.  
Active-site Tyrosyl residues are Targets in the Irreversible Inhibition of a Class Mu Glutathione Transferase by 2-(S-Glutathionyl)-3,5,6-Trichloro-1,4-Benzoquinone  
*J. Biol. Chem.* **269**, 26890-26897 (1994)
5. S. Jespersen, W. M. A. Niessen, U. R. Tjaden and J. van der Greef.  
Quantitative Bioanalysis Using Matrix-assisted Laser Desorption Mass Spectrometry.  
*J. Mass Spectrom.* **30**, 357-364 (1995)
6. F. A. van Golen, K. W. Li, R. P. J. de Lange, S. Jespersen and W. P. M. Geraerts  
Mutually exclusive neuronal expression of peptides encoded by the FMRFa gene underlies a differential control of copulation in *Lymnaea*  
*J. Biol. Chem.* **270**, 28487-28493 (1995)
7. S. Jespersen, W. M. A. Niessen, U. R. Tjaden, J. van der Greef, E. Litborn, U. Lindberg and J. Roerade.  
Picoliter Vials: a New Sample Handling Technique for Matrix-assisted Laser Desorption/Ionization Mass Spectrometry.  
*Mass Spectrometry in the Biological Sciences*, Eds. A. L. Burlingame & S. A. Carr, Humana Press, Clifton, Totowa, New Jersey. 217-226 (1996)

8. C. J. M. Rompelberg, J. H. T. M. Ploemen, S. Jespersen, H. Verhagen, J. van der Greef and P. J. van Bladeren.  
Inhibition of Rat, Mouse and Human Liver Cytosol and Major Rat Human Glutathione S-Transferase Isoenzymes by Eugenol and its Oxidation Products  
*Chemico-Biological Interactions* **99**, 85-97 (1996)
  
9. S. Jespersen, J. H. T. M. Ploemen, P. J. van Bladeren, W. M. A. Niessen, U. R. Tjaden and J. van der Greef.  
Identification of Multiple Target Sites for a Glutathione Conjugate on Glutathione-S-Transferase by Matrix-Assisted Laser Desorption/Ionization Mass Spectrometry.  
*J. Mass Spectrom.* **31**, 101-107 (1996)
  
10. F. J. van Strien, S. Jespersen, J. van der Greef, B. G. Jenks and E. W. Roubos  
Identification of POMC processing products in single melanotrope cells by matrix-assisted laser desorption/ionization mass spectrometry.  
*FEBS Letters* **379**, 165-170 (1996)
  
11. S. Jespersen, J. Koedam, C. M. Hoogerbrugge, J. L. van den Branden, U. R. Tjaden and J. van der Greef.  
Characterization of O-glycosylated precursor insulin-like growth factor by matrix-assisted laser desorption/ionization mass spectrometry.  
*J. Mass Spectrom.* **31** 893-900 (1996)
  
12. S. Jespersen, W. M. A. Niessen, U. R. Tjaden, and J. van der Greef  
Basic Matrices in the Analysis of Non-covalent Complexes by Matrix-assisted Laser Desorption/ Ionization Mass Spectrometry  
*J. Mass Spectrom.* **33**, 1088-1093 (1998)
  
13. R.M. Vazquez-Martinez, M.M. Malagon, F.J.C. van Strien, S. Jespersen, J. van der Greef, E.W. Roubos and F. Gracia-Navarro  
Analysis of POMC-derived Peptides in Two Subpopulations of Melanotrope Cells from *Rana Ridibunda* by Matrix-Assisted Laser Desorption/Ionization Mass Spectrometry.  
*Life Science* (in press)
  
14. S. Jespersen, P. Chaurand, F.J.C. van Strien, B. Spengler and J. van der Greef  
Direct sequencing of neuropeptides in biological tissue by PSD-MALDI mass spectrometry.  
*Anal. Chem.* (in press)

## Stellingen

behorende bij het proefschrift

### Matrix-Assisted Laser Desorption/Ionization Mass Spectrometry in Biological Sciences

1. Quantitation in Matrix-assisted laser desorption/ionization mass spectrometry (MALDI-MS) without the use of a closely related internal standard can generate erroneous results.  
(this thesis)
2. There is not a strong correlation between the matrix solution pH and the ability of the matrix in the analysis of non-covalent bound complexes, by MALDI-MS.  
(this thesis)  
L. R. H. Cohen, K. Strupat and F. Hillenkamp, *J. Am. Soc. Mass Spectrom.*, **1997**, *8*, 1046-1052
3. PSD MALDI mass spectrometry offers sufficient peptide sequence information to successfully search protein and nucleotide databases.  
(this thesis)
4. Although MALDI peptide maps can be generated very quickly from sample probes which have been activated through the covalent immobilization of enzymes, the substantial time and effort required to prepare the active probe surface should also be taken into account.  
(this thesis)  
D. Dogruel, P. Williams and R. W. Nelson, *Anal. Chem.* **1995**, *67*, 4343-4348
5. The additional information that UV MALDI-MS peptide mapping of proteins directly from gels offers over the IR MALDI-MS analysis of intact proteins directly from membranes is underestimated.  
C. Eckerskorn, K. Strupat, D. Schleuder, D. Hochstrasser, J.-C. Sanchez, F. Lottspeich and F. Hillenkamp. *Anal. Chem.*, **1997**, *69*, 2888-2892

6. The sudden drop in mass resolution above the 20 kDa mass range, in delayed extraction MALDI-MS, can be avoided if extraction conditions and matrix are optimized.  
U. Bahr, J. Stahl-Zeng, E. Gleitsmann and M. Karas, *J. Mass Spectrom.*, **1997**, 32, 1111-1116
7. The definition of "normality" for packet-cell volume set by the international sports controlling authority, encourages the elite athletes with a physiologically lower packet-cell volume to increase their level by doping products such as epoetin (EPO).  
J.J.M. Marx and P.C.J. Vergouwen, *The Lancet*, **1998**, 352, 451-451
8. The finding that neurons in the adult human brain can be regenerated after all, is no argument to drink too much.  
P.S. Eriksson, P. Perfilieva, T. BjorkEriksson, A.M. Alborn, C. Nordborg, D.A. Peterson and F.H. Gage, *Nat. Med.*, **1998**, 4, 1313-1317
9. Outbreaks of infections with the vero cytotoxin producing *Escherichia coli* 0157 can be prevented by educating the public to send back pink undercooked beefburgers.  
S.M. Parry, R.L. Salmon, G.A. Willshaw and T. Cheasty, *The Lancet*, **1998**, 351 1019-1022.
10. Product of science and technology is mainly what separates our modern way of life from that of our cave dwelling ancestors.
11. The tolerance towards the admittance of illegal drugs (cocaine, XTC, etc.) is in sharp contrast to the admittance of legalized pharmaceuticals.
12. Though we might not find it appealing to get old, the alternative "dying young" seems a much worse destiny.

S. Jespersen

Leiden, 18 Februari 1999



